

ABSTRACT

Title of Thesis: COMPARING SSM/I SNOW DEPTH ESTIMATES TO IN-SITU
AND INTERPOLATED MULTI-SOURCE MEASUREMENTS

Susan Amee Chin-Murray, Master of Science, 2011

Thesis directed by: Associate Professor Kaye L Brubaker
Department of Civil and Environmental Engineering

Spaceborne remote sensing data from the Special Sensor Microwave Imager (SSM/I) have been used for several decades to estimate snow depth over large regions. The SSM/I snow depth accuracy is not well quantified in non-uniform terrain. In this study, SSM/I snow depth estimates for the Columbia River Basin and surroundings in the Western USA and Canada are compared with in-situ manual snow-course measurements and interpolated snow water equivalent from the National Operational Hydrologic Remote Sensing Center. Snow depth is estimated for 25-km pixels from SSM/I brightness temperatures with the widely used Chang algorithm, adjusted for canopy cover. Interactive Data Language and ESRI ArcGIS are used to generate maps and time-series graphs, and to analyze the agreement between SSM/I snow depth and the other data sources. Measures of agreement are cross-tabulated with quantitative landscape descriptors, including: mean pixel elevation, elevation standard deviation (a measure of terrain complexity), and evergreen canopy cover.

COMPARING SSM/I SNOW DEPTH ESTIMATES TO
IN-SITU AND INTERPOLATED MULTI-SOURCE MEASUREMENTS

By

Susan Amee Chin-Murray

Thesis submitted to the Faculty of the Graduate School of the
University of Maryland, College Park in partial fulfillment
of the requirements for the degree of
Master of Science
2011

Advisory Committee:

Associate Professor K Brubaker, Chair
Associate Professor E Kasischke
Professor R Pinker

©Copyright by

Susan Amee Chin-Murray

2011

ACKNOWLEDGMENT

This work was partially supported by the National Aeronautics and Space Administration through Grant NAG 5-11600. Dr. Ed Josberger, USGS Washington Water Science Center, provided the processed SSM/I data and much technical advice. This support is gratefully acknowledged.

DEDICATION

I dedicate this work to my mother Caroline Chin, my husband Thomas and my two wonderful boys Jonathan and Benjamin.

Many heartfelt thanks with great appreciation to Dr Kaye Brubaker and Dr Henry Snyder. Their wisdom and guidance made it possible for me to complete this thesis.

Table of Contents

Chapter 1 Introduction	1
Study Goal	1
Study Location	2
Objectives	2
Chapter 2 Literature Review	3
Importance of Snow	3
Snow depth and density	4
Snow Water Equivalent	5
Remote Sensing of Snow Depth and Snow Water Equivalent	5
EASE Grid	8
Snow course	10
NOHRSC	11
Chapter 3 Methods	13
Location of study region in EASE-GRID	13
Calculating SSM/I snow depth	13
Obtaining station data	14
Mapping Stations in EASE grid coordinates	15
Numerical measures of agreement	17
Comparing NOHRSC Snow Water Equivalent to SSM/I Snow depth	20
Obtaining SWE Data and Mapping in EASE-GRID	20
Numerical measures of agreement	22
Correlation	23
Relative Density	25
Analyzing agreement	29
Categories of Landscape Properties	31

Tabulating Agreement and Landscape Properties	31
Chapter 4 Results	34
Graphically Comparing SSM/I to Surface Snow Depth	34
Comparing Station Measurements to Time-Averaged SSM/I Snow Depth	40
Comparing NOHRSC SWE to SSM/I SD	44
Analyzing agreements between the ground stations with SSM/I snow depth	51
Analyzing agreements between SWE with SSM/I snow depth	54
Chapter 5 Discussion and Conclusions.....	59
Comparing SSM/I snow depth to ground station snow depth	59
Comparing SSM/I SD to NOHRSC SWE	59
Conclusion	60
Appendix A Index Maps of Study Region.....	59
Appendix B Lists of All Pixels containing at least one Agreement	59
Appendix C Time Series Graphs of Ground-Measured and SSM/I Snow Depth for all pixels containing Ground Stations.....	59
Appendix D Series Graphs of SSM/I Snow Depth and NOHRSC SWE for Pixels in the Columbia Basin	59
Reference	59

LIST OF TABLES

Table 2-1 Typical densities of snow in different forms.....	4
Table 4-1– 12 Best agreements with correlation of greater than 0.7 and relative density of less than 0.4.	49
Table 4-2 Ground Snow Depth and Mean Elevation Class.....	52
Table 4-3 Evergreen Canopy Class and SSM/I – Ground Snow Depth Agreement (number of pixels)	53
Table 4-4 SSM-I Snow Depth – NOHRSC SWE Agreement Score by Mean Elevation Class (number of pixels)	55
Table 4-5 SSM-I Snow Depth – NOHRSC SWE Agreement Score by Elevation Standard Deviation (number of pixels).....	56
Table 4-6 SSM-I Snow Depth – NOHRSC SWE Agreement Score by Percentage of Evergreen Coverage.....	57

LIST OF FIGURES

Figure 2-1 Northern Hemisphere EASE-Grid projection (Polar Azimuthal Equal-Area). The red box shows the study location in Western USA and Canada	9
Figure 3-1 Locations of the ground stations and the EASE-GRID 25-km pixels that contain them	16
Figure 3-2 Pixel (202,263) in black box contains 12 stations and Pixel (201,264) in green box contains 1 station	17
Figure 3-3 Time Series of ground station and SSM/I Snow depth, pixel (170, 286)	18
Figure 3-4 Time Series of ground station and SSM/I Snow depth, pixel (186, 268)	19
Figure 3-5 Time series of SSM/I Snow Depth and NOHRSC Snow Water Equivalent, pixel (177, 269)	21
Figure 3-6 Time Series of SSM/I Snow Depth and NOHRSC Snow Water Equivalent, Pixel (177,284)	22
Figure 3-7 For pixel (200,286), the correlation between SSM/I Snow Depth and NOHRSC SWE is -0.72481.	24
Figure 3-8 For pixel (170,274), the correlation between SSM/I Snow Depth and NOHRSC SWE is 0.865425	25
Figure 3-9 For the pixel (194,255) the relative density (NOHRSC SWE / SSM/I Snow Depth) is 0.289429	26
Figure 3-10 For pixel (206,285) the relative density (NOHRSC SWE / SSM/I Snow Depth) is 0.297567	27
Figure 3-11 SSM/I Snow Depth and NOHRSC SWE for pixel (203,275), one of the best agreements with correlation of 0.813344 and relative density of 0.242506.	28
Figure 3-12 SSM/I Snow Depth and NOHRSC SWE for pixel (206,272), one of the best agreements with correlation of 0.718215 and relative density of 0.210978.	29
Figure 3-13 SRTM Elevation [m above sea level] averaged to 25-km EASE-Grid pixels, Columbia Basin.	32
Figure 3-14 SRTM Elevation Standard Deviation [m] in EASE-Grid pixels, Columbia Basin.	33
Figure 4-1 SSM/I Snow depth in pixel (209, 273) and manually measured snow depth at the station in the pixel. This is one of the best pixels observed with 4 agreements.	34
Figure 4-2 SSM/I Snow depth in pixel (200, 263) and manually measured snow depth at the station in the pixel. This is one of the best with two agreements observed.	35
Figure 4-3 SSM/I Snow depth in pixel (202, 262) and manually measured snow depth at three stations in the pixel. Agreement is good for one station, but not for the other stations at higher elevation	35
Figure 4-4 SSM/I Snow depth in pixel (204, 270) and manually measured snow depth at the station in the pixel. This is one of the best agreements observed with three agreements.	36
Figure 4-5 SSM/I Snow depth in pixel (183, 273) and manually measured snow depth at three stations in the pixel. This is considered poor agreement. The increase of snow depth with elevation is evident in the station data.	36
Figure 4-6 SSM/I Snow depth in pixel (183, 285) and manually measured snow depth at the station in the pixel. This is considered poor agreement.	37

Figure 4-7 SSM/I Snow depth in pixel (187, 288) and manually measured snow depth at two stations in the pixel. This is considered poor agreement. The increase of snow depth with elevation is evident in the station data. At these high elevations, the canopy cover correction does not make up the difference between SSM/I and station SD.	38
Figure 4-8 SSM/I Snow depth in pixel (199, 282) and manually measured snow depth at four stations in the pixel. The SSM/I estimates agree somewhat with the lowest elevation station, but not with the increased snow depth at higher elevation.	39
Figure 4-9 SSM/I Snow depth in pixel (188, 271) and manually measured snow depth at two stations in the pixel. This is considered very poor agreement. The increase of snow depth with elevation is evident in the station data.	39
Figure 4-10 SSM/I Snow depth in pixel (182, 264) and manually measured snow depth at the station in the pixel. This is considered poor agreement; however, at this low elevation, less difference is observed between ground station and SSM/I snow depth.....	40
Figure 4-11 Station snow depth measurements with lower and upper bounds of 95% confidence interval for time-averaged SSM/I (4 or 5 pentads centered on the ground measurement date). All stations from British Columbia, Montana, Idaho, Oregon and Washington. If ground SD lies within the confidence interval, the two are considered in agreement for that date.	41
Figure 4-12 Number of agreements per pixel which ground snow depth observations were compared to 95% confidence interval for SSM/I snow depth (4 or 5 pentads centered on the ground measurement date). If ground SD lies within the confidence interval, the two snow depths are considered in agreement for that date	42
Figure 4-13 Percentage of Agreements per pixel. The fraction of agreement is the number of agreements divided by the total number of ground observations in the pixel.....	43
Figure 4-14 Number of ground observations per pixel (station-date pairs). Pixels contain from 1 to 27 ground snow depth observations.	44
Figure 4-15 SSM/I Snow Depth and NOHRSC Snow Water Equivalent for pixel (169, 287). Although the time series show some similarity in pattern, the magnitudes are wrong; SD must be greater than SWE.	45
Figure 4-16 SSM/I Snow Depth and NOHRSC Snow Water Equivalent for pixel (171, 280). Good relative density but poor pattern consistency	45
Figure 4-17 SSM/I Snow Depth and NOHRSC Snow Water Equivalent for pixel (196, 287). This result is among the worst: poor correlation in time, and SD less than SWE	46
Figure 4-18 Correlation of SWE and SSM/I snow depth. Strong positive correlations indicate good agreement; strong negative correlations indicate a linear relationship, but lack of agreement.	47
Figure 4-19 Relative density (Average NOHRSC SWE / Average SSM/I Snow Depth) – Up to 0.4 is considered good agreement. Values above one are physically impossible, and high fractions (near 1.0) unlikely.....	48
Figure 4-20 - 12 blue pixels represents 12 best agreements with correlation of greater than 0.7 and relative density of less than 0.4.....	49
Figure 4-21 Shallow snow depth shows good agreement.....	50
Figure 4-22 Despite canopy cover of 57%, shallow snow depths yield good agreement for the pixel (187,263)	50
Figure 4-23 This is one best 12 pixels with the most snow depth about 110cm.	51
Figure 4-24 Mean pixel elevation class and number of pixels with no agreement and at least one agreement between SSM/I and ground snow depth.....	52
Figure 4-25 Evergreen canopy class and SSM/I - ground snow depth agreements (number of pixels).	53

Figure 4-26 Evergreen Canopy Coverage and locations of 50 pixels with at least one agreement	54
Figure 4-27 SSM/I Snow Depth and NOHRSC SWE Agreement Score by Mean Elevation Class	55
Figure 4-28 SSM/I Snow Depth and NOHRSC SWE Agreement Score by Elevation Standard Deviation Class.....	566
Figure 4-29 SSM/I Snow Depth and NOHRSC SWE Agreement Score by Percentage of Evergreen Coverage	58

Chapter 1 Introduction

Understanding snowpack characteristics through various types of physical measurement allows for the prediction of snowmelt runoff and better management of scarce water supply. The knowledge is also extremely valuable for flood forecasting purposes especially in the early spring. In mountainous regions, the snow-covered area is too vast, remote, and hazardous to cover by manual snowpack measurements. Satellite remote sensing, however, can cover these areas spatially and temporally. Remote sensing gives hope to cover vast space with abundant data.

Special Sensor Microwave Imager (SSM/I) snow retrieval has been used for several decades. The SSM/I algorithm estimates snow depth or snow water equivalent from a spectral gradient. The model was calibrated and has been confirmed in areas of uniform terrain and with shallow snowpack; its performance in complex terrain, such as mountains, is less well quantified. The algorithm was recently revised to include a canopy factor.

Study Goal

The SSM/I snow depth retrieval algorithm is tested against available ground measurements. In addition, independent snow water equivalent data from National Operational Hydrologic Remote Sensing Center (NOHRSC) are compared to the SSM/I snow depth retrieval. The goal is to assess how well the SSM/I estimates compare to the ground measurements and NOHRSC estimates, and to identify terrain characteristics where the SSM/I performs well or poorly.

Study Location

This study focuses on the Columbia River Basin in the western US and Canada.

Additional nearby locations in the Rocky Mountains but outside the Columbia Basin are also included.

Objectives

The objectives of this study are to:

1. Compare the SSM/I snow depth estimates to ground measurements in the Columbia River Basin and nearby Rocky Mountains;
2. Compare the SSM/I snow depth estimates to NOHRSC SWE estimates in the Columbia River Basin; and
3. Analyze agreement and non-agreement between the SSM/I snow depth and the other data sources, specifically how the agreement varies with elevation, terrain complexity, and canopy cover.

Chapter 2 Literature Review

Importance of Snow

The occurrence of precipitation in the form of snow can change the drainage basin's response to the input of water. The modified hydrological response is due to the fact that snow is held in storage over an extended period of time before it enters in the runoff process (Rango, 1997).

Several variables affecting the occurrence of seasonal snow cover in a basin include the time of year, weather patterns, moisture sources, latitude, elevation, and landscape features. When the seasonal snow cover is deposited, several factors can affect the distribution of the snow, depending on the type of the basin. In a flat lowland basin, the type and number of winter storms are the primary factor affecting the amount of the snow accumulation, with terrain and landscape features as secondary factors. In the mountain basins, elevation is the primary factor with storm track and landscape features as secondary factors influencing the amount of snow accumulation. In some basins, wind is an important factor that strongly affects the original deposition pattern by moving and redepositing the snow. In many mountain basins, snow may still be accumulating at the higher elevations while the snow may have already disappeared at the lower elevations (Rango, 1997).

Snow depth and density

Snow depth is the vertical distance from the ground to the top of the snow pack. Snow accumulation or snowfall is the vertical depth of fresh snow deposited over a defined period (generally 24 hours) (Geer, 1996; Singh and Singh, 2001)

Snow density (mass per volume) varies according to the amount of air and liquid water in the snow. Fresh snow density can vary from 0.06 to 0.18 gm/cc, but the average density of fresh snow is about 0.1gm/cc and this value is usually used when actual measurements are not made (Singh and Singh, 2001).

The microstructure of snow changes over time, which affects the density of the snowpack. Table 2-1 shows how density increases with the age of the snow.

Table 2-1 Typical densities of snow in different forms

Snow Type	Density (gm/cc)
Wild snow (new snow at low temperature in calm)	0.01-0.03
New snow (immediately after falling in calm)	0.05-0.07
Damp new snow	0.10-0.20
Settled snow	0.20-0.30
Depth hoar	0.20-0.30
Wind packed snow	0.35-0.40
Firn*	0.40-0.65
Very wet snow and firn*	0.70-0.80
Glacier ice	0.85-0.91

(Source: Singh and Singh, 2001)

*Firn is the type of snow that survived at least one complete summer melt season and could be considered as an intermediate stage between fresh snow and ice.

Snow Water Equivalent

The water equivalent of snow is defined as the depth of water that would be produced by melting the snow, given in units of vertical depth [millimeter or inch]. The snow water equivalent of a snowpack having different layers of different density can be defined as

$$SWE = \sum_{i=1}^n d_i \rho_i = \bar{\rho} D \quad 2-1$$

where the index i refers to one layer of the snow, ρ_i is that layer's density, d_i is that layer's depth, $\bar{\rho}$ is average density, and D is total snow depth (Singh and Singh, 2001).

Remote Sensing of Snow Depth and Snow Water Equivalent

Research has shown the microwave band has most potential for use in remote sensing applications for snow hydrology. Frequencies 37 and 19 GHz were found to be most useful for the SWE data.

Chang et al. (1987) presented a multi-frequency approach to estimate SWE from raw brightness temperature data using the 37-GHz and 18-GHz frequencies of the Scanning Multichannel Microwave Radiometer (SMMR). The algorithm was later revised for the 37- and 19-GHz frequencies of the SSM/I instrument (Chang, 1990). The 37 GHz frequency senses the near-surface (0-50cm) temperature, emissivity and surface roughness. The 19GHz frequency is useful to obtain the information about the internal characteristics of the snow pack (Butt, 2009).

The spatial resolution at these frequencies is poor, about 25km or greater. Observation times were limited to once every few days, depending on the latitudes. With this poor resolution, Rango (1997) stated that use of the SSM/I data to estimate SWE was limited to flat and relatively homogeneous terrain.

The earlier SMMR algorithm was revised to a snow depth (SD)/brightness temperature (T) relationship for a uniform snowfield. The algorithm to estimate the snow depth is based on the assumption of the entire snowpack consisting of snow density of 0.3 g/cm^3 , corresponding to a snow crystal radius of 0.3 mm (Foster, 2005). This algorithm expresses SD [cm] as proportional to the difference between the microwave brightness temperature at the 37 and 19 SSM/I channels as follows,

$$SD = 1.59(T_{19H} - T_{37H}) \quad 2-2$$

where T_{18H} and T_{37H} are the brightness temperature at 18 and 37 GHz, horizontal polarizations, respectively, and 1.59 is a constant derived by using the linear portion of the 37 and 18GHz responses to obtain a linear fit of measured snow depth to the differences between these two channels. This approximation limits the use of the algorithm to detection of snow up to 1m deep. Snow at the margins of snow-covered area is believed to be underestimated since shallow, dry snow (< 2.5cm) is nearly transparent to microwave emission (Chang, 1990).

Forest poses a serious problem by obscuring the snowpack. A forest canopy over the snowpack can cause lower certainty of the SWE estimations by attenuating the microwave signal from the snowpack and at the same time emitting the forest microwave. In the extremely dense forest area with a significant snowpack, the apparent snow water equivalent can drop to zero. This indicates a need for finding a method to correct the forest cover's effect on the passive microwave snow signature (Rango,1997).

Most of the aircraft-derived SWE over flight lines without extensive forest covers are consistent with the SWE derived from SSM/I data. Over the forested regions, SWE retrievals without correcting for the forested cover gave much lower values than the

ground measurements (Chang, 1997). Foster (1997) incorporated the factor of forest canopy and produced a revised algorithm for North American, Eurasia and other non-Eurasia area.

Foster (2005) writes,

“Because of low loss when snow is dry, part of the radiation emitted by the underlying ground is scattered within the snowpack and part contributes to the observed signal when the total snow depth is less than 10–100 times the microwave wavelength (Rango, 1983). Therefore, in most cases, additional scattering does not result when snow thickness exceeds 0.8 m—the approximate saturation limit for 37 GHz frequencies. For most locations in North America, usually, snow does not accumulate to these depths over an entire PM pixel (37 km x 28 km for SSM/I). In portions of the Rocky Mountains and the Alaska Ranges, and perhaps in a few isolated areas in the boreal forests of Quebec, depths of 1 m or more can be reached, but our analysis indicates that these pixels make up less than 2% of all the pixels in North America.”

Mizukami (2011) writes,

“Several algorithms for retrieving SWE from passive microwave data have been developed in the past two decades (e.g., Chang et al., 1987; Goodison and Walker, 1995; Foster et al., 1997; Tait, 1998; Pullianinen and Hallikainen, 2001; Josberger and Mognard, 2002; Koenig and Forster, 2004; Gan et al., 2009). However, there has been little success in developing analogous algorithms for mountainous areas, partly due to the complex physiographic features and

significant variations in snow distribution within each microwave pixel (approximately 25 x 25 km). Furthermore, there is a limitation of the passive microwave data to estimate large SWE due to passive microwave signal saturation (Tait and Armstrong, 1996; Dong et al., 2005). Dong et al., (2005) reported approximately 150 mm of SWE for this threshold. The mountainous areas typically receive well above this snow amount. Airborne gamma radiation SWE surveys, such as the one operated by the National Weather Service's National Operational Hydrologic Remote Sensing Center (e.g., Carroll, 2001), can provide reliable mean areal SWE estimates along flight lines (approximately 10 km x 300 m; e.g., Cline et al., 2009), but this approach is not feasible when continuous estimates of SWE over large areas are needed.....”

Mizukami (2011) reported several other studies that demonstrate little success in developing analogous algorithms for mountainous areas due to complex physiographic features and significant variation in snow distribution within each microwave pixel (approximately 25 x 25km). Furthermore, there is a limitation of the passive microwave data to estimate large SWE due to passive microwave signal saturation.

EASE Grid

The Equal-Area Scalable Earth Grid (EASE-GRID) is a versatile tool for using and displaying global-scale gridded remote sensing data. The Northern Hemisphere is one of several possible projections in the EASE-GRID family (Figure 2-1)

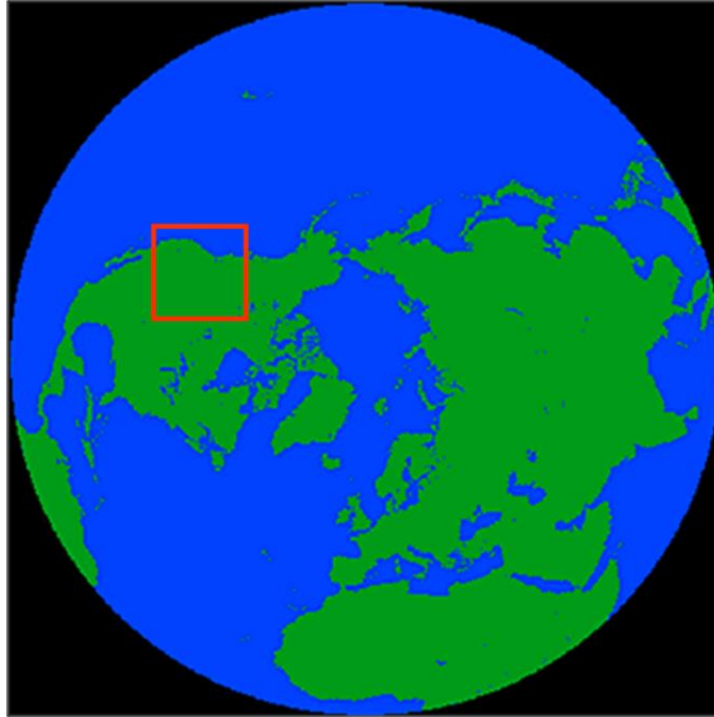


Figure 2-1 Northern Hemisphere EASE-Grid projection (Polar Azimuthal Equal-Area). The red box shows the study location in Western USA and Canada (Source: National Snow and Ice Data Center, 2011a)

A spherical earth model was chosen over elliptical model because of the reduced error introduced in the gridding geolocation in this model choice (NSIDC, 2011a). The projection is easier to project with known latitude and longitudes value which can be related to the column and row coordinates. A grid in the EASE-Grid family is described by four elements: the map projection, the numbers of columns and rows, the number of grid cells per map unit and the grid cell that corresponds to the map's origin.

The original SSM/I Grids were defined as 25-km grids for the SSM/I Level 3 Pathfinder project at NSIDC, which also included gridded Passive Brightness Temperatures. The Northern Hemisphere EASE- Grid is 721 rows by 721 columns. These grids have a nominal cell size of 25km x 25km; the actual cell size is slightly larger: 25.067525km.

The grid coordinates in decimal real numbers (r,s) start at the upper left corner as (0,0) with r, increasing from left to right as columns, and s increasing from top to bottom as rows. Rounding the (r,s) grid coordinates (rounding up at 0.5) gives an integer grid cell number. This grid cell (i,j) = (column,row) is centered at grid coordinates (r,s) = (i+0.5,j+0.5) and is bounded by: $i - 0.5 \leq r < i + 0.5$, $j - 0.5 \leq s < j + 0.5$.

In units of meters, the Map Origin is at the Pole, 90.0N latitude and 0.0 longitude. The map origin corresponds to grid cell (360,360).

Snow course

Snow survey in the Western USA began around 1906. Snow courses were established in permanent sites for trained observers to take manual measurement of snow depth and snow water equivalent, usually around the first of the month during winter and spring; they are generally situated in small meadows protected from the wind (NRCS, 2009a). For this study, four states (Oregon, Washington, Montana and Idaho) are chosen as they are part of Columbia basin and Rocky Mountain area. The Natural Resource Conservation Service (NRCS) lists over 1090 sites in these four states, but only 516 sites are active.

Manual snow surveys in British Columbia are usually conducted up to 8 times per year around the beginning of the month from January to June, with extra measurements in the mid month of May and June (British Columbia River Forecast Centre, 2011). The snow surveys are ideally located in a relatively sheltered area with least tree canopy overhead and as wide as possible with the forest clearing at least as wide as the height of the tree.

Sites were selected to be representative of the elevation between 1000 to 2000 meters above sea level, with snow for at least a portion of the winter.

Five or ten points within the area are chosen with reference to a tree or other markers. Snow depth and snow water equivalent are measured with graduated aluminum tubes with a cutter affixed to the tubing section. The tubes are known as Standard Federal Snow Samplers. The tubes are driven through the snow to the ground, then withdrawn and the snow core extracted. The core and tube are first weighed, then the weight of the core is determined by difference; this weight gives the measurement of snow water equivalent in cm. Then the snow depths and snow water equivalents are averaged based on all measurements taken at the site during each sampling period. (British Columbia River Forecast Centre, 2011).

NOHRSC

The National Operational Hydrologic Remote Sensing Center (NOHRSC) provides remotely sensed and modeled hydrology products covering the USA. Estimates of snow water equivalent data are one of such products; they are assimilated by several dynamic data sources including satellite imagery, airborne gamma radiation survey, snow water equivalent data sets, and station observations. For the SWE data used in this study, satellite imagery was acquired daily at a variety of resolutions from variety of sensors such as Advanced Very High Resolution Radiometer (AVHRR) and Geostationary Operational Environmental Satellite (GOES). Each data type was analyzed and processed by its corresponding system (Hartman, 2011a).

Operational Processing of Multi-Source Snow Data is a system that processes all data from several sources to generate hydrologic products by streamlining and integrating all snow estimation data in one operational system. The spatial data processing algorithms were developed and used to produce snow estimation products from all input data sources. OPPS is capable of integrating raster data with point, line and area vector data. First satellite imagery were acquired and analyzed to produce a map of the areal extent of the snow cover. Then SWE station observations were spatially interpolated and stratified by elevation band. The SWE observations were averaged within each elevation band for individual hydrologic basins. (Hartman, 2011a).

National Weather Service Office of Hydrology developed a methodology to generate real-time gridded snow water equivalent estimates that were from ground-based airborne snow data collected over the Western United States. The spatial variability of the snowpack caused by the orographic effect in the West was incorporated in the gridded snow water equivalent estimates. Due to the difficulty in accurately estimating the precipitation in the mountains, Snow Estimation and Updating System (SEUS) was created for this task. SEUS mainly does analysis of historical snow observation data, and calibrating the parameters needed for estimating the snow water equivalently operational, updating and administering the gridded snow water equivalent (Hill, 2011). Since the process of SEUS implementation is somewhat laborious, only about 25 percent of the mountainous Western US could be estimated. This could lead to questionable accuracy of individual pixel estimates from SEUS. Gridded snow water equivalent could be estimated with simpler model but its accuracy and reliability may not be as high as SEUS's product (Hartman, 2011b).

Chapter 3 Methods

Location of study region in EASE-GRID

North America is in the upper left quadrant of the Northern Hemisphere version of EASE-GRID (Fig. 2-1). The latitudes and longitudes for this study region are from N40 to N53 and W108 to W125 respectively. The study location includes rows 168 to 218 (51 rows) and columns 243 to 302 (60 columns).

Calculating SSM/I snow depth

Brightness temperatures T_{19} and T_{37} in EASE Grid format were obtained from Dr. Ed Josberger, who processed the SSM/I data. Data were provided by pentad (5-day period) for water year 1997. Here, the water year is defined from September 23 1996 to September 24 1997. The pentad is identified by the middle date of the 5-day set. For example, Sept. 25 pentad represents Sept. 23 to Sept. 27. The next pentad would be Sept. 30 (Sept. 28 to Oct. 2). The data set for water year 1997 includes 70 pentads. The Chang equation including forest canopy (Foster, 1997) was applied to compute SSM/I snow depth:

$$SD = \frac{1.59(T_{19H} - T_{37H})}{1.00 - f} \quad (3-1)$$

where f = fraction of the EASE-grid cell covered by the forest canopy

If Eq. 3-1 results in a negative SD value, it is set to zero.

Forest canopy data in EASE-Grid were obtained from National Snow and Ice Data Center (2011b). The data set gives the percent coverage of each land cover class in each

25-km EASE-Grid pixel. The data set has 17 classes of land cover, including Evergreen Needleleaf and Evergreen Broadleaf. Both evergreen classes were added together to give forest canopy coverage in percentage, providing a value of f in Eq. (3-1) for each pixel.

Obtaining station data

Canadian ground measurement station data were obtained from the British Columbia River Forecast Centre online resource SNOWHIST (BCRFC, 2011). SNOWHIST provided a file containing snow depth and SWE from 440 ground measurement and pillow stations throughout BC for the years 1935 to 2007. Snow depth stations report up to 8 measurements per year in cm: generally on the first of the month from January to June, with additional 15th day of the month during May and June. The 115 stations that lie in the Columbia basin were identified and extracted.

Surface measurements of snow depth in the USA are available online from the Natural Resources Conservation Service (formerly Soil Conservation Service) (NRCS, 2011). The data are provided by state; data are available from as early as 1915 to the current year, with up to 6 measurements per year taken around the first of the month from January to June. The Columbia basin lies in four states: Montana, Oregon, Idaho and Washington. Surface snow depth measurements were gathered from all four states: 273 Idaho stations, 259 Montana stations, 313 Oregon stations, and 229 Washington stations.

Out of nearly 1200 ground stations from BC and 4 states, only 458 have data for Water Year 1997. These stations' data were entered into a spreadsheet in a consistent format and units. US snow depth reports (in) were converted to cm.

Mapping stations in EASE grid coordinates

The ground measurement station data provided the latitude/longitude location of each station. The stations were mapped to EASE grid coordinates, using the transformation equations for the North polar azimuthal equal-area projection provided by the National Snow & Ice Data Center (NSIDC, 2011a):

$$r = 2 * R / C * \sin(\lambda) * \sin(\pi/4 - \phi/2) + r_0 \quad 3-2(a)$$

$$s = 2 * R / C * \cos(\lambda) * \sin(\pi/4 - \phi/2) + s_0 \quad 3-2(b)$$

where:

r = column coordinate

s = row coordinate

λ = longitude in radians

ϕ = latitude in radians

R = Radius of the Earth, set to 6371.228 km for EASE-Grid

C = nominal cell size (25067.525 m)

(r_0 , s_0) = map origin column, row (360,360 for the North azimuthal grid)

With r and s computed, the stations could be assigned (x,y) locations in the EASE-GRID projection

$$x = (r - 360) * C \quad 3-3(a)$$

$$y = (360 - s) * C \quad 3-3(b)$$

The station point locations can be viewed in ArcMap (Figure 3-1). Some EASE-Grid pixels contain as many as 14 stations.

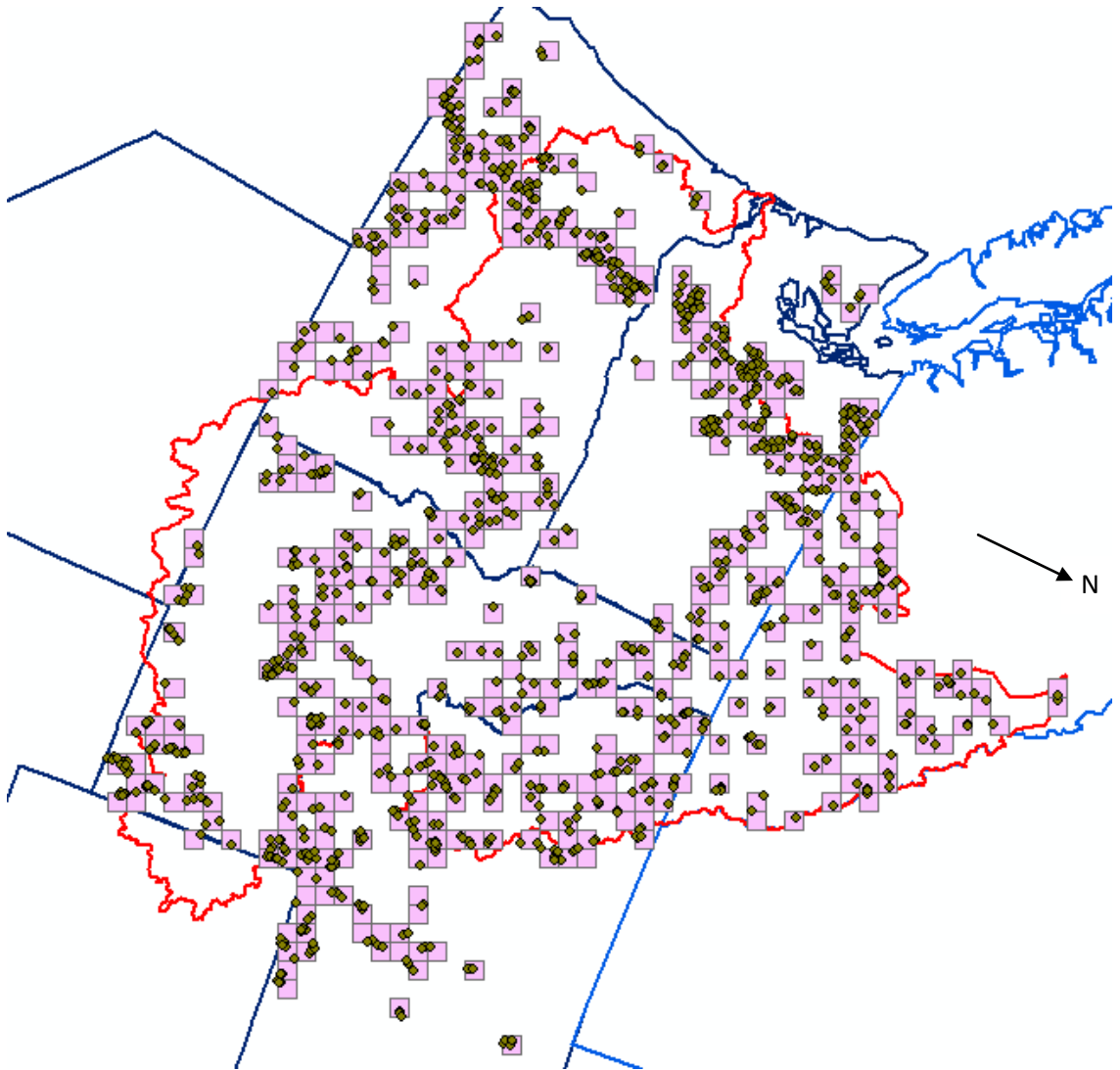


Figure 3-1 Locations of the ground stations and the EASE-GRID 25-km pixels that contain them. Red line indicates the Columbia Basin boundary.

Interactive Data Language (IDL) was used to generate time series graphs of snow depth for all pixels that contain at least one ground station and for which SSM/I SD estimates are available. A pixel's center coordinates lie halfway between integer values of r and s . Therefore, any station can be assigned to a pixel by rounding its (r,s) coordinates to the nearest integer. For example, the station located at $(r,s) = (273.4, 301.9)$ is mapped to pixel $(273,302)$. If the pixel contains multiple ground stations, they are all included in the

graph. For example, pixel (202,263), containing 12 stations, and pixel (201,264), containing a single station, are shown in Figure 3-2.

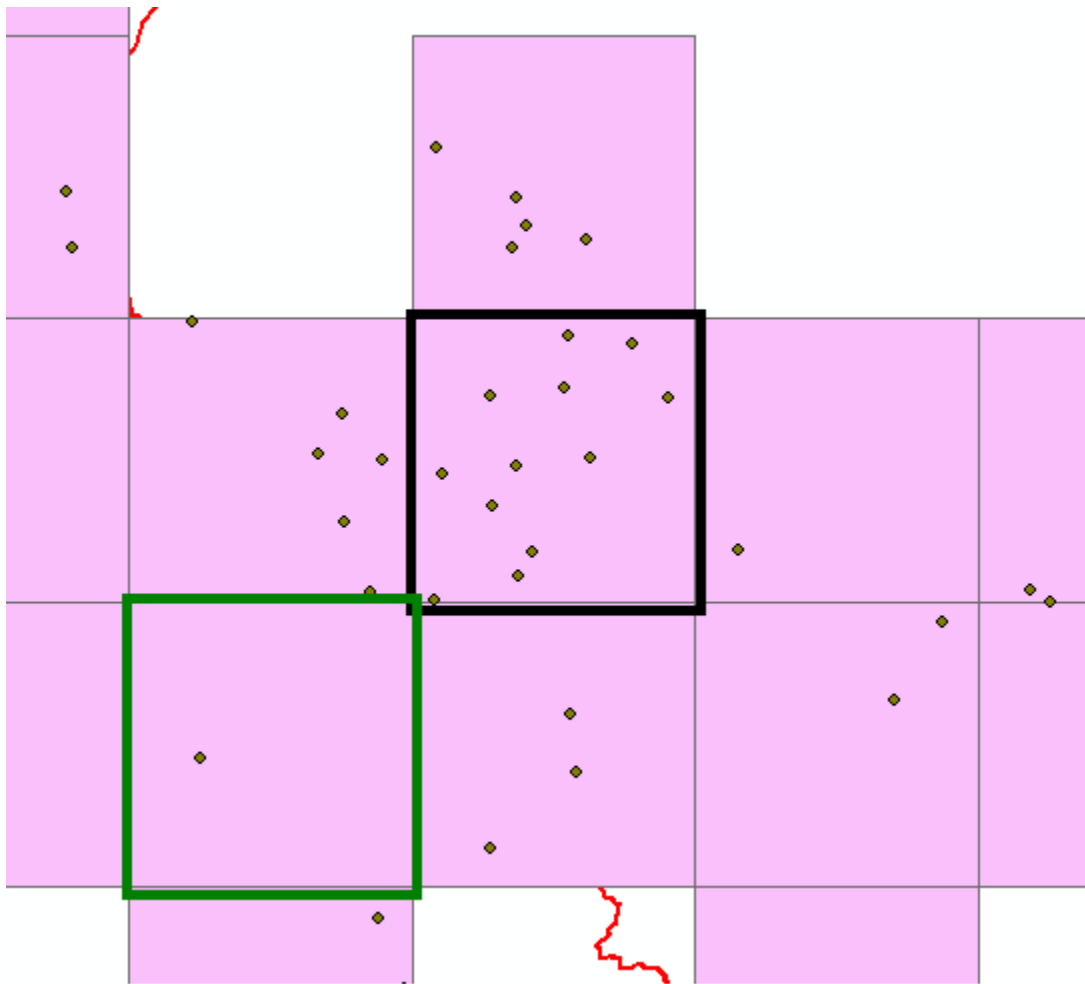


Figure 3-2 Pixel (202,263) in black box contains 12 stations and Pixel (201,264) in green box contains 1 station

Numerical measures of agreement

In general, the ground stations report SD once a month – at best, twice a month. Because they are collected in situ, according to a standard protocol, they can be assumed very accurate at a point scale. The SSM/I SD estimates are provided every 5 days; they

represent an estimated value over a 25x25 km area. Temporal variability in the SSM/I SD can be observed in Figure 3-3 and Figure 3-4.

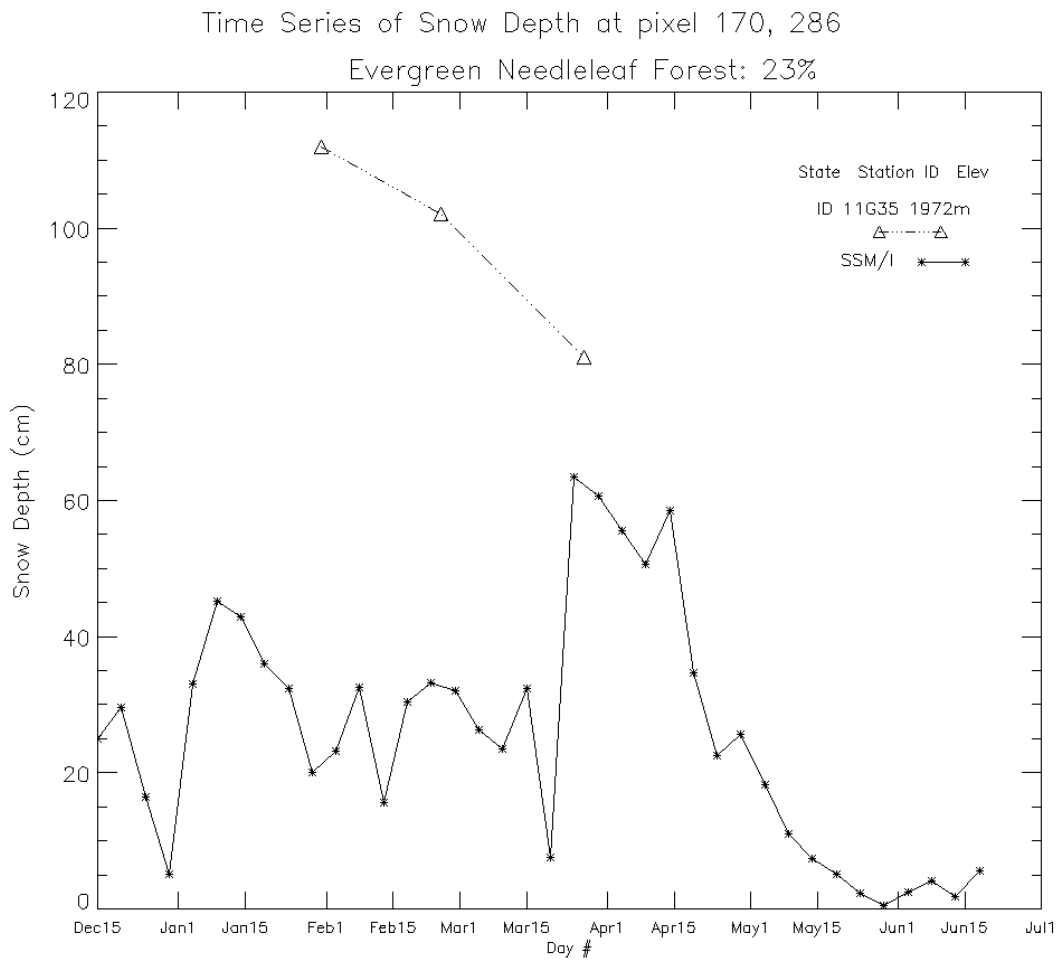


Figure 3-3 Time Series of ground station and SSM/I Snow depth, pixel (170, 286)

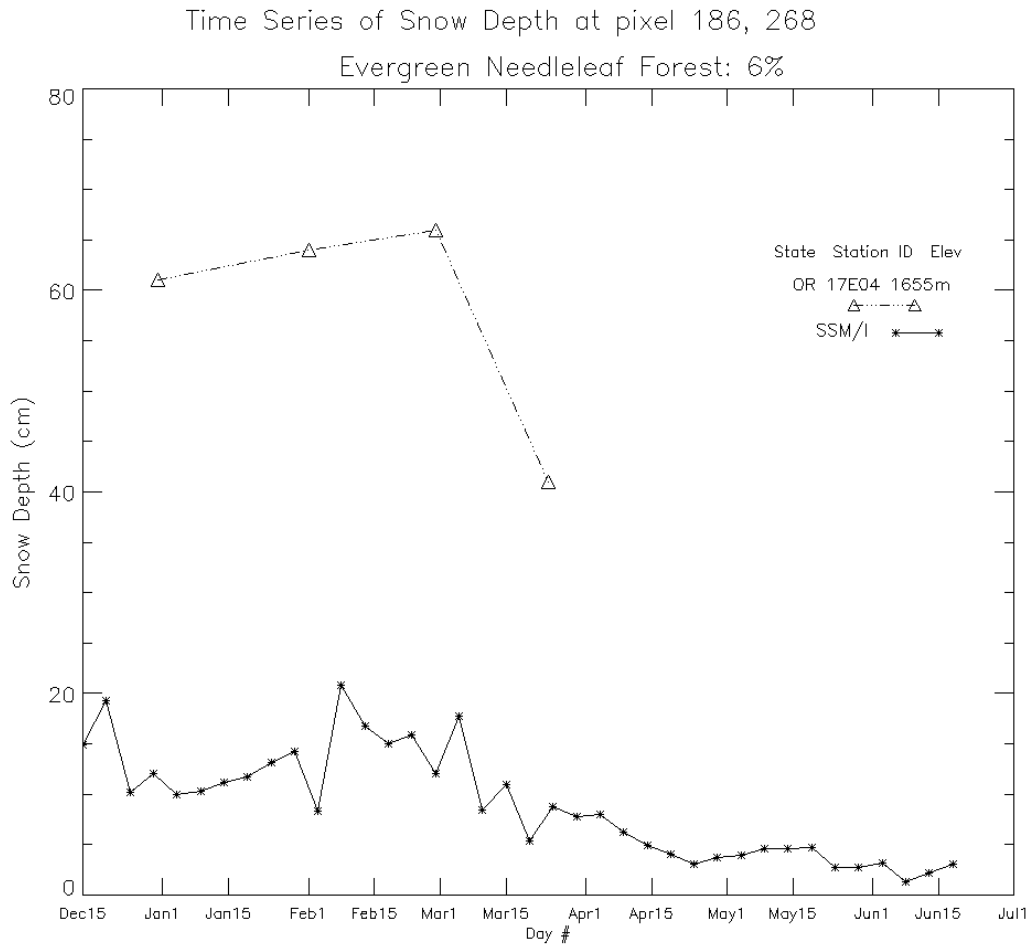


Figure 3-4 Time Series of ground station and SSM/I Snow depth, pixel (186, 268)

In this analysis, the 4 or 5 pentad values surrounding the surface measurement date were treated as a sample from which the mean value of SSM/I on the surface observation date was estimated. If ground measurement day falls on the center day of a pentad, i , then

$$SD_SSMI(\text{day } i) = \text{Sum}_{j=i-2 \text{ to } i+2} [SD_SSMI(j)]/5 \quad 3-4$$

Otherwise, i is set equal to the first pentad center before the ground measurement day, and

$$SD_SSMI(\text{day } i) = \text{Sum}_{j=i-1 \text{ to } i+2} [SD_SSMI(j)]/4 \quad 3-5$$

In other words, 2 pentad values are taken each from 10 days before and 10 days after the measurement date. If the measurement date is the center of a pentad, this date is the 5th pentad value.

A confidence interval (CI) can also be calculated for the mean SD_SSM/I using the t-distribution,

$$CI = t_{\alpha} * StdDev(SD_SSMI) / \text{sqrt}(n) \quad 3-6$$

where StdDev is the standard deviation of the 4 or 5 SSM/I SD measurements flanking the ground measurement, n equals either 4 or 5, and t_alpha is the value of the t statistic corresponding to n-1 degrees of freedom and a selected level of significance (alpha) . A 95% confidence interval was applied (alpha = 0.05). Confidence intervals were calculated in an MS Excel spreadsheet using the “CONFIDENCE” function. If the confidence interval contains the ground measurement value on that date, then the SSM/I estimate is said to agree with that ground measurement on that date. For each pixel, the number of agreements is tallied.

Comparing NOHRSC Snow Water Equivalent to SSM/I Snow depth

Obtaining SWE Data and Mapping in EASE-GRID

SWE data from January 1997 to June 1997 were obtained from a CD distributed by the National Operational Hydrologic Remote Sensing Center (NOHRSC, 1997). The values are provided on a 1km resolution grid in geographic coordinates. The gridded data were reprojected and resampled to the 25-km resolution EASE-GRID.

Using IDL, time-series graphs were plotted showing NOHRSC SWE and SSM/I SD for each pixel location. Examples are shown in Figure 3-5 and Figure 3-6.

Time Series of Snow Depth & SWE at pixel 177, 269

Evergreen Needleleaf Forest: 0%

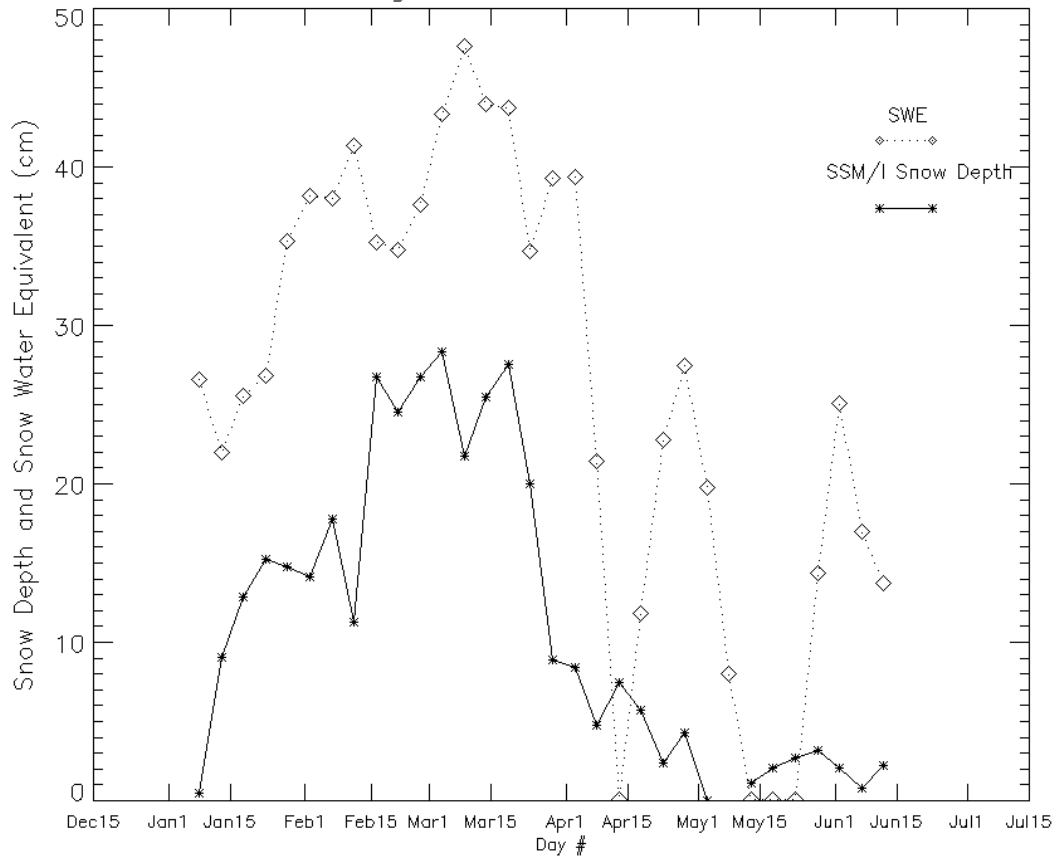


Figure 3-5 Time series of SSM/I Snow Depth and NOHRSC Snow Water Equivalent, pixel (177, 269)

Time Series of Snow Depth & SWE at pixel 177, 284

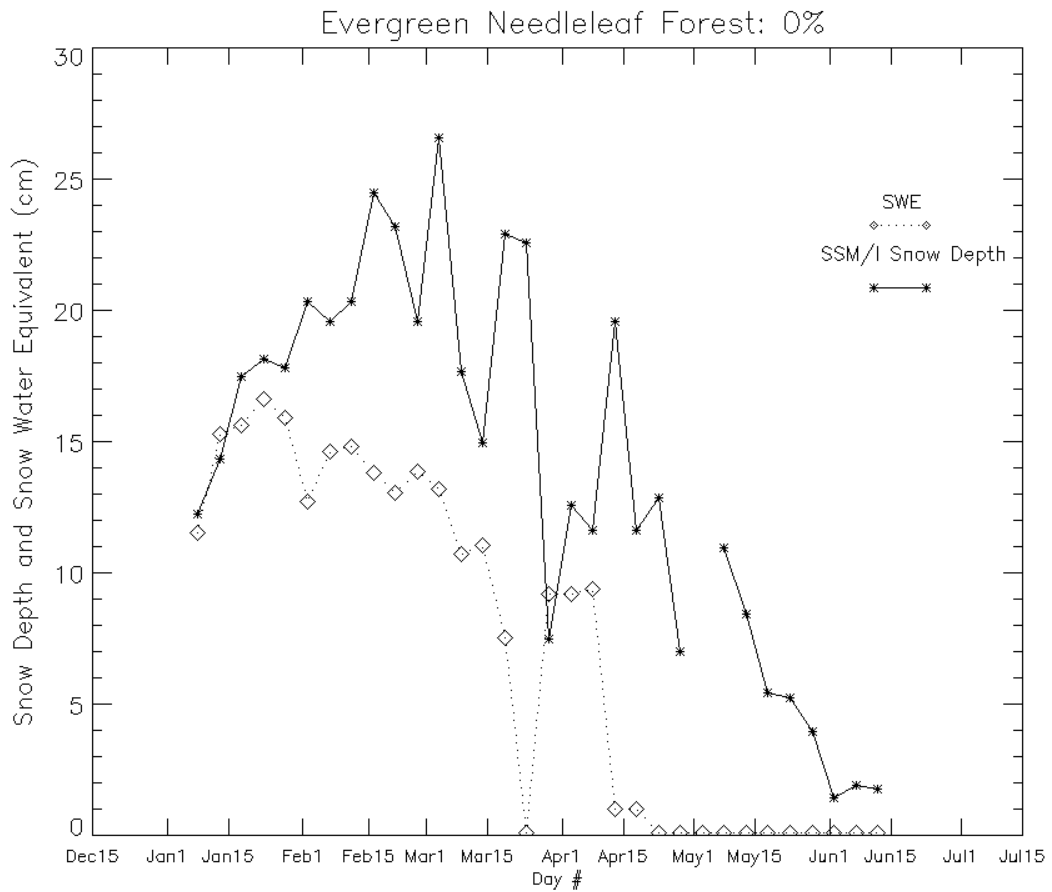


Figure 3-6 Time Series of SSM/I Snow Depth and NOHRSC Snow Water Equivalent, Pixel (177,284)

Numerical measures of agreement

Due to the time-varying density of snow, time series of SWE and SD cannot be directly compared. However, they would be expected to follow the same general trend or pattern, and when given in the same units (cm) SWE should be less than SD, with the ratio SWE/SD lying in the range of expected values for relative density of snow, 0.01 to 0.4. Two overall measures were selected as measures of agreement between the two time

series: correlation as a measure of similar pattern, and a bulk relative density indicating the general relationship between SWE values and SD values over the season.

Correlation

For each pixel, correlation coefficient was computed for SWE and SSM/I snow depth, paired by date, and excluding dates on which either measurement was missing. The correlations were calculated in IDL and the resulting values were arranged in grid form for viewing in ARCMAP. A strong positive correlation is interpreted as good agreement. Although a strong negative correlation indicates a linear relationship, in this case, it does not indicate good agreement. Pixels with at least 0.7 correlation are considered to be good agreement in terms of pattern. For the examples shown in Figure 3-7 and Figure 3-8, the correlation coefficients are -0.72481, and 0.865425, respectively.

Time Series of Snow Depth & SWE at pixel 200, 286

Evergreen Needleleaf Forest: 72%

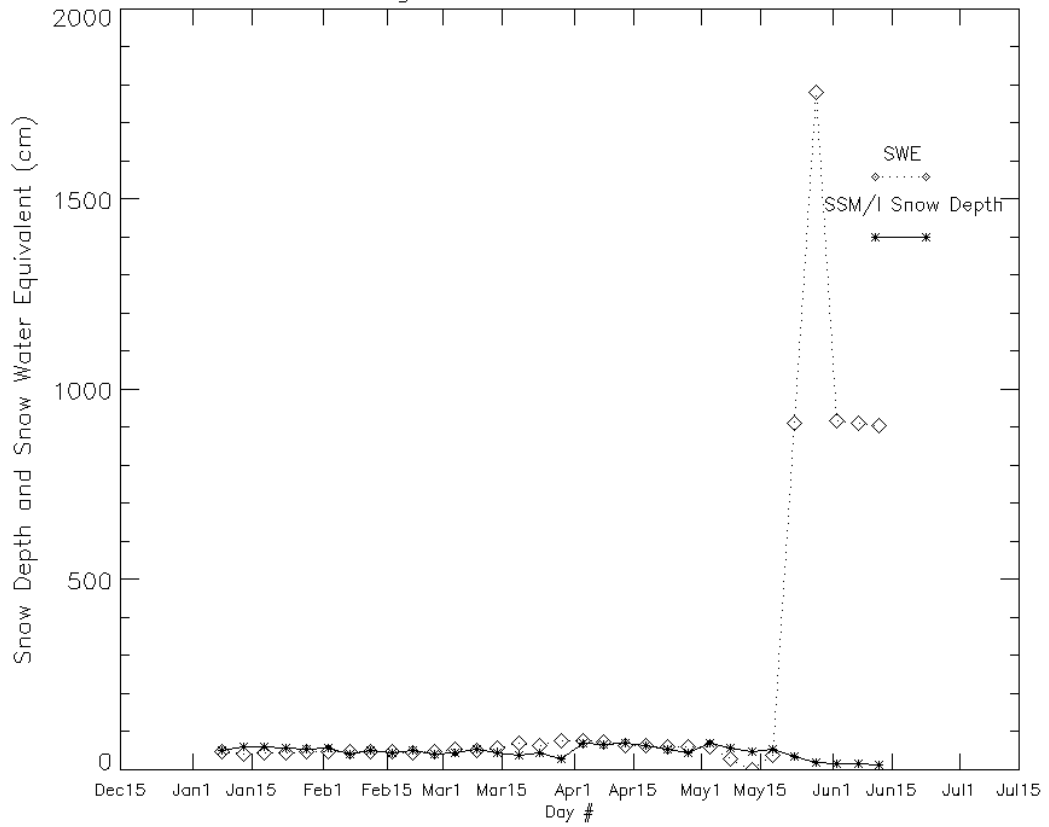


Figure 3-7 For pixel (200,286), the correlation between SSM/I Snow Depth and NOHRSC SWE is **-0.72481**.

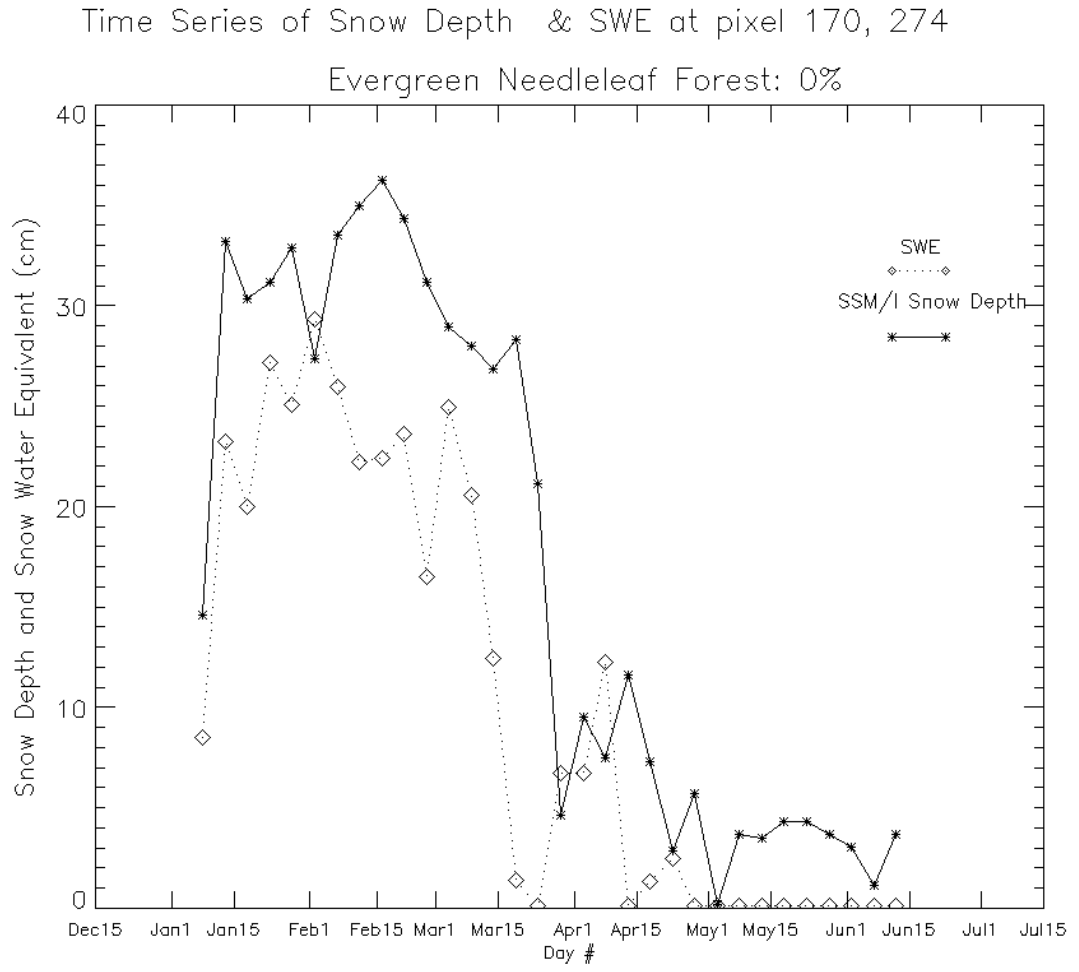


Figure 3-8 For pixel (170,274), the correlation between SSM/I Snow Depth and NOHRSC SWE is 0.865425

Relative Density

Relative density was computed for each pixel by dividing the average of SWE over the measurement period by the average of snow depth over the period. Relative density of up to 0.3 is considered to be good agreement in terms of magnitude. For the examples shown in Figure 3-9 and Figure 3-10 the relative density values are 0.289429 and 0.297567 respectively. Relative density was calculated in IDL and output in gridded form for viewing in ArcMAP.

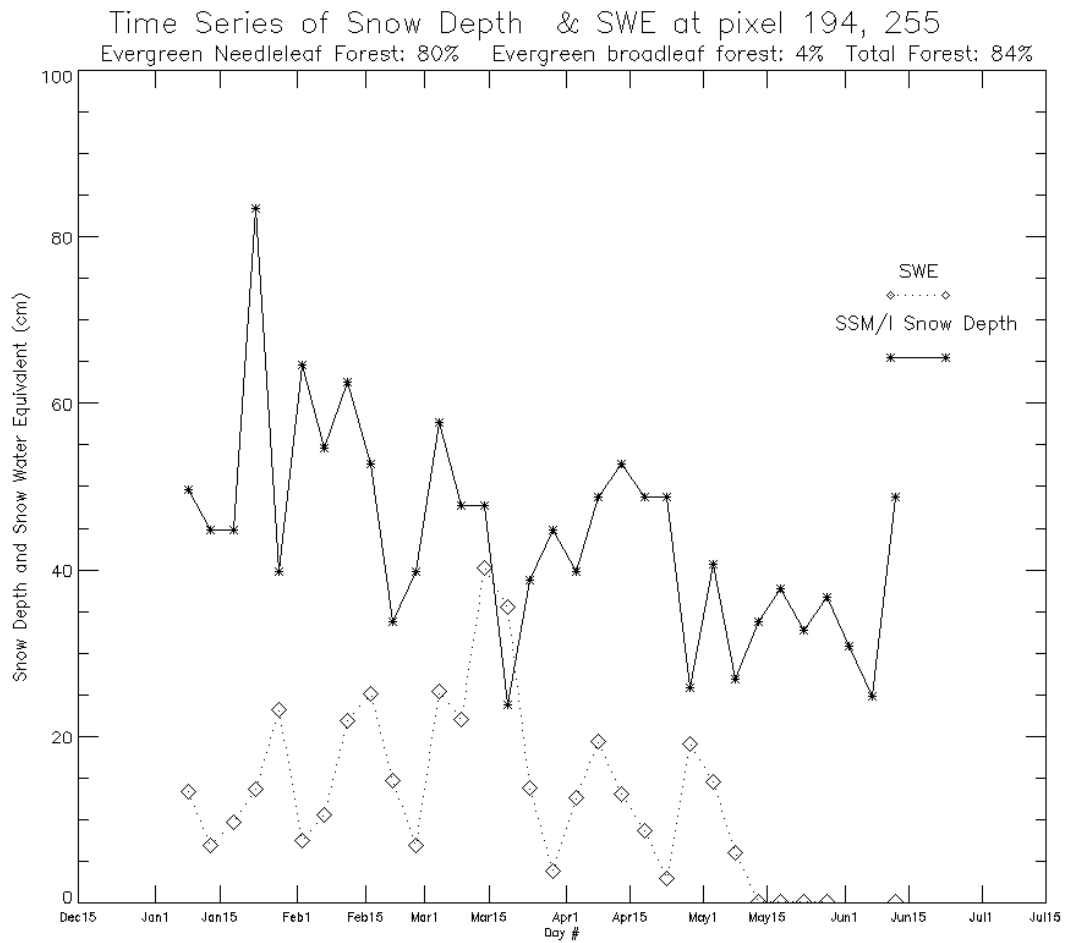


Figure 3-9 For the pixel (194,255) the relative density (NOHRSC SWE / SSM/I Snow Depth) is 0.289429

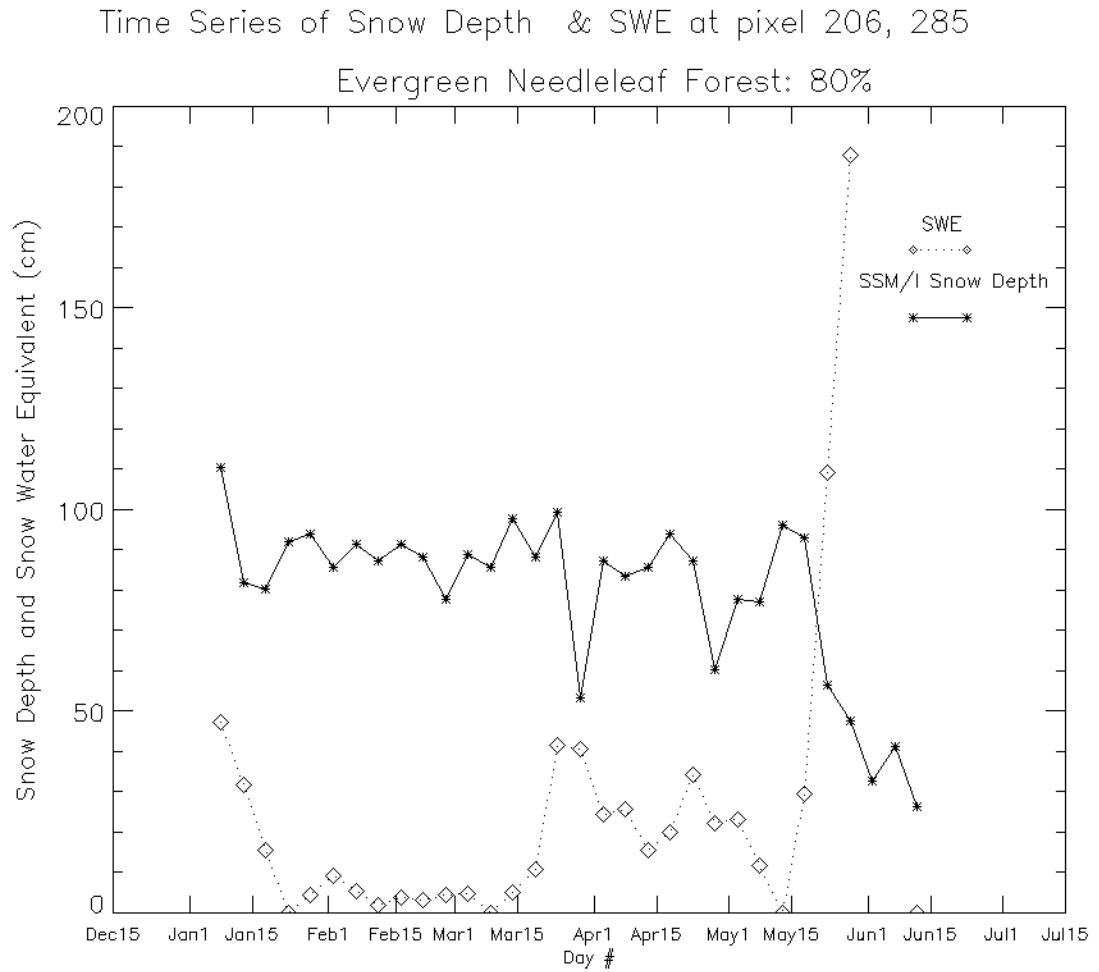


Figure 3-10 For pixel (206,285) the relative density (NOHRSC SWE / SSM/I Snow Depth) is 0.297567

Overall, SSM/I SWE is said to agree with NOHRSC SWE if agreement is found by both measures: strong positive correlation, and a physically reasonable relative density.

Examples of good agreement by these measures are shown in Figure 3-11 and Figure 3-12.

Time Series of Snow Depth & SWE at pixel 203, 275
 Evergreen Needleleaf Forest: 84%

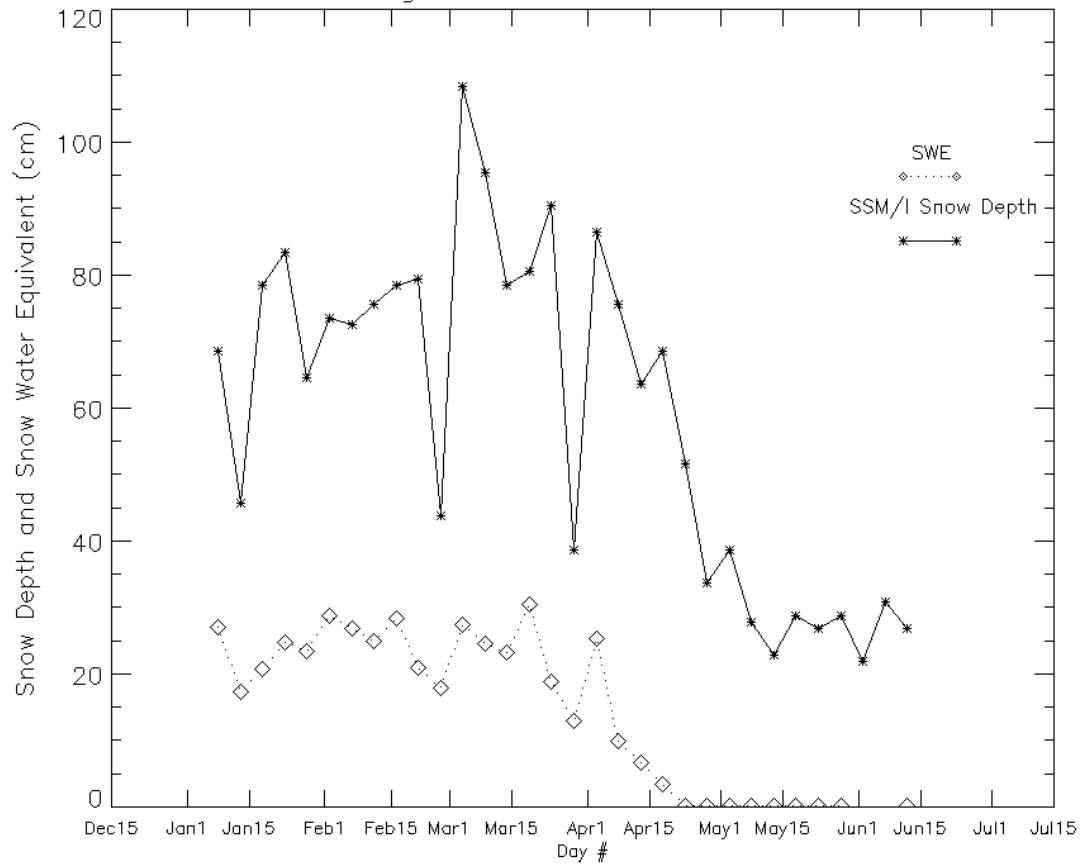


Figure 3-11 SSM/I Snow Depth and NOHRSC SWE for pixel (203,275), one of the best agreements with correlation of 0.813344 and relative density of 0.242506.

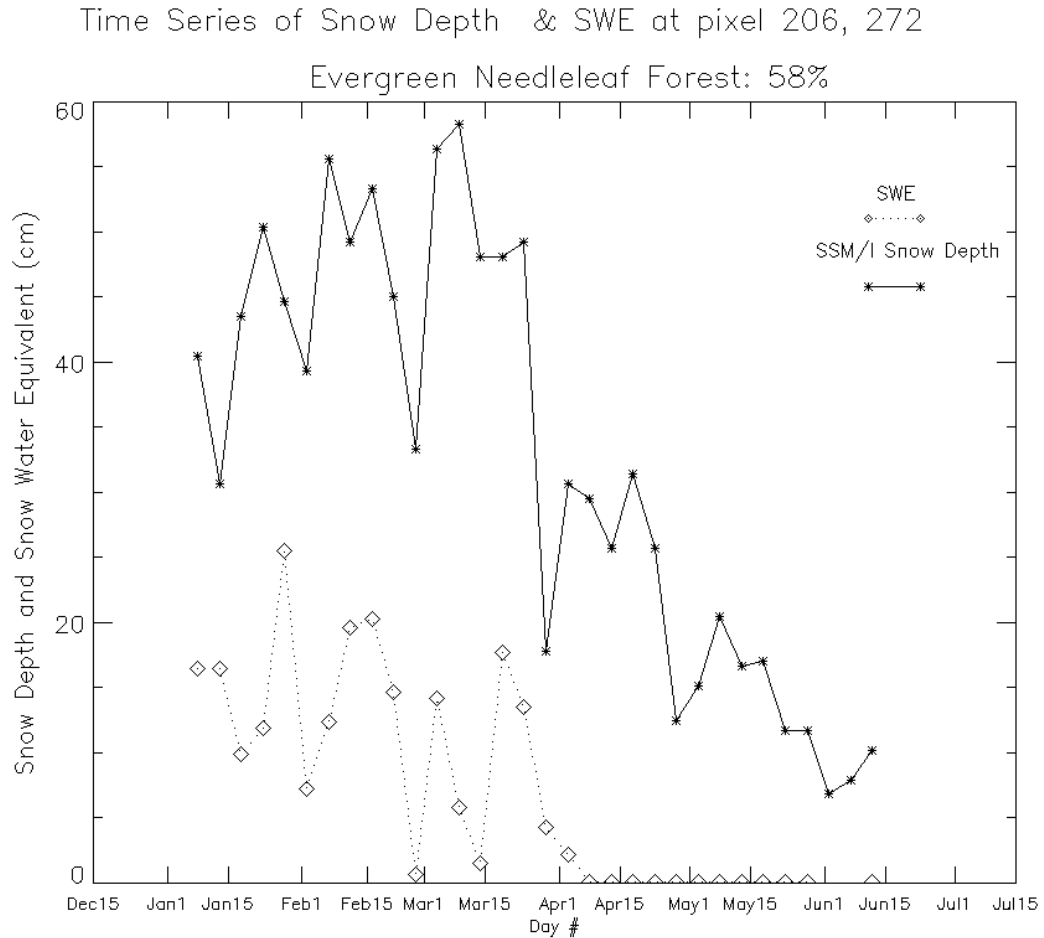


Figure 3-12 SSM/I Snow Depth and NOHRSC SWE for pixel (206,272), one of the best agreements with correlation of 0.718215 and relative density of 0.210978.

Analyzing agreement

For each EASE-Grid pixel analyzed, the following quantities were arranged in grid form and viewed in ArcMap:

- Ground – SSM/I SD number of agreements and agreement fraction
- SSM/I SD – NOHRSC SWE Correlation
- SSM/I SD – NOHRSC SWE Relative Density

Using ArcMap tools, these results were stratified into agreement scores using the following rules.

For Ground/SSM/I SD, pixels were identified as either “having at least one agreement” (score 1) or “no agreement” (score 0). Given the differences in the number of stations and station-date pairs in the pixels, this was selected as the simplest overall treatment.

For SSM/I SD – NOHRSC SWE Correlation, scores were assigned from poor to excellent, as follows

correlation - 0.725 – - 0.3	score 1
correlation - 0.3 – 0.3	score 2
correlation 0.3 – 0.5	score 3
correlation 0.5 – 0.7	score 4
correlation > 0.7	score 5

For SSM/I SD – NOHRSC SWE relative density, scores were assigned from poor to excellent, as follows:

density 0.0005 – 0.005 or > 0.8	score 1
density 0.005 – 0.007	score 2
density 0.007 – 0.3	score 3
density 0.3 – 0.4	score 5
density 0.4 – 0-0.8	score 4

A total SSM/I SD – NOHRSC SWE score was calculated by multiplying the correlation score and the relative density score. Total scores could range from 1 to 25. The total scores were stratified to 5 levels: 1-5, 6-8, 9-12, 15-16, and 20-25.

Categories of Landscape Properties

The SRTM elevation data are given at 100-m resolution. ArcMap's Zonal Statistics tool was used to find the mean and standard deviation of elevation in each 25x25km EASE-Grid pixel, in the Columbia Basin for the SSM/I – NOHRSC comparison, and in the Ground Station pixels for the Ground – SSM/I comparison. Standard deviation of elevation is an estimate of terrain complexity in the pixel. For each data set, mean elevation and standard deviation were split into five categories by equal area (quantiles). The EASE-Grid evergreen canopy cover was also split into five categories for each data set.

Tabulating Agreement and Landscape Properties

ArcMap tools were used to tabulate the number of pixels in the analysis (the Columbia Basin domain for SSM/I – NOHRSC and the Ground station pixels for Stations – SSM/I) corresponding to each agreement score – landscape category combination. These tables and their 3-D column graph equivalents reveal any association between agreement and the landscape characteristics mean elevation, terrain complexity, and canopy cover. Six tables were produced, three for each analysis.

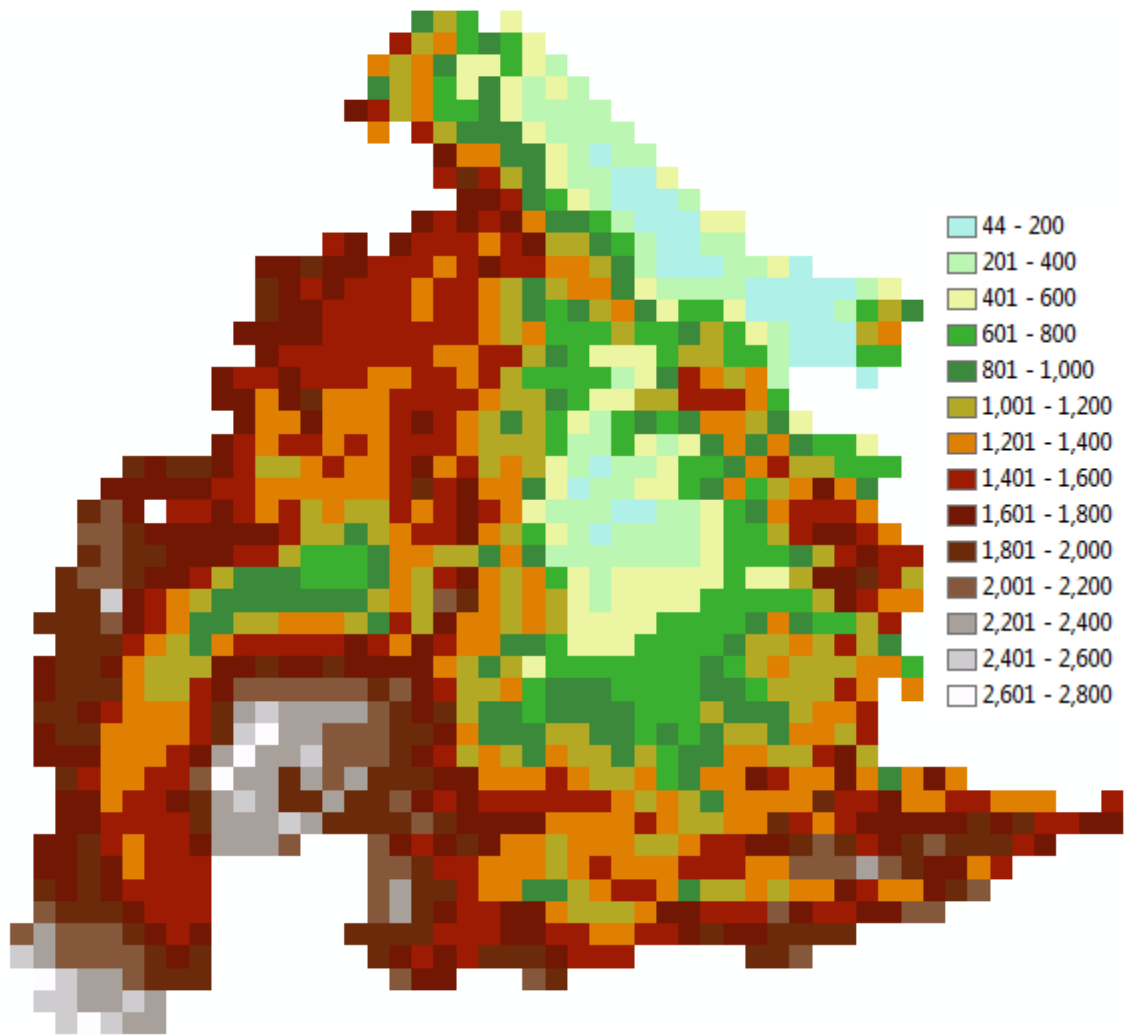


Figure 3-13 SRTM Elevation [m above sea level] averaged to 25-km EASE-Grid pixels, Columbia Basin.

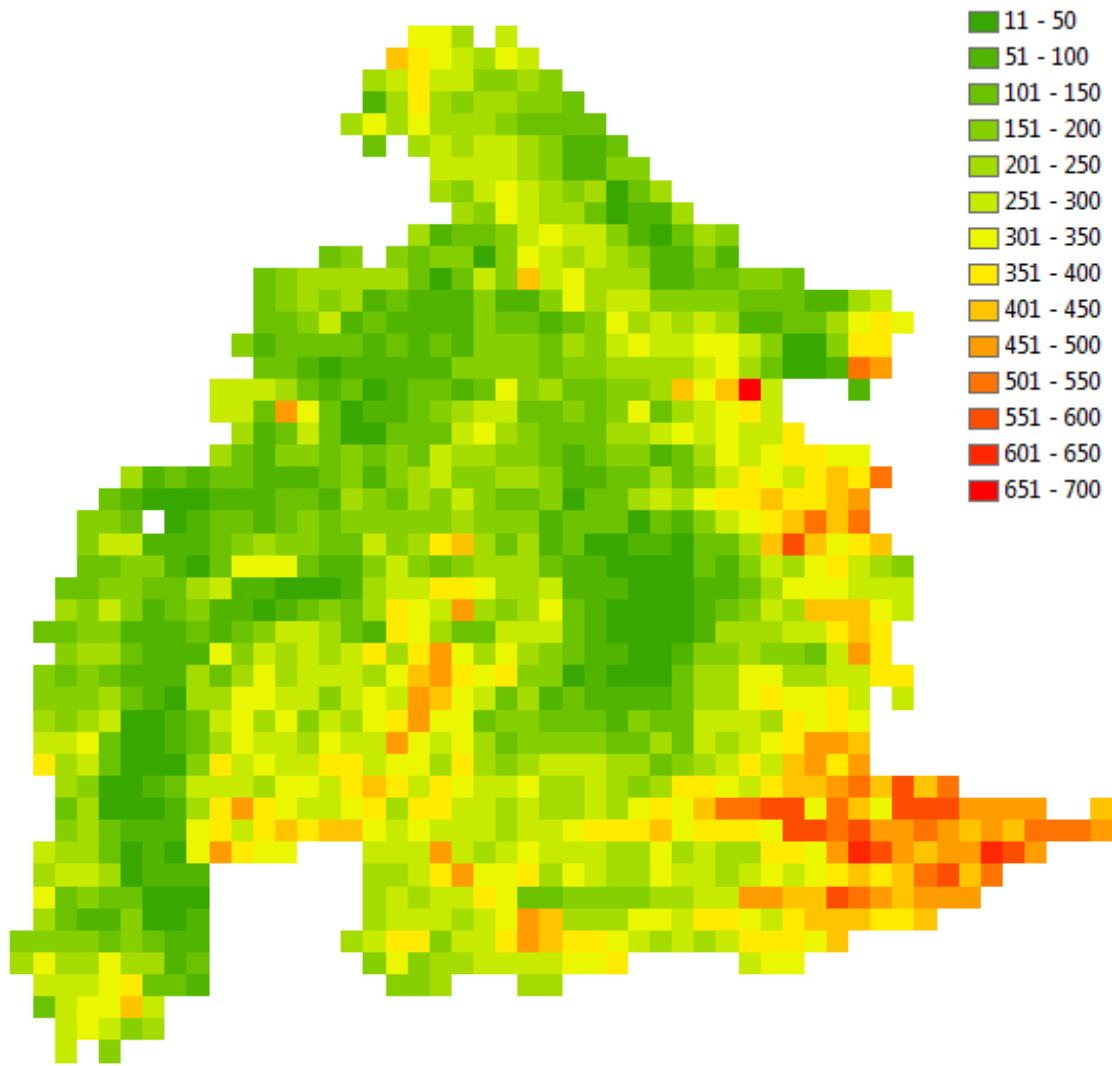


Figure 3-14 SRTM Elevation Standard Deviation [m] in EASE-Grid pixels, Columbia Basin.

Chapter 4 Results

Graphically Comparing SSM/I to Surface Snow Depth

307 graphs of time series of snow depths were generated and visually inspected. The majority showed a similar trend: ground station snow depths were much greater than SSM/I snow depths. Figure 4-1 to Figure 4-4 show the best locations and Figure 4.5 to Figure 4-10 the worst locations, by inspection. Among the worst locations, the greater the elevation, the greater the manually measured snow depth, and the greater the discrepancy between SSM/I and manual measurement.

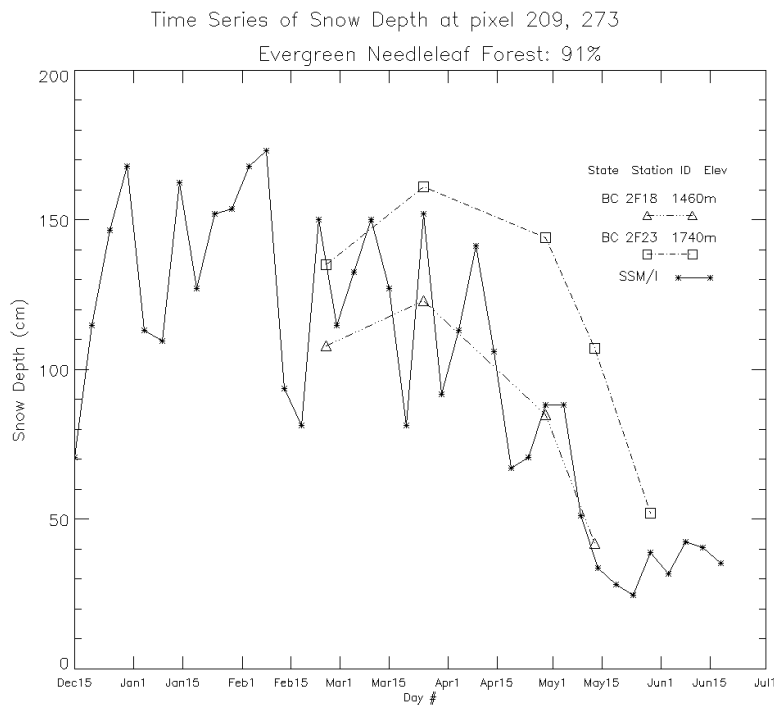


Figure 4-1 SSM/I Snow depth in pixel (209, 273) and manually measured snow depth at the station in the pixel. This is one of the best pixels observed with 4 agreements.

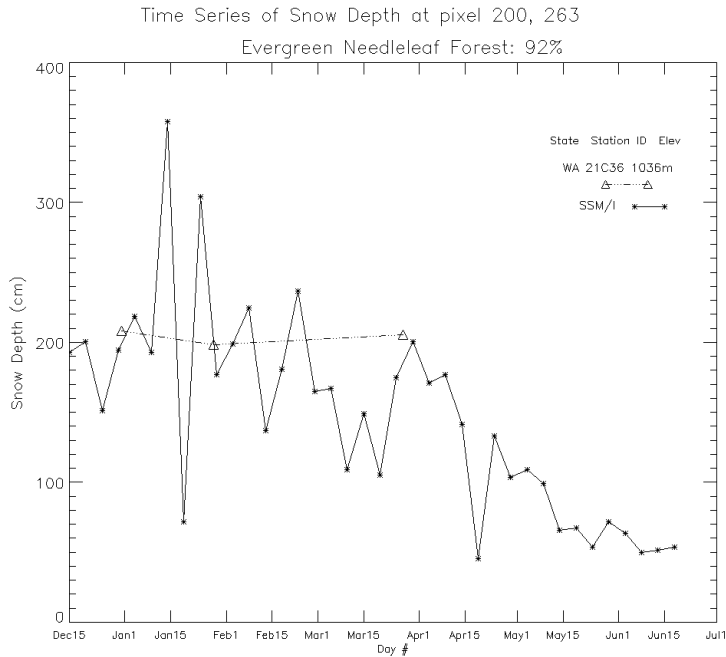


Figure 4-2 SSM/I Snow depth in pixel (200, 263) and manually measured snow depth at the station in the pixel. This is one of the best with two agreements observed.

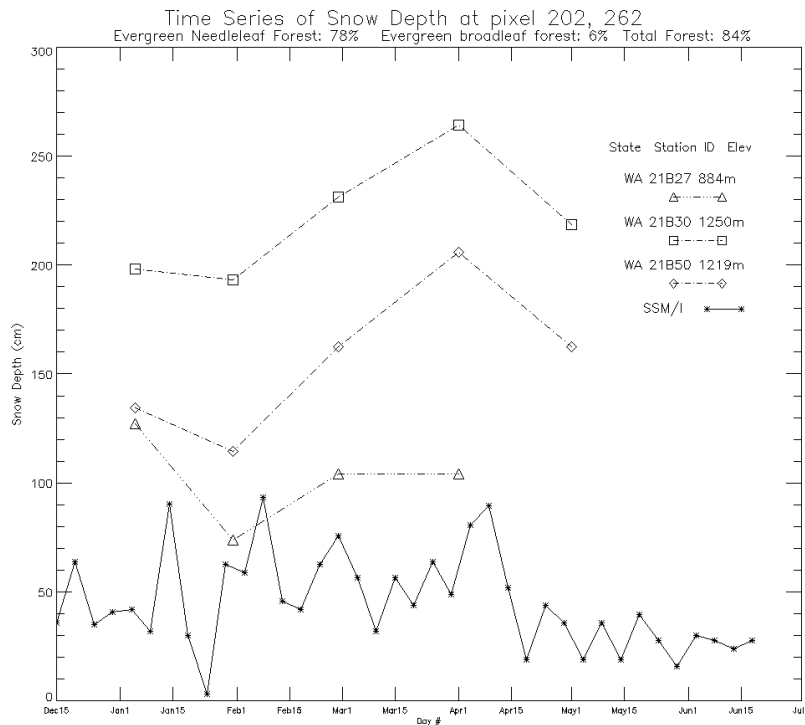


Figure 4-3 SSM/I Snow depth in pixel (202, 262) and manually measured snow depth at three stations in the pixel. Agreement is good for one station, but not for the other stations at higher elevation

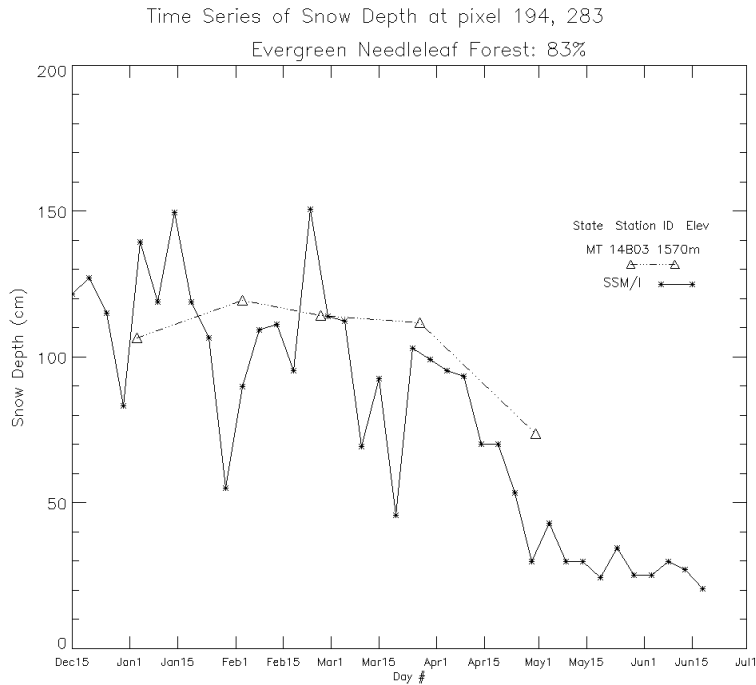


Figure 4-4 SSM/I Snow depth in pixel (204,270) and manually measured snow depth at the station in the pixel. This is one of the best agreements observed with three agreements.

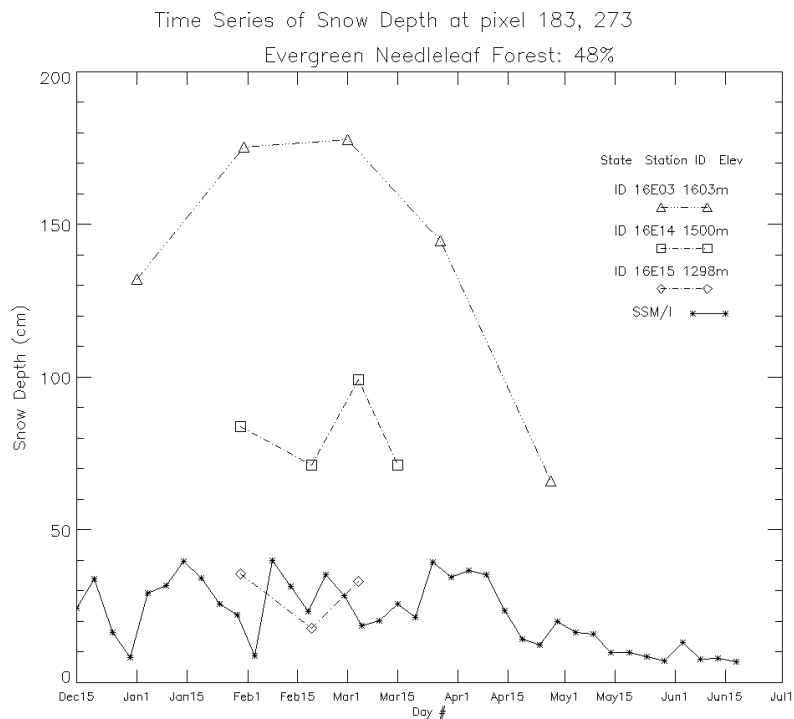


Figure 4-5 SSM/I Snow depth in pixel (183, 273) and manually measured snow depth at three stations in the pixel. This is considered poor agreement. The increase of snow depth with elevation is evident in the station data.

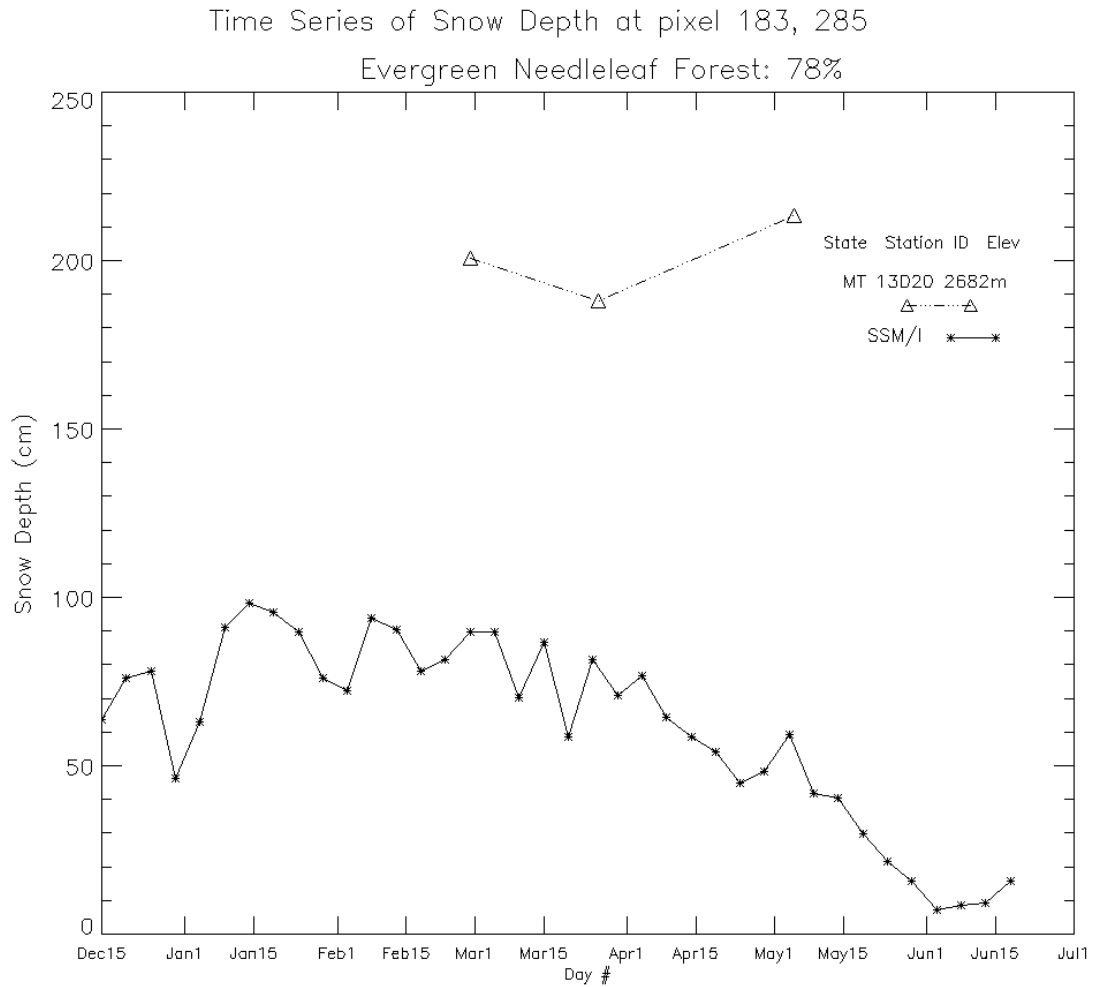


Figure 4-6 SSM/I Snow depth in pixel (183, 285) and manually measured snow depth at the station in the pixel. This is considered poor agreement.

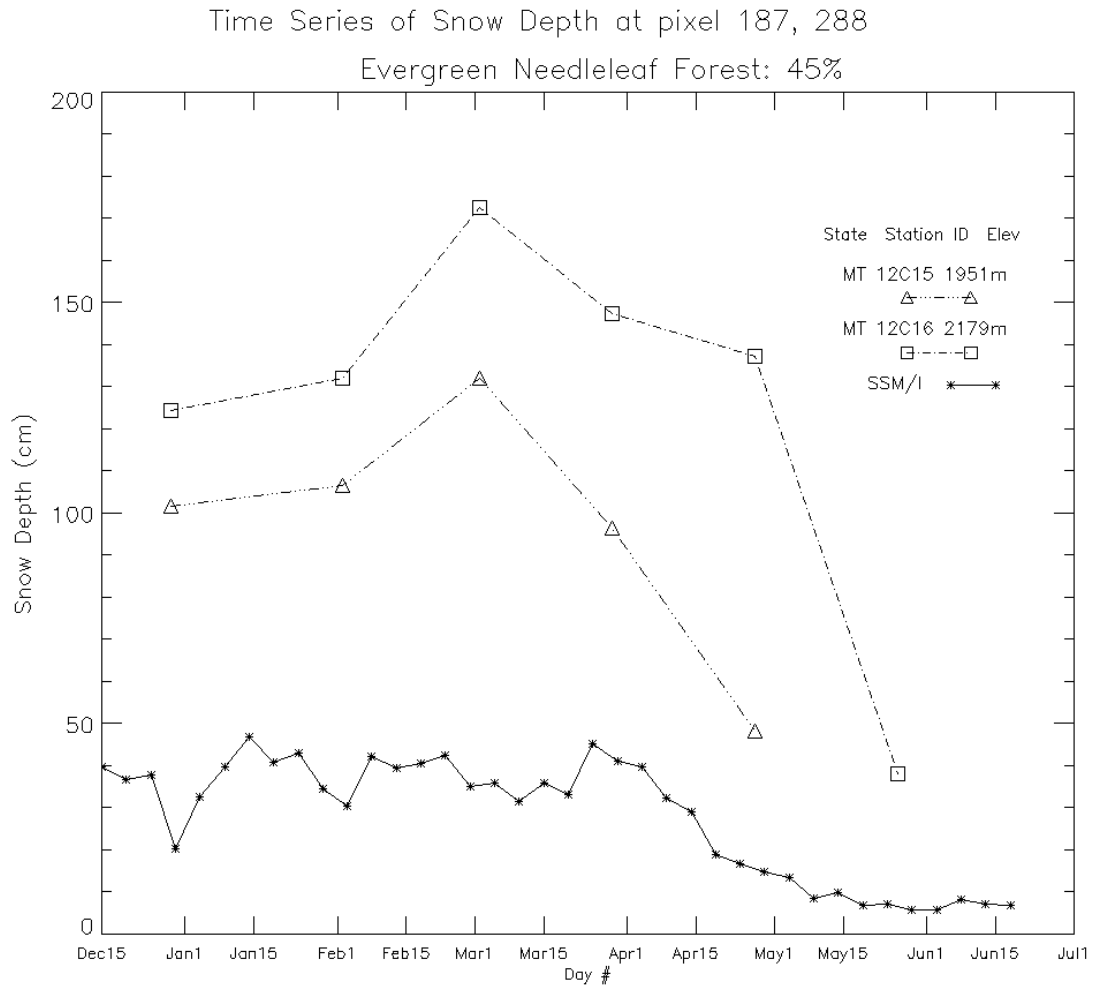


Figure 4-7 SSM/I Snow depth in pixel (187, 288) and manually measured snow depth at two stations in the pixel. This is considered poor agreement. The increase of snow depth with elevation is evident in the station data. At these high elevations, the canopy cover correction does not make up the difference between SSM/I and station SD.

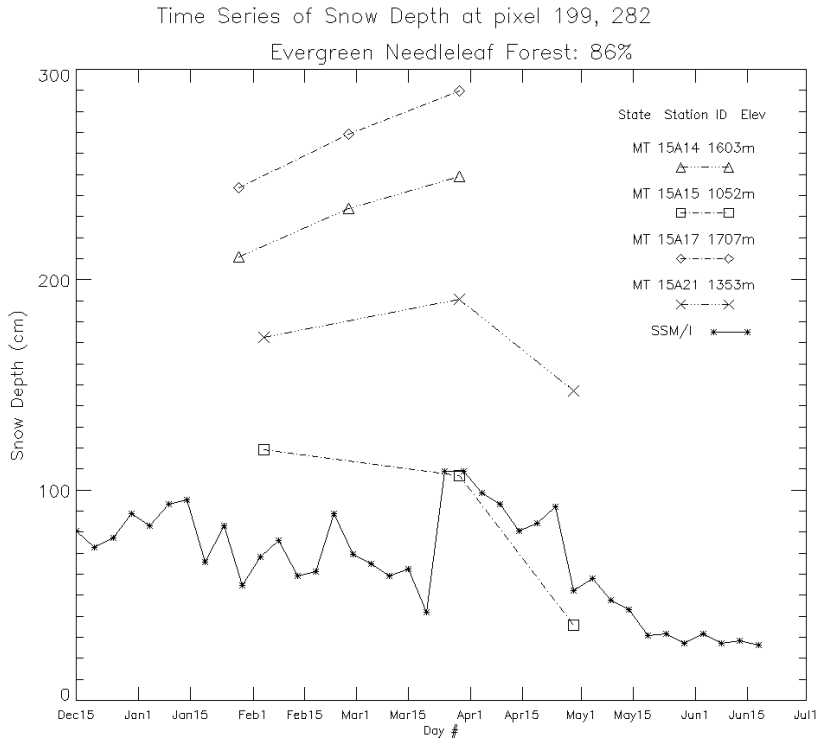


Figure 4-8 SSM/I Snow depth in pixel (199, 282) and manually measured snow depth at four stations in the pixel. The SSM/I estimates agree somewhat with the lowest elevation station, but not with the increased snow depth at higher elevation.

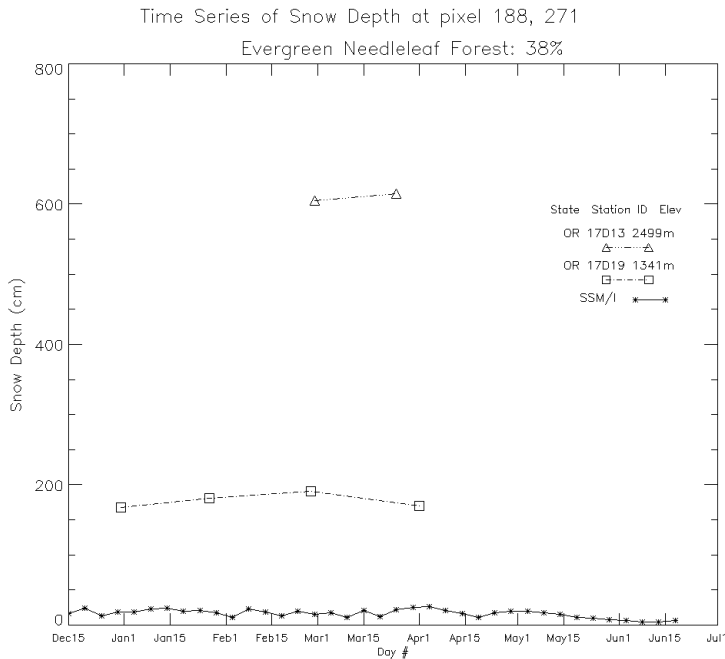


Figure 4-9 SSM/I Snow depth in pixel (188, 271) and manually measured snow depth at two stations in the pixel. This is considered very poor agreement. The increase of snow depth with elevation is evident in the station data.

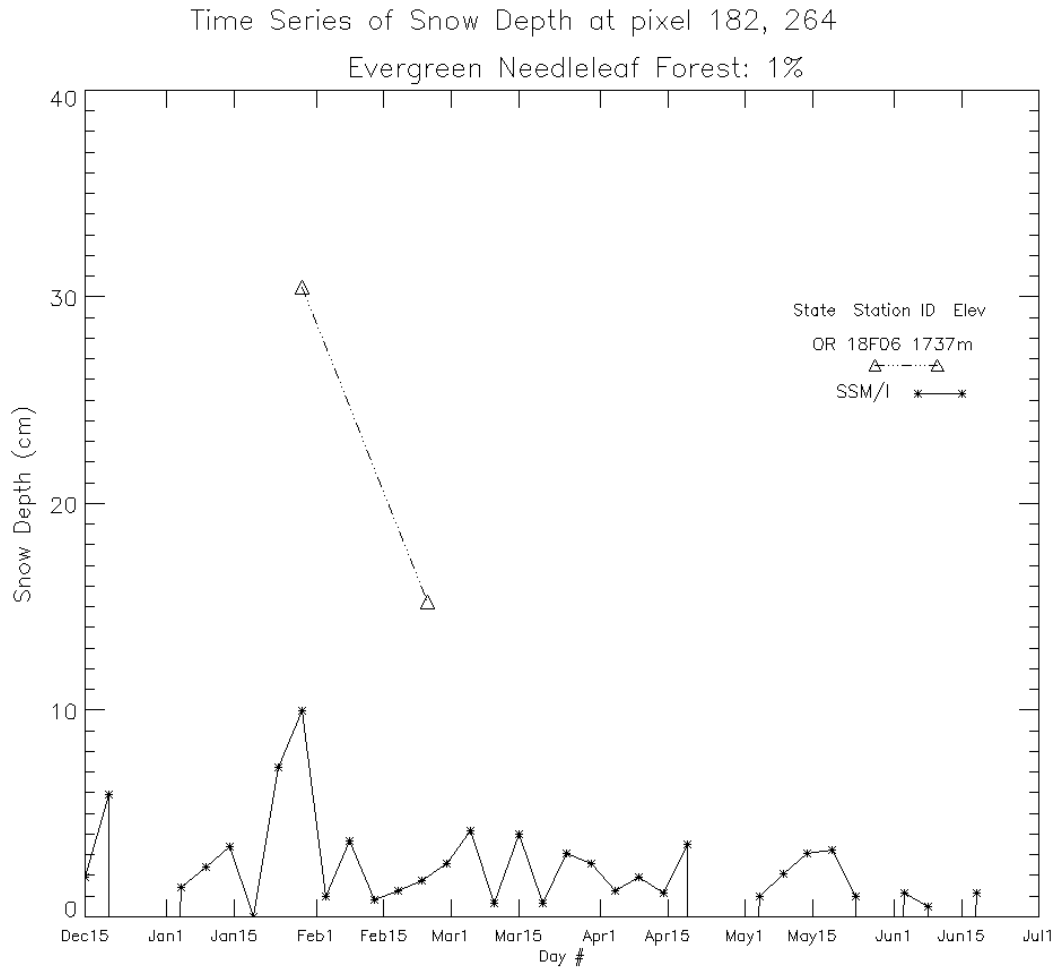


Figure 4-10 SSM/I Snow depth in pixel (182, 264) and manually measured snow depth at the station in the pixel. This is considered poor agreement; however, at this low elevation, less difference is observed between ground station and SSM/I snow depth

Comparing Station Measurements to Time-Averaged SSM/I Snow Depth

Confidence intervals on the mean of 4-5 pentads of SSM/I snow depth were calculated for each available ground station measurement. All results are graphed in Figure 4-11

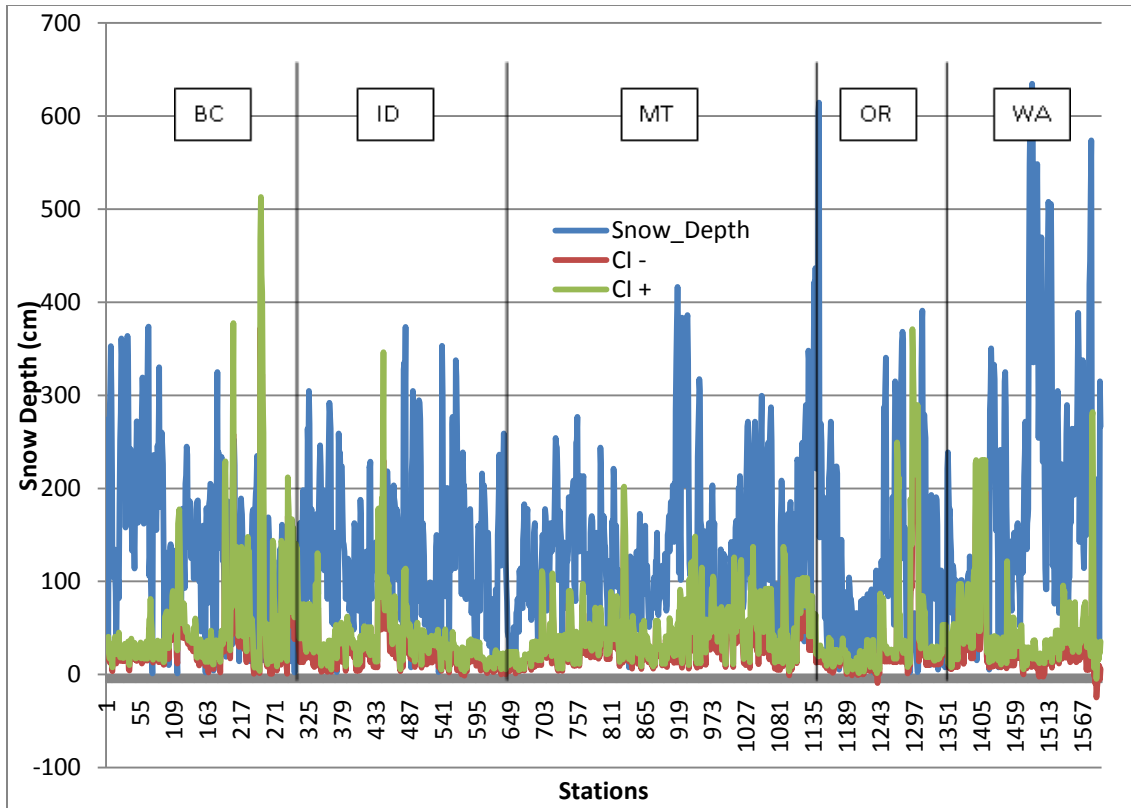


Figure 4-11 Station snow depth measurements with lower and upper bounds of 95% confidence interval (CI) for time-averaged SSM/I (4 or 5 pentads centered on the ground measurement date). All stations are from British Columbia, Montana, Idaho, Oregon and Washington. If ground SD lies within the confidence interval, the two are considered in agreement for that date.

As described in the “Numerical measures of agreement” section of Chapter 3, the numbers of agreements in each pixel were tallied (Figure 4-12). The fraction of agreement (Figure 4-13) is the number of agreement divided by the total number of ground observations in the pixel (Figure 4-14).

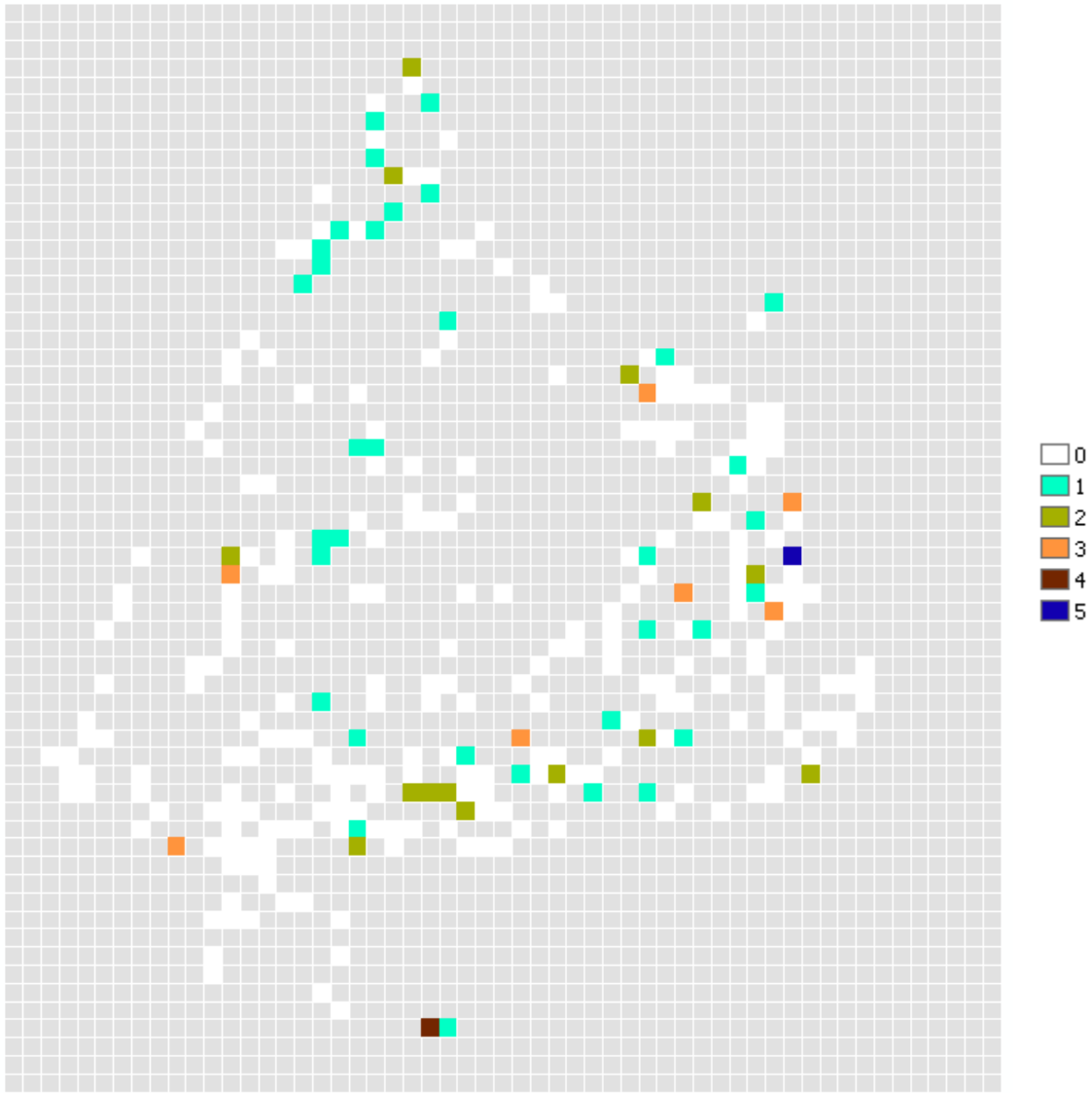


Figure 4-12 Number of agreements per pixel which ground snow depth observations were compared to 95% confidence interval for SSM/I snow depth (4 or 5 pentads centered on the ground measurement date). If ground SD lies within the confidence interval, the two snow depths are considered in agreement for that date

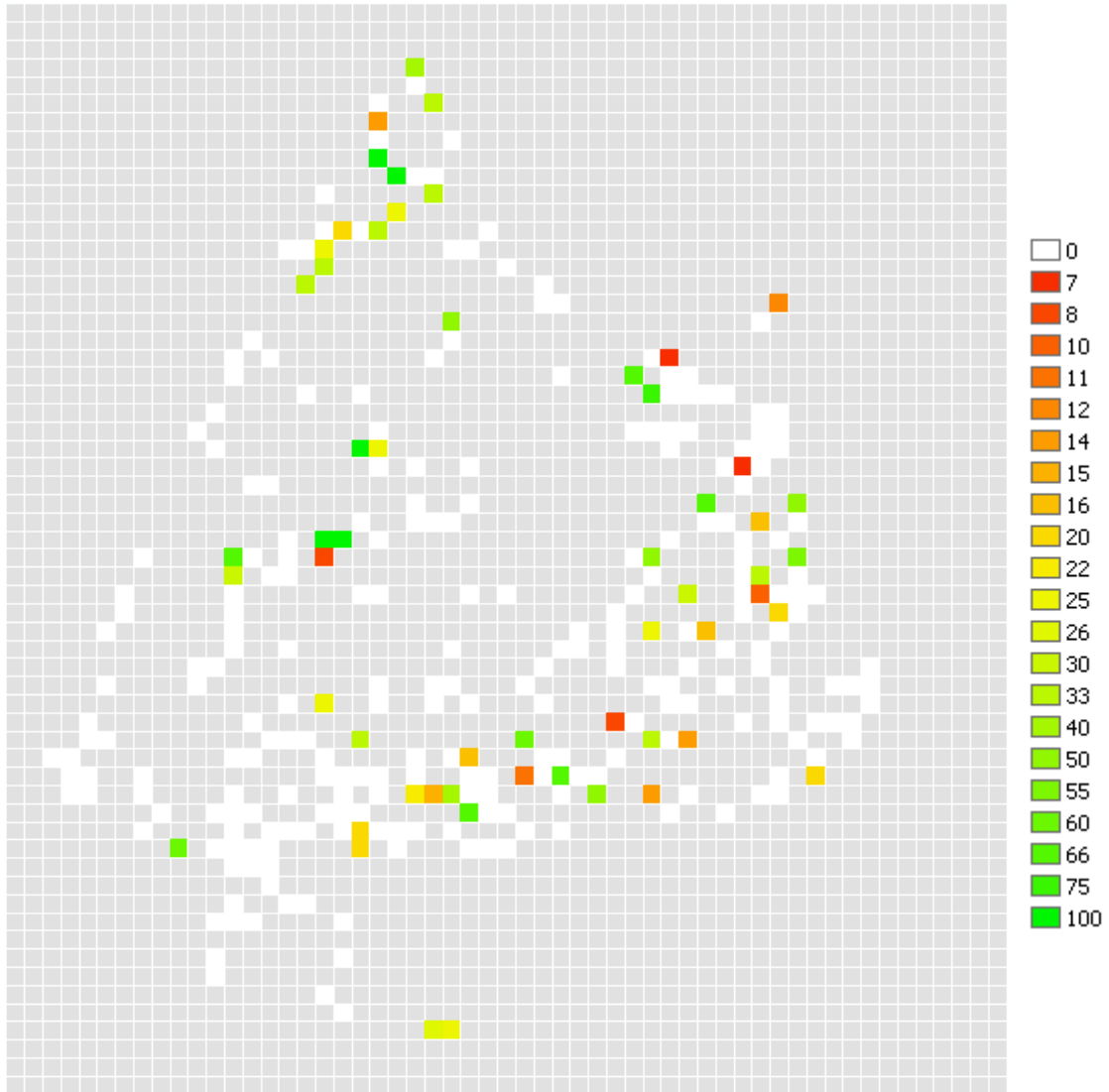


Figure 4-13 Percentage of Agreements per pixel. The fraction of agreement is the number of agreements divided by the total number of ground observations in the pixel

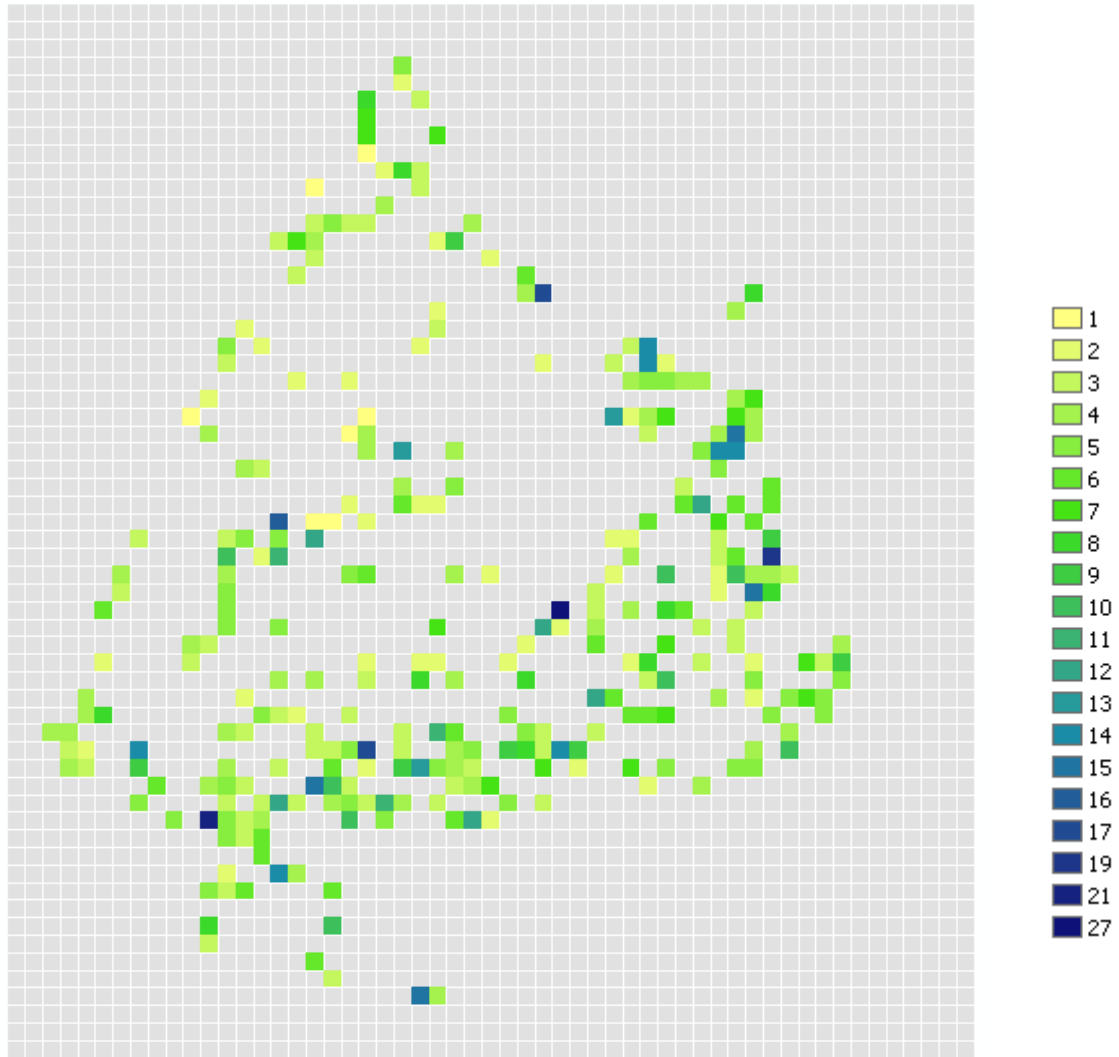


Figure 4-14 Number of ground observations per pixel (station-date pairs). Pixels contain from 1 to 27 ground snow depth observations.

Comparing NOHRSC SWE to SSM/I SD

IDL was used to plot the time series of NOHRSC SWE and SSM/I SD on the same graph by pixel for all pixels in the Columbia Basin study area. This generated over 1300 graphs of non-missing data. The majority of the graphs show poor agreement due to the general underestimation of SSM/I snow depth (SD); this underestimation is quickly apparent on visual examination of the graphs (for example, Figure 4-15); physically, SD must be

greater than SWE. Figure 4-16 is an example of a pixel where the relative density is physically realistic, but the temporal pattern does not match. Figure 4-17 shows both poor correlation and poor relative density.

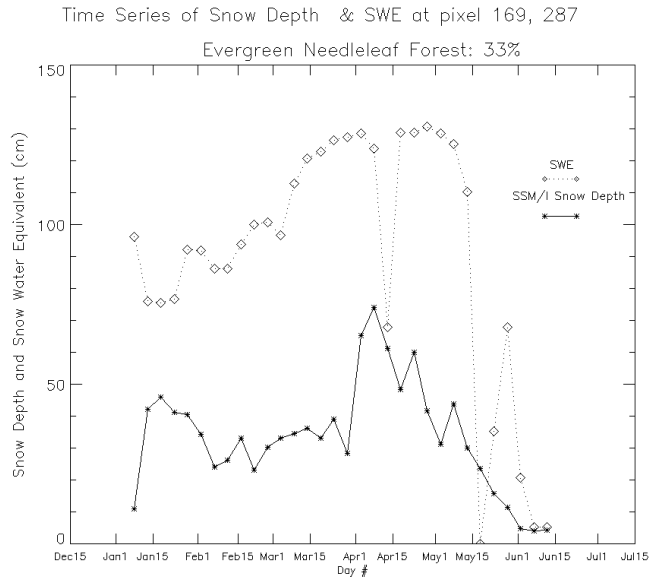


Figure 4-15 SSM/I Snow Depth and NOHRSC Snow Water Equivalent for pixel (169, 287). Although the time series show some similarity in pattern, the magnitudes are wrong; SD must be greater than SWE.

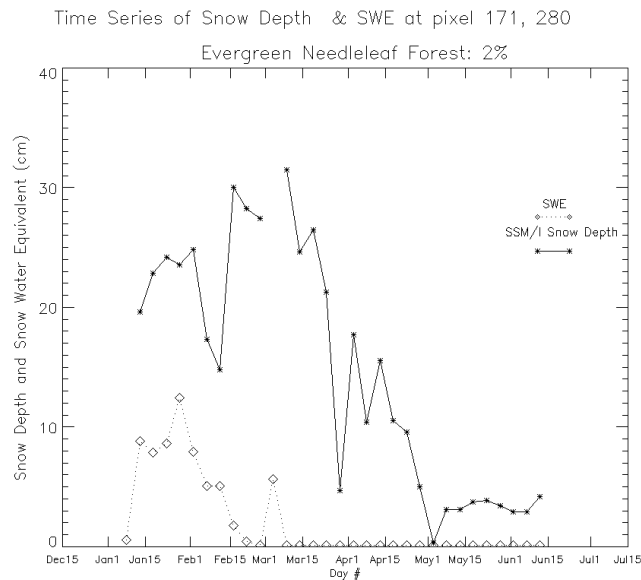


Figure 4-16 SSM/I Snow Depth and NOHRSC Snow Water Equivalent for pixel (171, 280). Good relative density but poor pattern consistency

Time Series of Snow Depth & SWE at pixel 196, 287

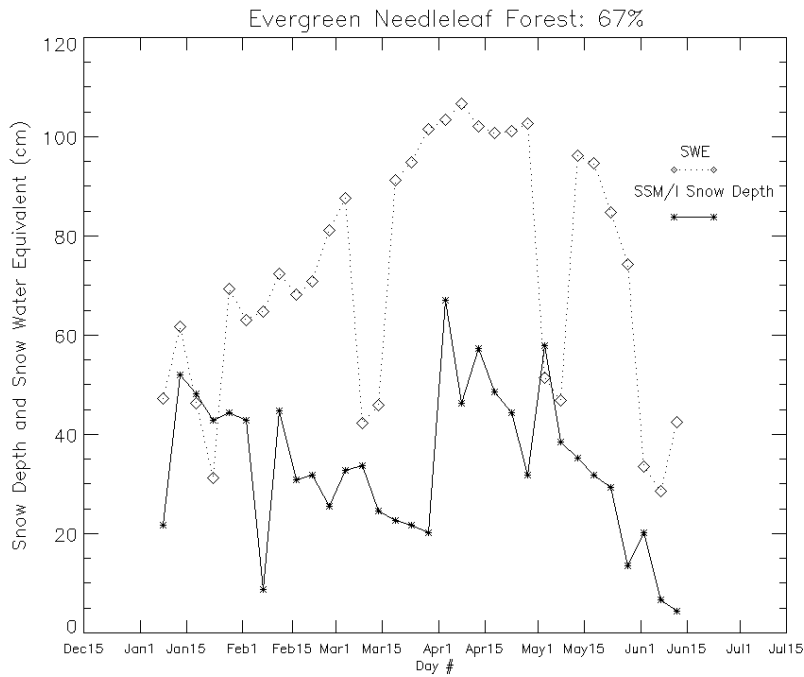


Figure 4-17 SSM/I Snow Depth and NOHRSC Snow Water Equivalent for pixel (196, 287). This result is among the worst: poor correlation in time, and SD less than SWE.

Figure 4-18 shows the temporal correlation between SSM/I SD and NOHRSC SWE for all pixels in the study area. Cluster of strong positive correlation are noted in the southeast corner of the region (lower left on map) and the north central part (right center on map). A striking cluster of strong negative correlation is found in the northeast corner of the region (lower right on map).

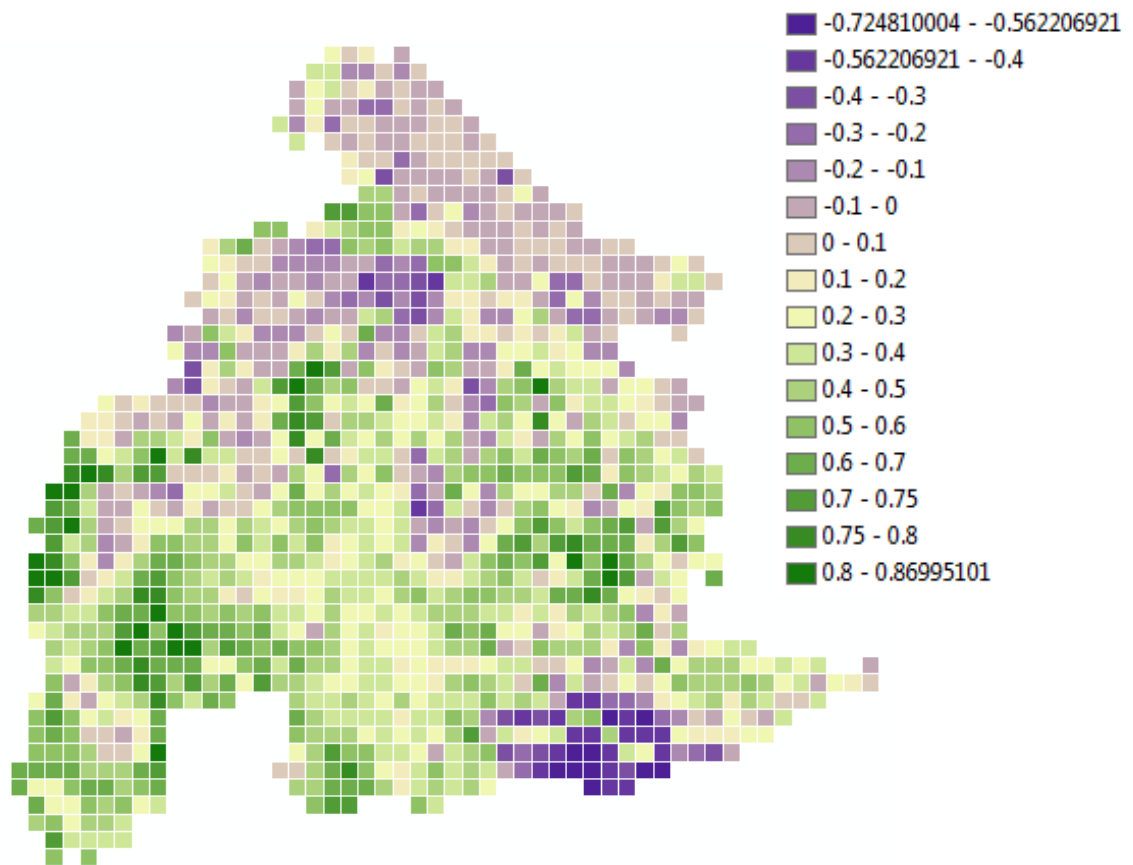


Figure 4-18 Correlation of SWE and SSM/I snow depth. Strong positive correlations indicate good agreement; strong negative correlations indicate a linear relationship, but lack of agreement.

Figure 4-19 shows the bulk seasonal relative density calculated (as described in the Relative Density Section of Chapter 3) by dividing average SWE by average SD. Any values over 1.0 are physically impossible, and correspond to time series such as the one shown in Figure 4-17. The very small relative density values are also physically unlikely over the course of a season.

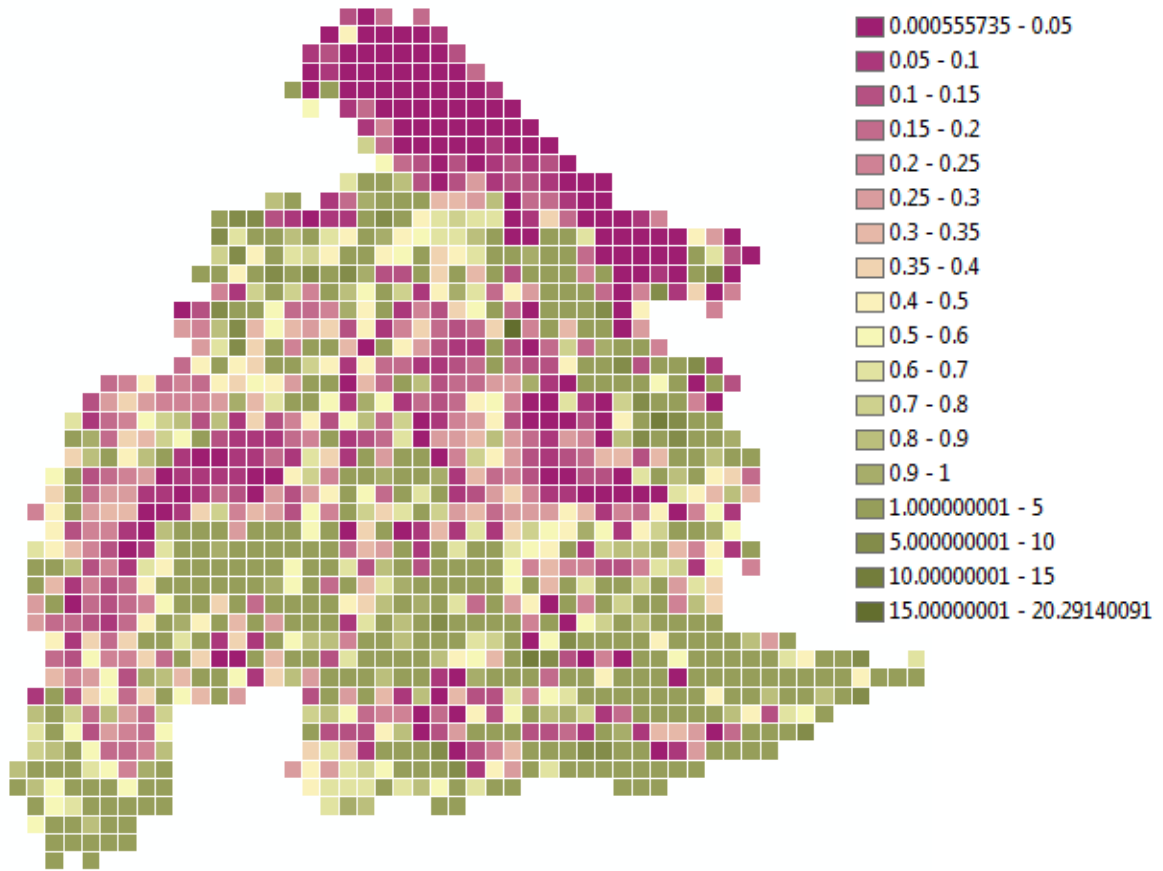


Figure 4-19 Relative density (Average NOHRSC SWE / Average SSM/I Snow Depth) – Up to 0.4 is considered good agreement. Values above one are physically impossible, and high fractions (near 1.0) unlikely.

Only 12 pixels were identified that have correlation above 0.7 and relative density below 0.4 (subjectively determined thresholds of agreement) as seen in Figure 4-20 and tabulated in Table 4-1 .

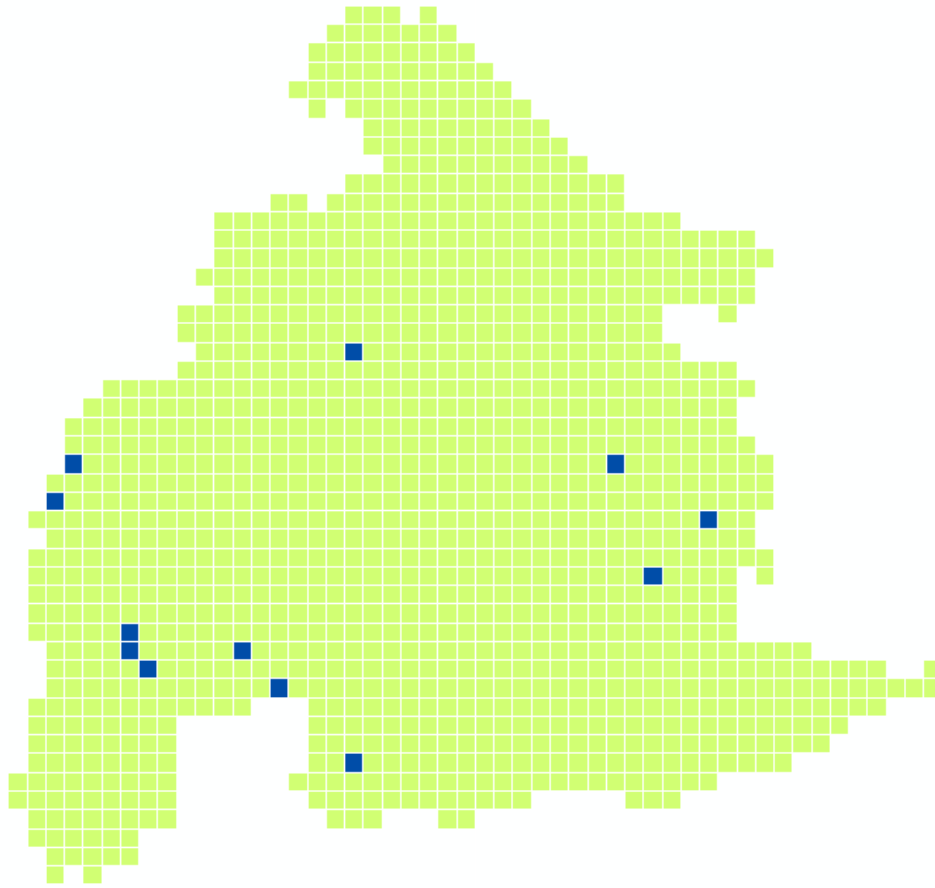


Figure 4-20 - Blue pixels represents 12 best agreements with correlation greater than 0.7 and relative density less than 0.4.

Table 4-1– Best agreements with correlation greater than 0.7 and relative density less than 0.4.

	R	S	Correlation	Relative Density
1	171	271	0.746523	0.375241
2	172	269	0.773299	0.363928
3	175	278	0.71962	0.192662
4	175	279	0.840386	0.391368
5	176	280	0.757374	0.397425
6	181	279	0.726029	0.385331
7	183	281	0.70592	0.378118
8	187	263	0.71165	0.315204
9	187	285	0.70233	0.346655
10	201	269	0.714258	0.307997
11	203	275	0.813344	0.242506
12	206	272	0.718215	0.210978

A few examples of best agreements based on greater than 0.7 correlation and less than 0.4 relative density can be seen in Figure 4-21 through Figure 4-23.

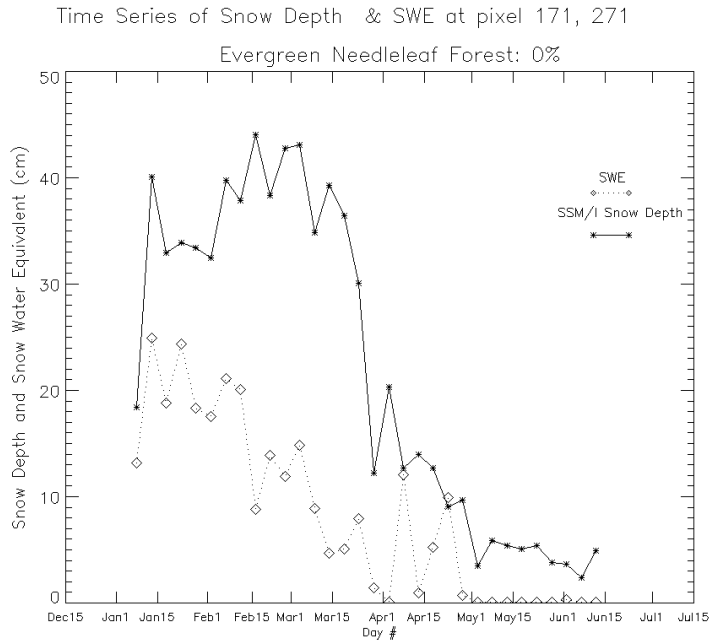


Figure 4-21 Shallow snow depth shows good agreement.

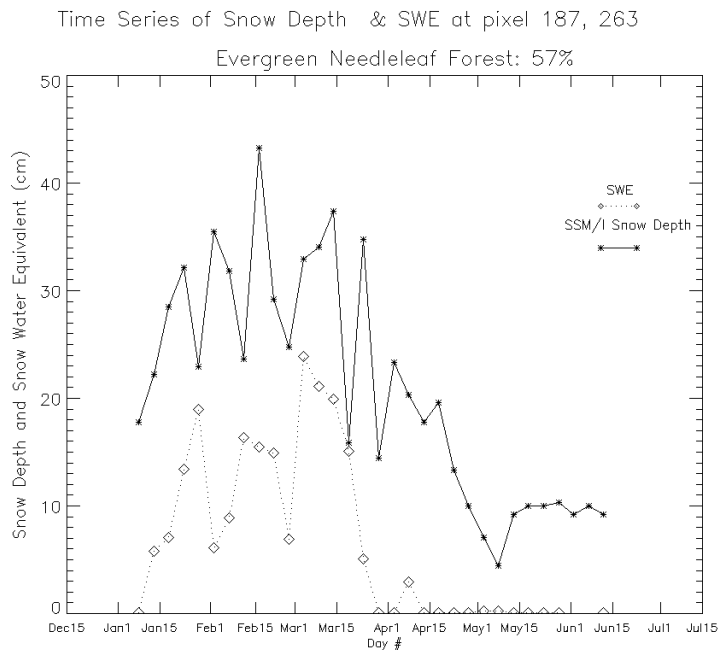


Figure 4-22 Despite canopy cover of 57%, shallow snow depths yield good agreement for the pixel (187,263)

Time Series of Snow Depth & SWE at pixel 203, 275
 Evergreen Needleleaf Forest: 84%

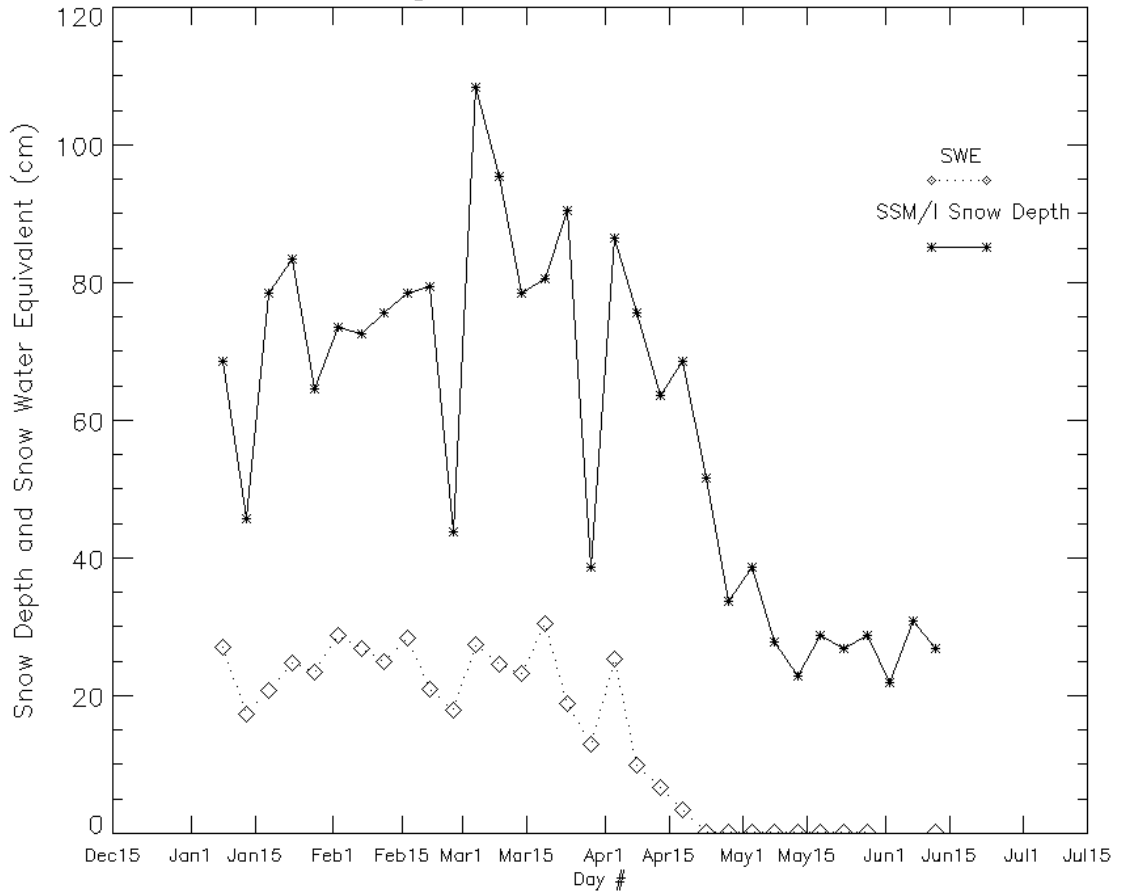


Figure 4-23 This is one of the best 12 pixels, with maximum snow depth about 110cm.

This result is consistent with other studies' findings that passive microwave snow retrieval is relatively good for measuring snow depth up to 120cm. (Mizukami, 2011).

Analyzing agreements between the ground stations with SSM/I snow depth

Out of 300 pixels, only 50 have at least 1 agreement, and the highest number in any one pixel is 4 agreements (refer to Figure 4-1).

Table 4-2 and Figure 4.24 show better agreement at the low to medium mean elevation.

The snow depths tend to increase with elevation, and this would result in poorer agreement between ground snow depth and passive microwave snow depth.

Table 4-2 SSM/I – Ground Snow Depth Agreement and Mean Elevation Class

	Low	Medium Low	Medium	High Medium	High
NO agreement	46	45	43	55	54
Agreement(s)	14	15	17	4	7

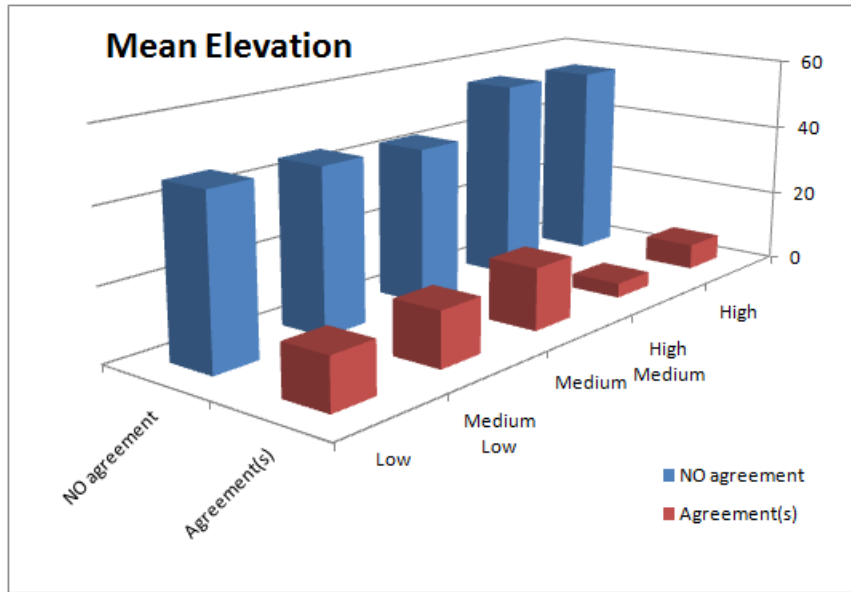


Figure 4-24 Mean pixel elevation class and number of pixels with no agreement and at least one agreement between SSM/I and ground snow depth.

Agreements were most frequent at higher evergreen canopy factor as seen in Table 4-3 and Figure 4.25. Low evergreen canopy factor is next best agreement group. Agreement in low evergreen canopy makes sense because the area is more uniform and less complex -- at least, with respect to vegetation. The second quantile seems to be the worst agreement, which may be due to patchy canopy and/or other vegetation type (Figure 4-26)

The best agreement groups are high and low evergreen canopy coverage, which matches the 12 pixels with best correlation and relative density in the NOHRSC SWE

– SSM/I SD comparison. **This indicates that high canopy factor and lack of canopy cover may have a positive impact on agreement.**

Table 4-3 Evergreen Canopy Class and SSM/I – Ground Snow Depth Agreement (number of pixels)

	Low	Medium Low	Medium	High Medium	High
NO agreement	48	60	49	50	36
Agreement(s)	10	4	9	8	26

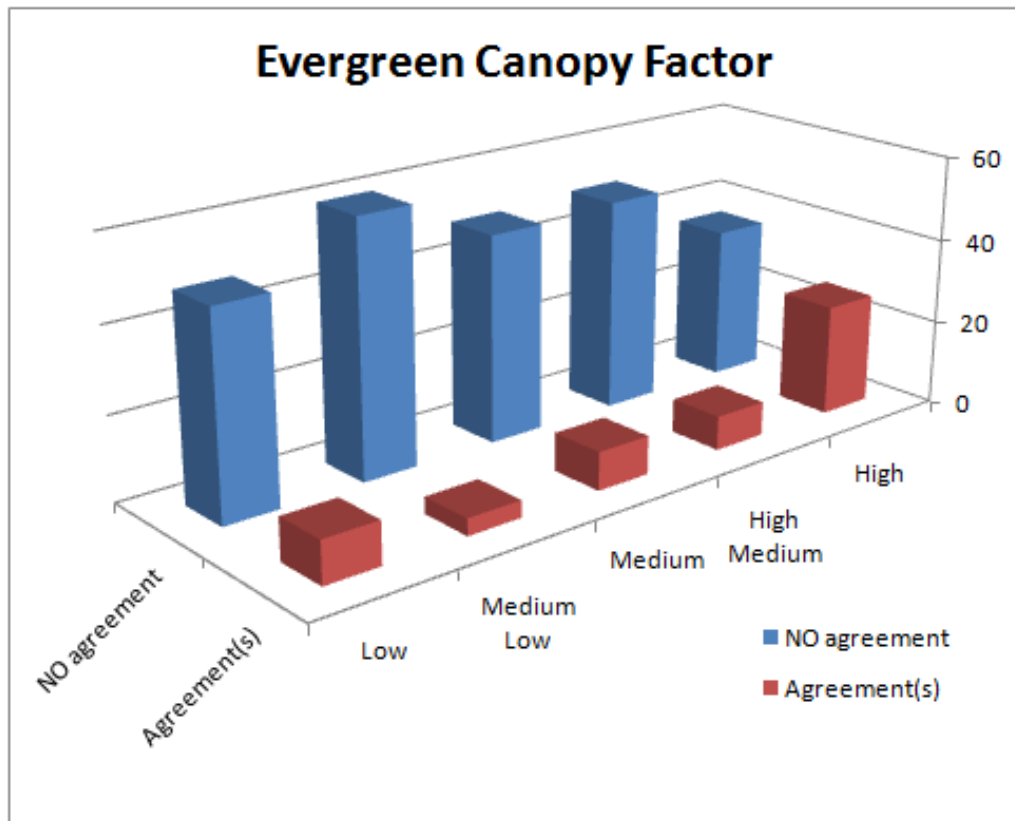


Figure 4-25 Evergreen canopy class and SSM/I – ground snow depth agreements (number of pixels).

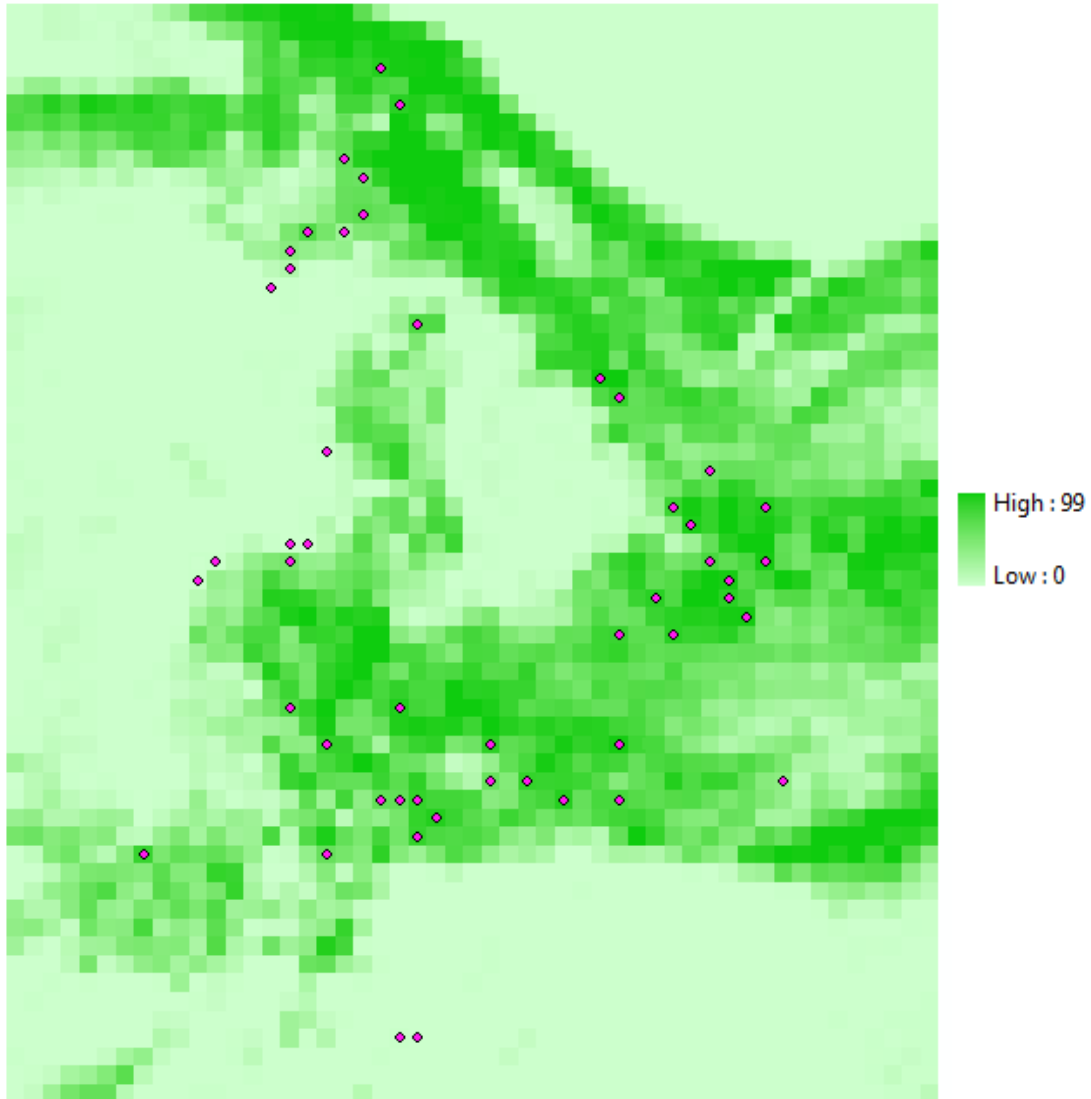


Figure 4-26 Evergreen Canopy Coverage and locations of 50 pixels with at least one agreement

Analyzing agreements between SWE with SSM/I snow depth

From Table 4.4 and Figure 4.27, about 10% of the 1279 pixels have good agreement with score of 4 or 5. Score of 1 have poor agreement between SWE and snow depth. The majority of snow depth was underestimated especially at higher elevation. Moderate to poor agreement at low elevation with score of 2 and 3 were unexpected and unexplained, similar trends to the Table 4.5 and Figure 4.28

Table 4-4 SSM-I Snow Depth – NOHRSC SWE Agreement Score by Mean Elevation Class (number of pixels)

Score	Low	Low – Medium	Medium	Medium-High	High	Count
5	7	7	4	10	22	55
4	8	14	13	15	15	69
3	59	60	95	61	49	327
2	127	96	57	50	13	345
1	51	76	84	117	154	483
						1279

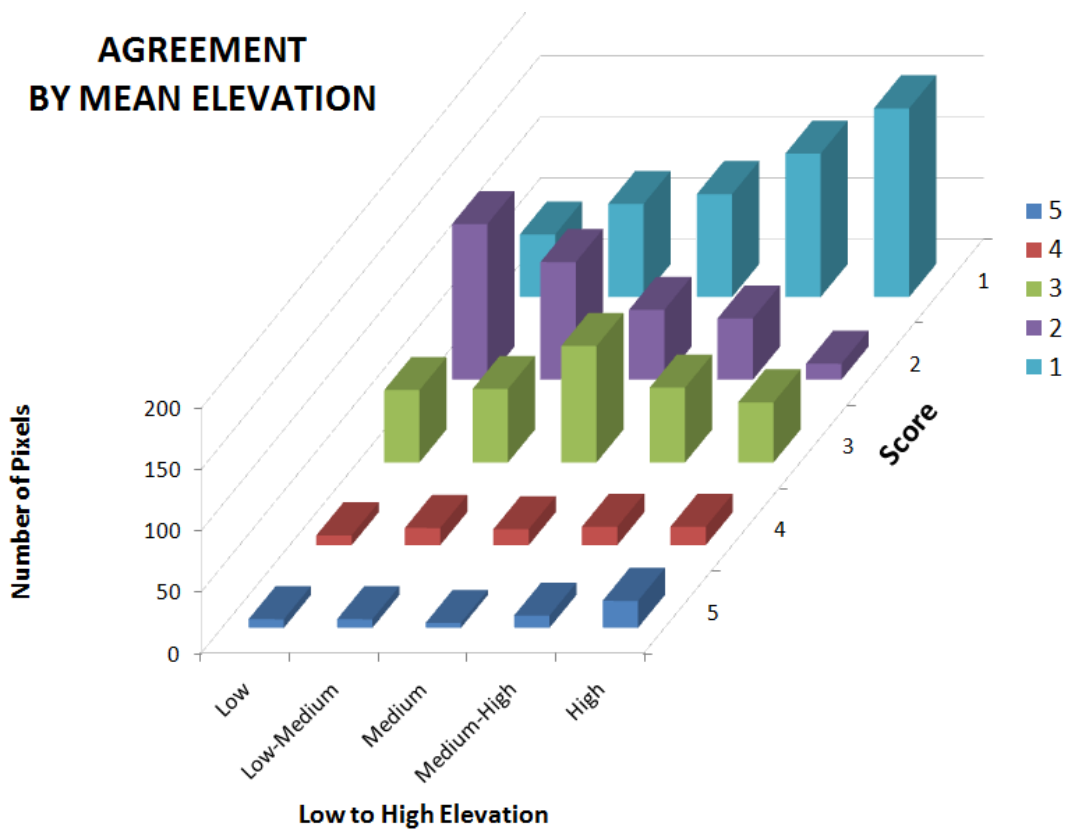


Figure 4-27 SSM/I Snow Depth and NOHRSC SWE Agreement Score by Mean Elevation Class.

Table 4-5 SSM/I Snow Depth – NOHRSC SWE Agreements by Elevation Standard Deviation Class (number of pixels)

Score	Low	Low-Medium	Medium	Medium-High	High
5	7	12	14	14	3
4	11	16	15	15	8
3	83	64	65	57	55
2	113	86	59	54	38
1	38	75	100	120	148

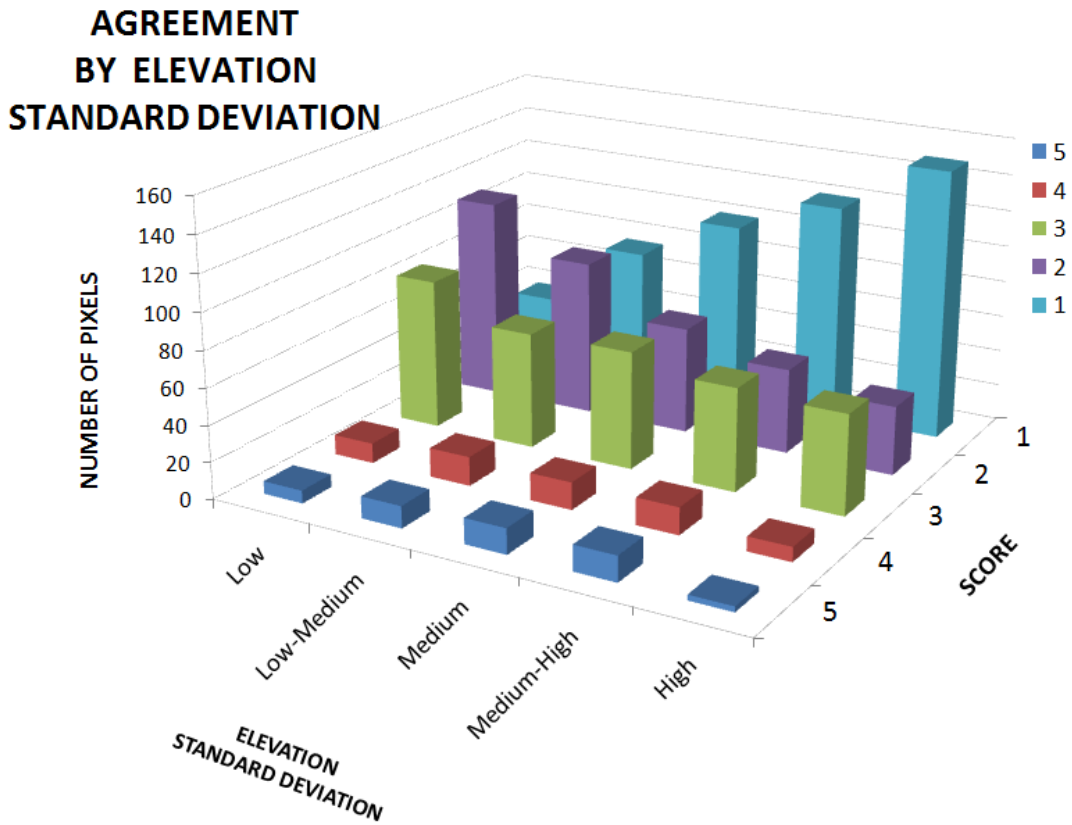


Figure 4-28 SSM/I Snow Depth – NOHRSC SWE Agreement Score by Elevation Standard Deviation Class

The trend for comparing high and low canopy between ground stations and SSM/I snow depth are seen similar in Table 4.6 and Figure 4.29. The better agreements are found either at higher or lower canopy coverage. For the lowest agreement score (1), the high and zero canopy are lower than their counterparts.

Table 4-6 SSM/I Snow Depth – NOHRSC SWE Agreement Score by Percentage of Evergreen Coverage

Score	Low	Low - Medium	Medium	Medium-High	High
5	19	11	5	8	7
4	11	19	16	8	11
3	93	69	53	42	67
2	106	57	57	57	67
1	35	94	126	139	89

**AGREEMENT
BY PERCENTAGE OF
EVERGREEN COVERAGE**

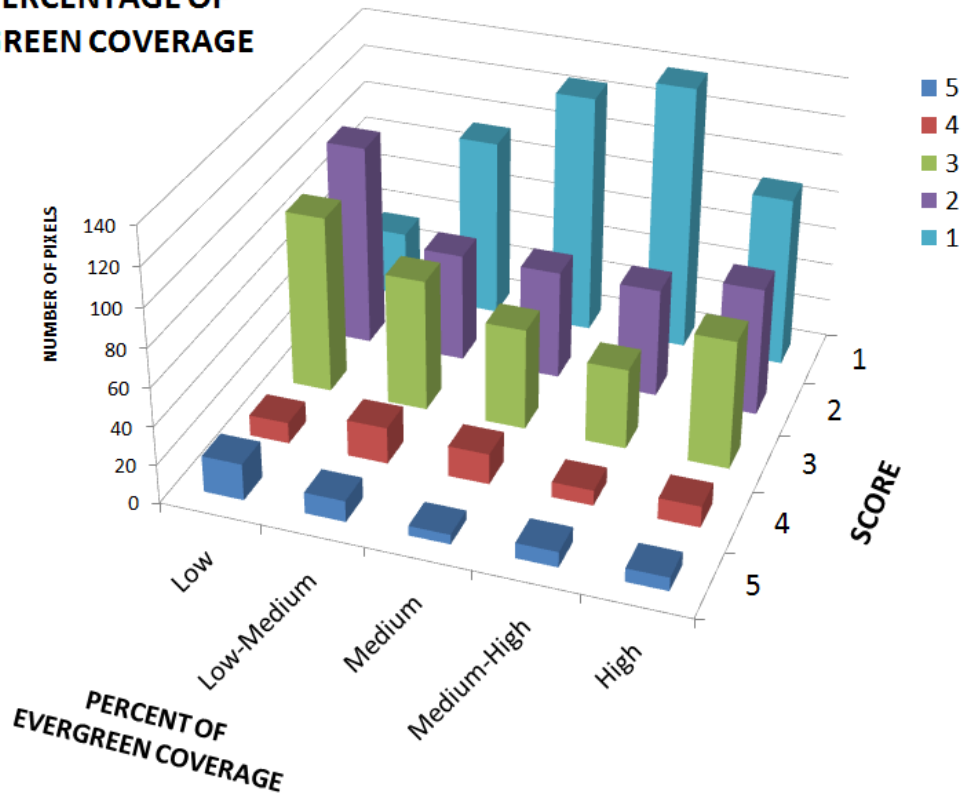


Figure 4-29 SSM/I Snow Depth – NOHRSC SWE Agreement Score by Percentage of Evergreen Coverage

Chapter 5 Discussion and Conclusions

Comparing SSM/I snow depth to ground station snow depth

From observing 307 graphs, the majority of the graphs show that SSM/I snow depth is significantly underestimated. About 80 percent of the ground measurements were at least twice the value of the SSM/I snow depth. Passive microwave satellite data have good agreements for locations with 120cm of snow depth or less. This supports several other studies' findings that the Chang algorithm seriously underestimates deep snow.

Under conditions of high canopy coverage, low elevation, low elevation standard deviation, and shallow snow depth, the SSM/I estimates have better agreements with either interpolated snow water equivalent or in situ snow depth.

Most likely the landcover type in two different areas may affect the microwave retrieval. Another consideration may be the slope and orientation of the terrain, as well as the SSM/I instrument's angle of view.

Comparing SSM/I SD to NOHRSC SWE

From over 1300 graphs of the time series of NOHRSC SWE and SSM/I, the majority indicate that SSM/I snow depth was underestimated, in some cases quite significantly. This conclusion is based on examination of the relative density measure. Any relative density greater than 1.0 is physically impossible,

Even if the magnitude of snow depth estimate is incorrect, the SSM/I retrievals may be useful if they can track the pattern of SD as it increases during snow accumulation and decreases during the melt season. The correlation is a measure of this agreement between SSM/I SD and NOHRSC SWE. Figure 4-20 summarizes this correlation. The Cascade range (top of the map) shows poor correlation, as does Eastern British Columbia. The time series for pixel (200,286) in this area shows a spike in NOHRSC SWE in late June which is not reflected in the SSM/I estimate (Figure 3-7); a similar spike appears in other NOHRSC time series. These may represent real events, or errors in the NOHRSC interpolation algorithm. Ground measurements do not capture an increase on this date but this is not conclusive because a late snow could have fallen and melted between the once-a-month measurements. Ground stations report no snow beyond June 1, while SSM/I continues to report snow.

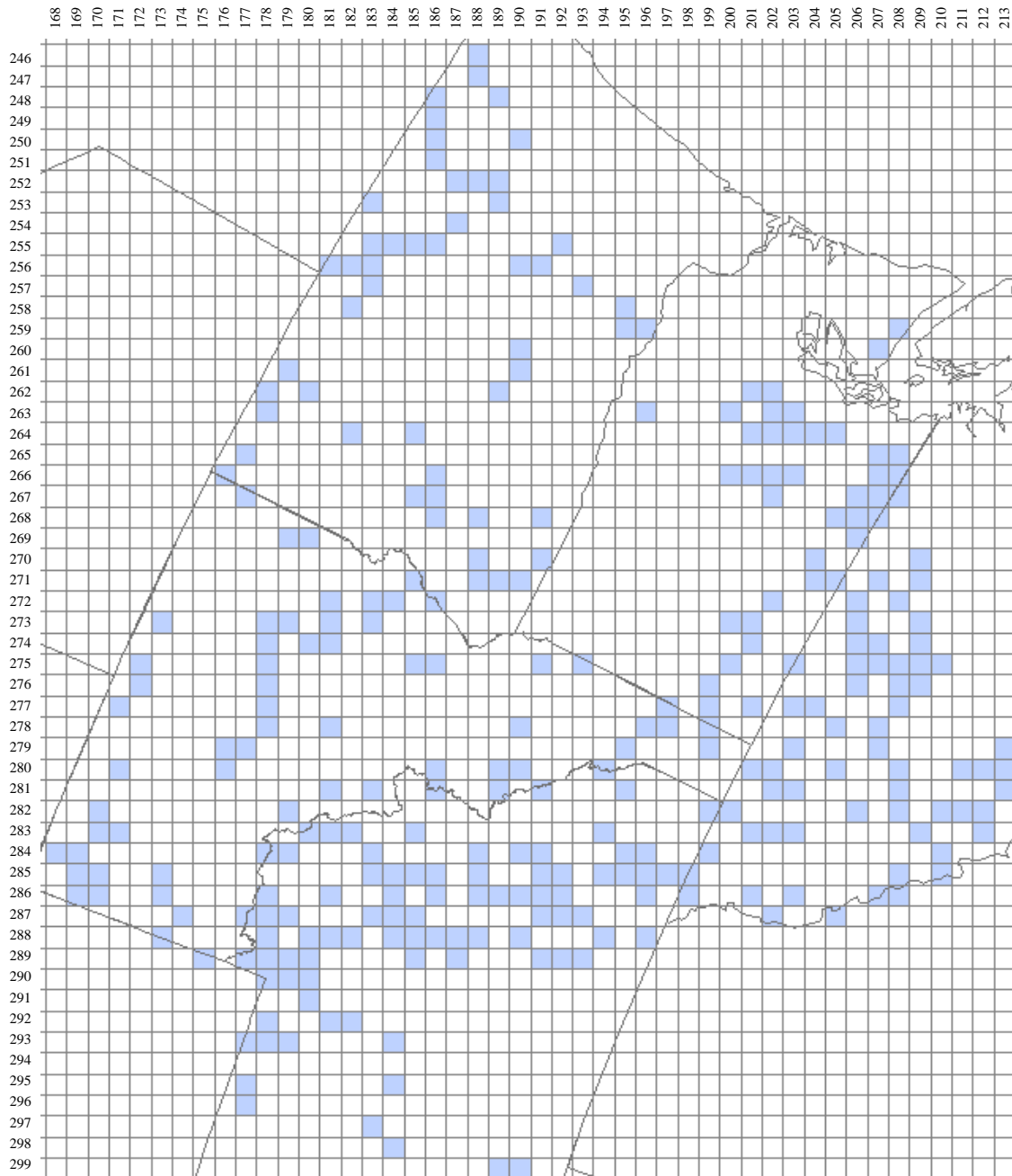
Conclusion

The current algorithm for SSM/I snow depth retrieval in the mountainous areas of the Western USA and British Columbia is poor, especially with snow depth greater than 200 cm. The results do not support any algorithm adjustments for elevation or terrain complexity. Further investigation is needed to include other considerations such as mountain orientation and slope

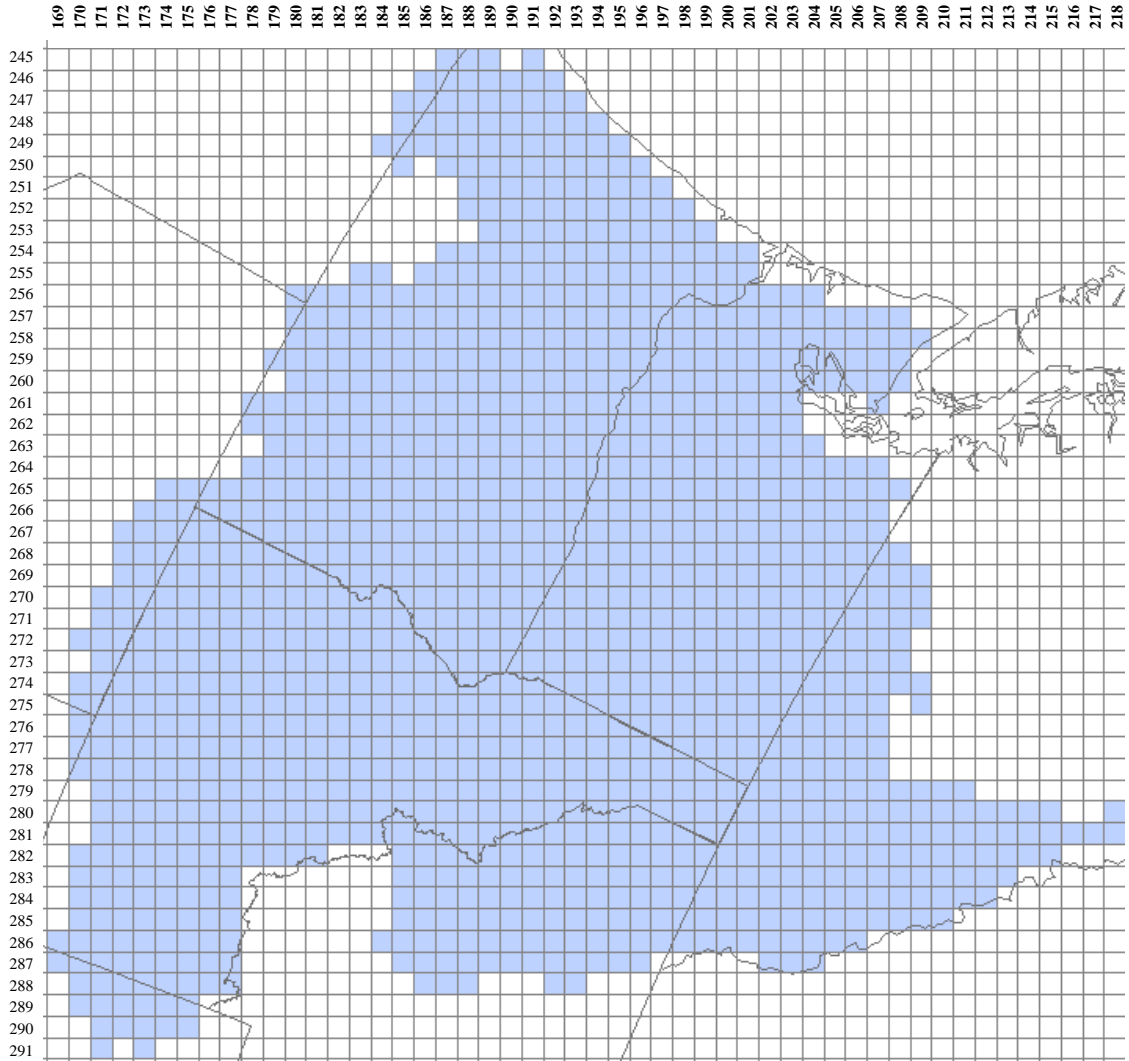
Appendix A

Index Maps of Study Region

The index map #1 below gives the (column, row) coordinates that identify the pixels containing ground stations.



The index map #2 below gives the (column, row) coordinates that identify the pixels in the Columbia Basin



Appendix B

Lists of All Pixels containing at least one agreement

The index maps in Appendix A show the locations of each pixel.

All Pixels containing
Only One Agreement

R	S	AGREEMENT
175	289	1
179	273	1
182	258	1
183	256	1
183	257	1
183	272	1
183	273	1
183	281	1
184	255	1
184	272	1
185	267	1
185	283	1
186	251	1
186	255	1
187	254	1
189	248	1
190	286	1
190	288	1
190	299	1
194	285	1
198	286	1
201	277	1
201	286	1
203	275	1
204	277	1
206	268	1
206	273	1
207	275	1

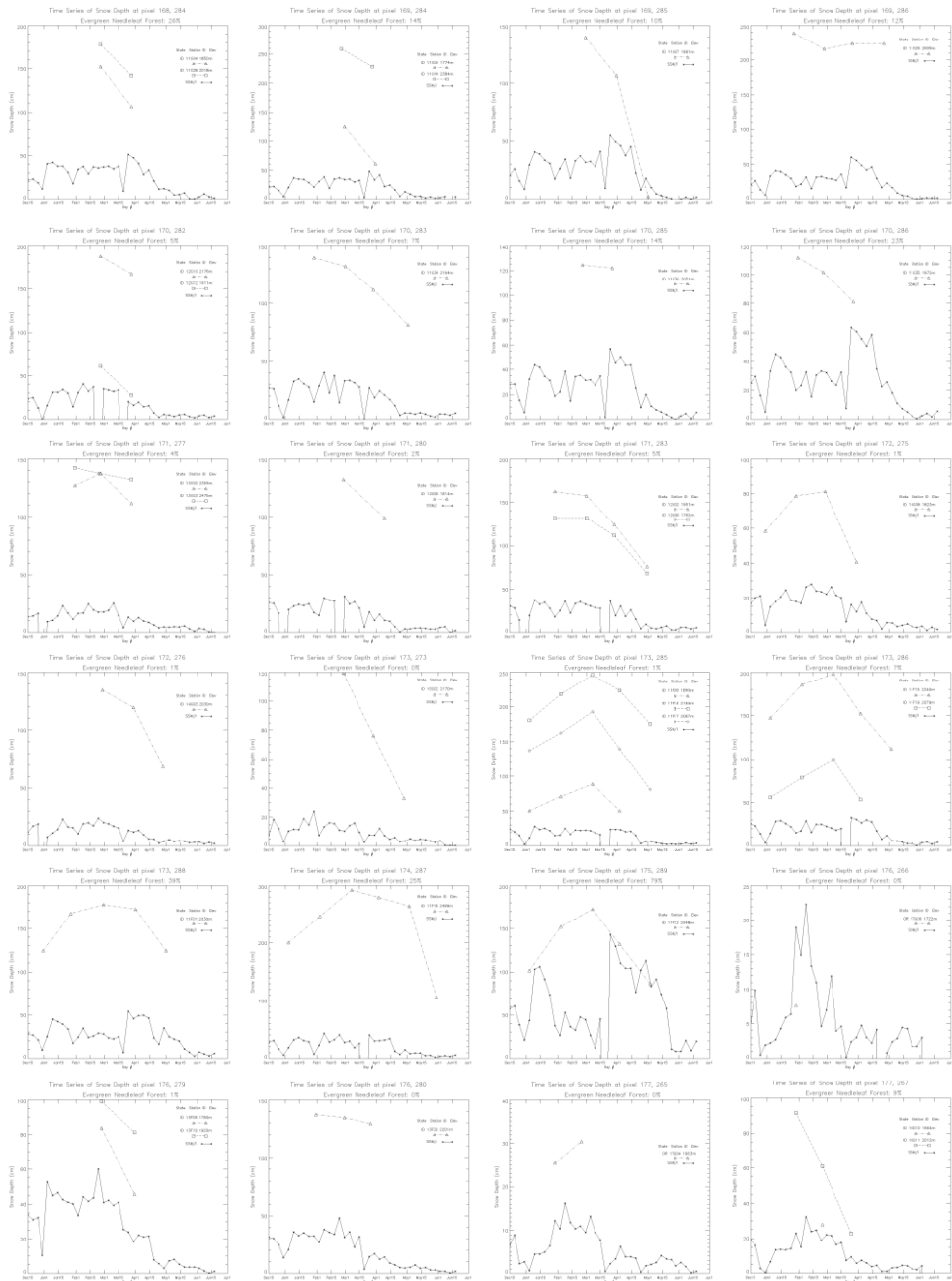
All Pixels containing
at least 2 Agreements

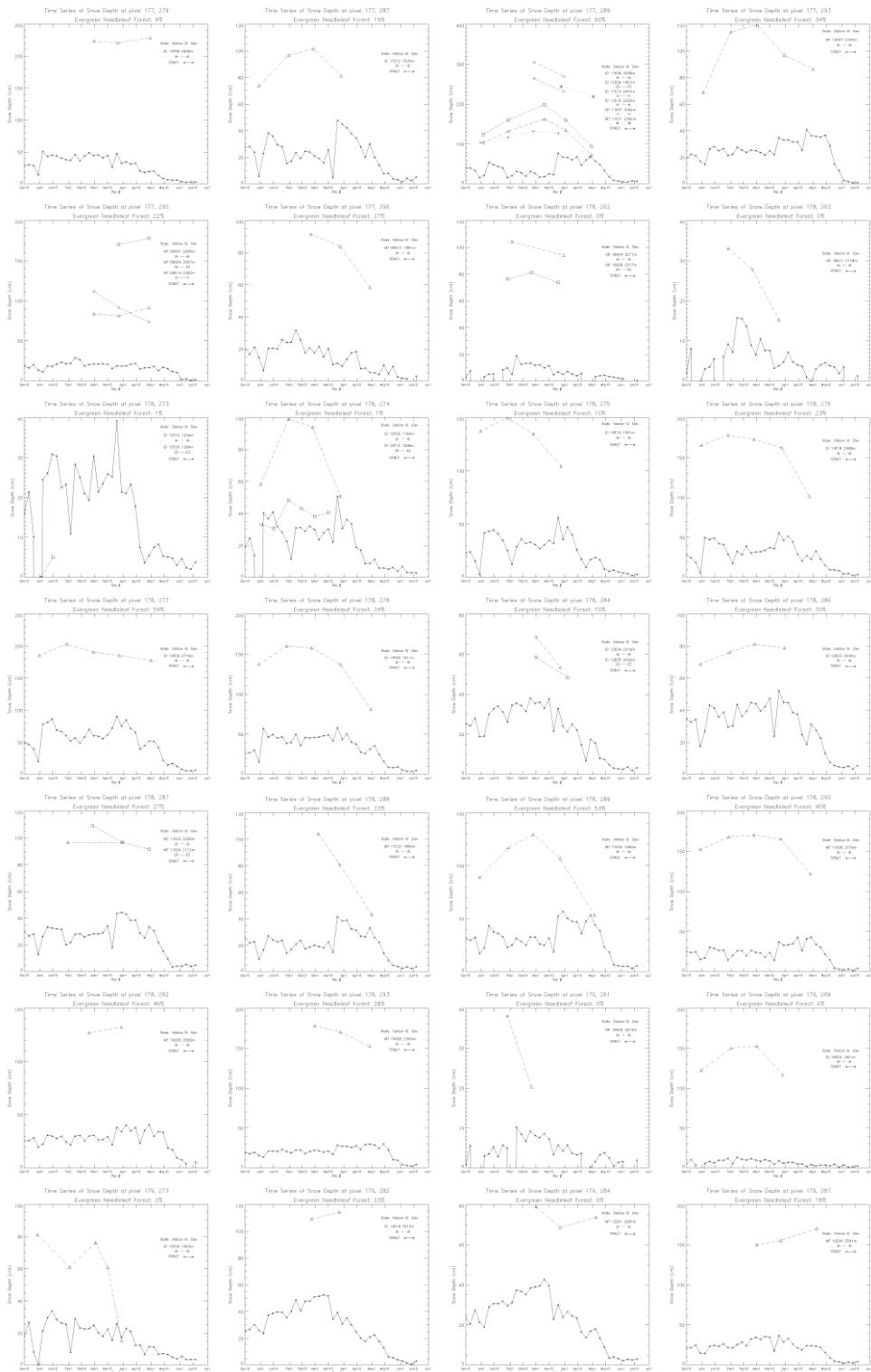
R	S	AGREEMENTS
178	274	2
185	289	2
187	252	2
188	246	2
188	286	2
189	281	3
189	286	2
189	299	2
190	260	2
191	287	2
194	283	2
196	285	2
200	263	2
201	264	3
201	283	3
204	270	2
205	271	2
207	274	3
208	276	3
209	270	3
209	273	4
210	285	2

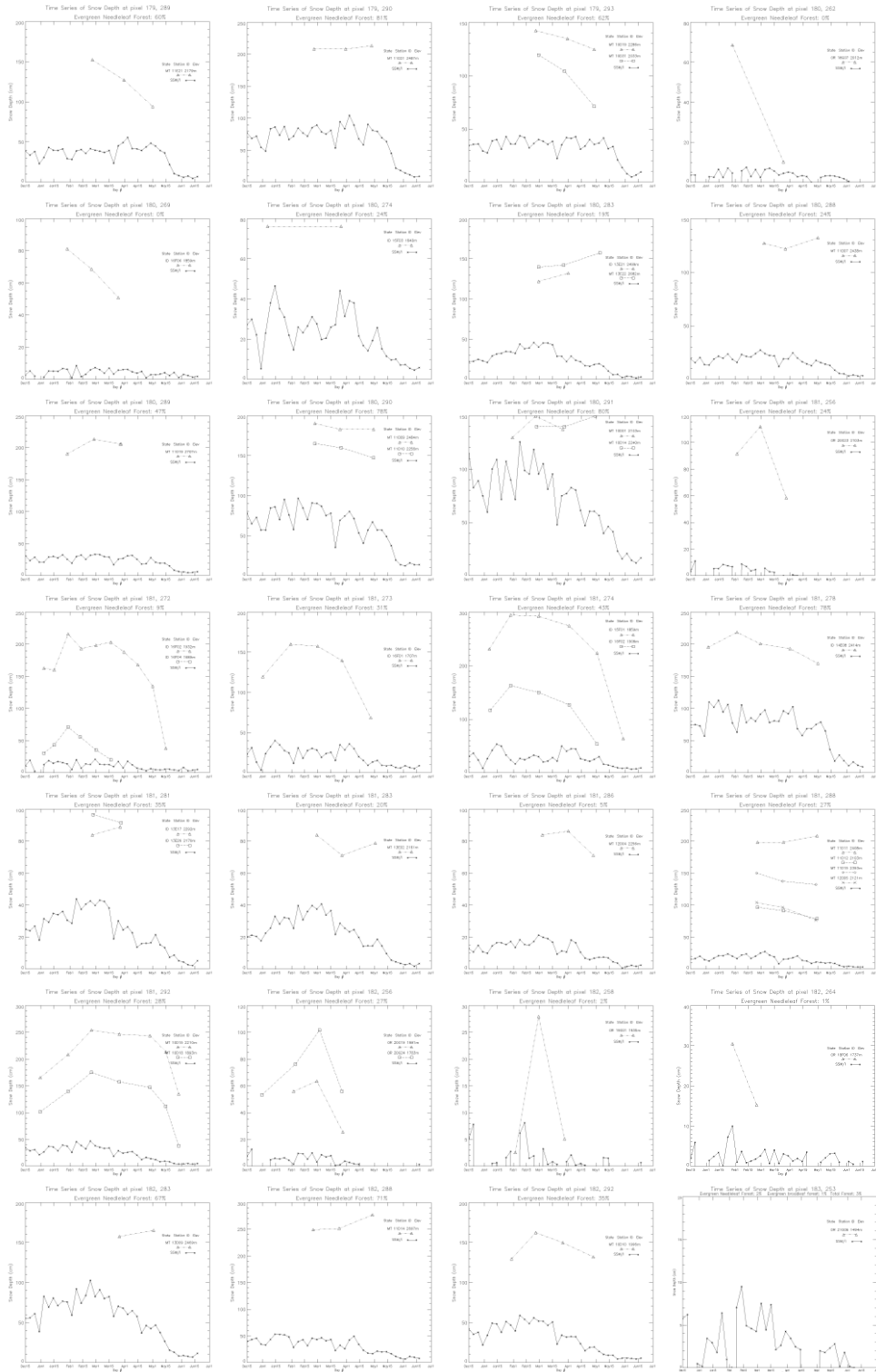
Appendix C

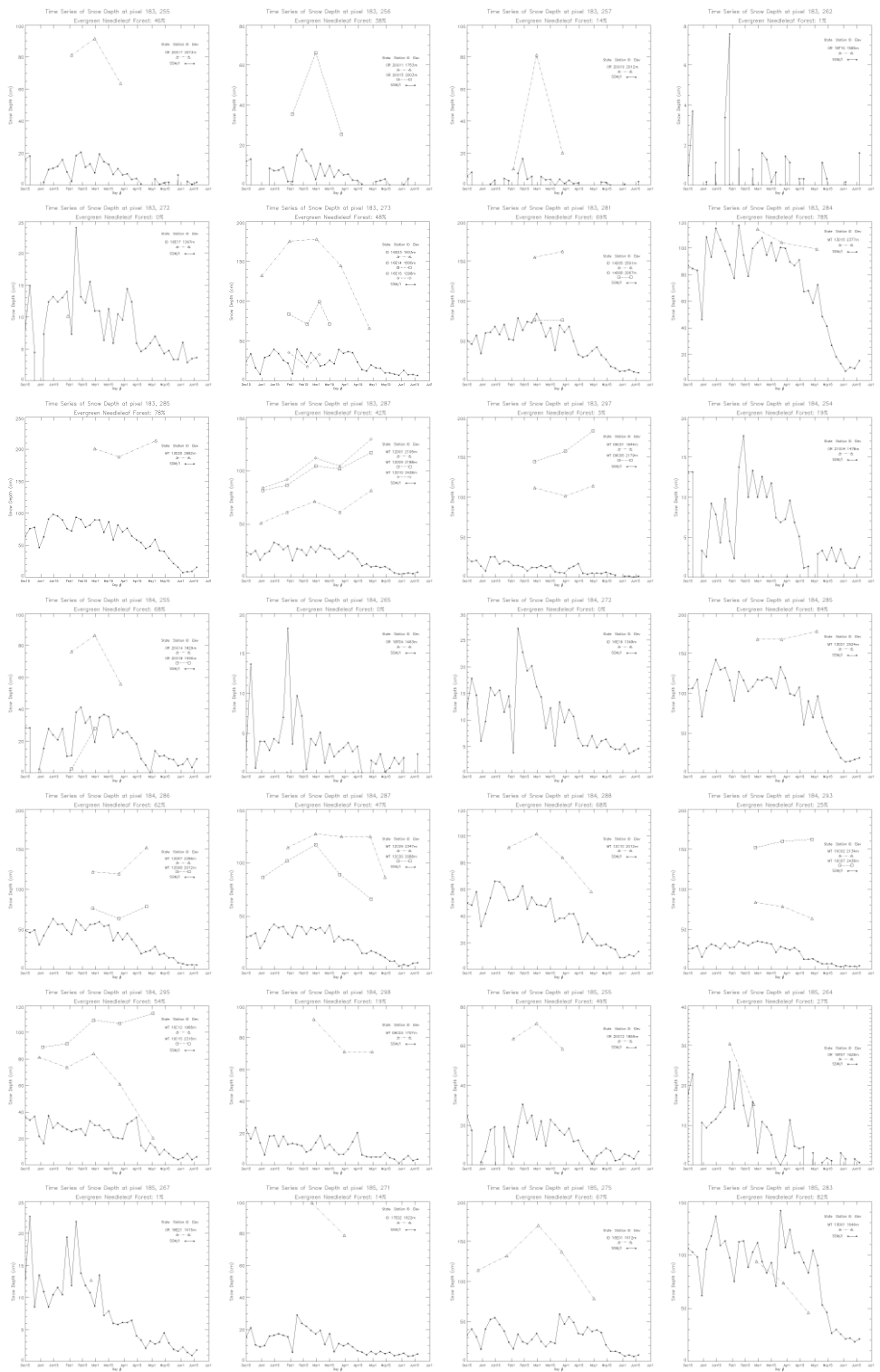
Time Series Graphs of Ground-Measured and SSM/I Snow Depth for All Pixels Containing Ground Stations

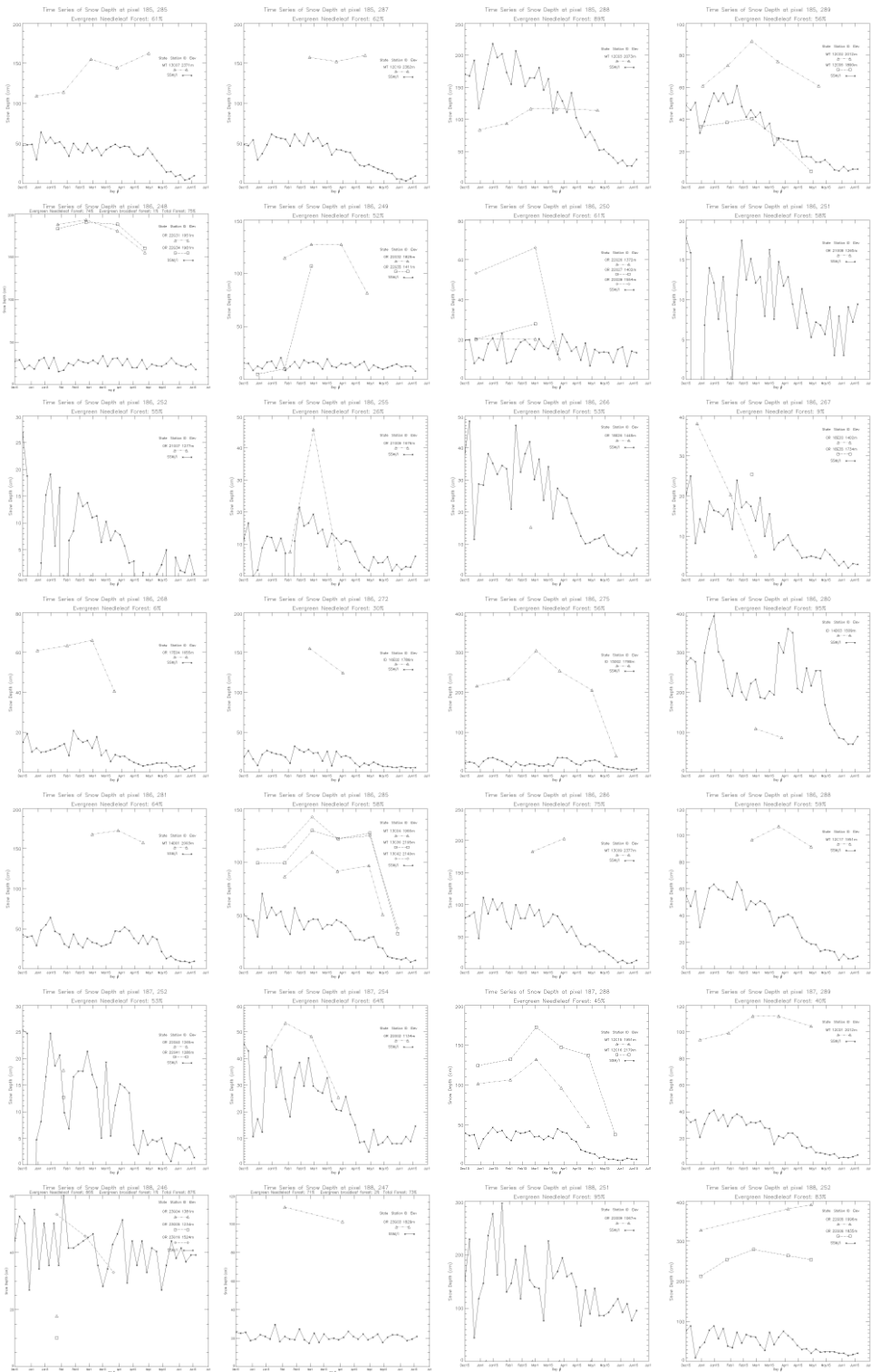
The index map #1 in Appendix A gives the (column, row) coordinates that identify the pixels containing ground stations.

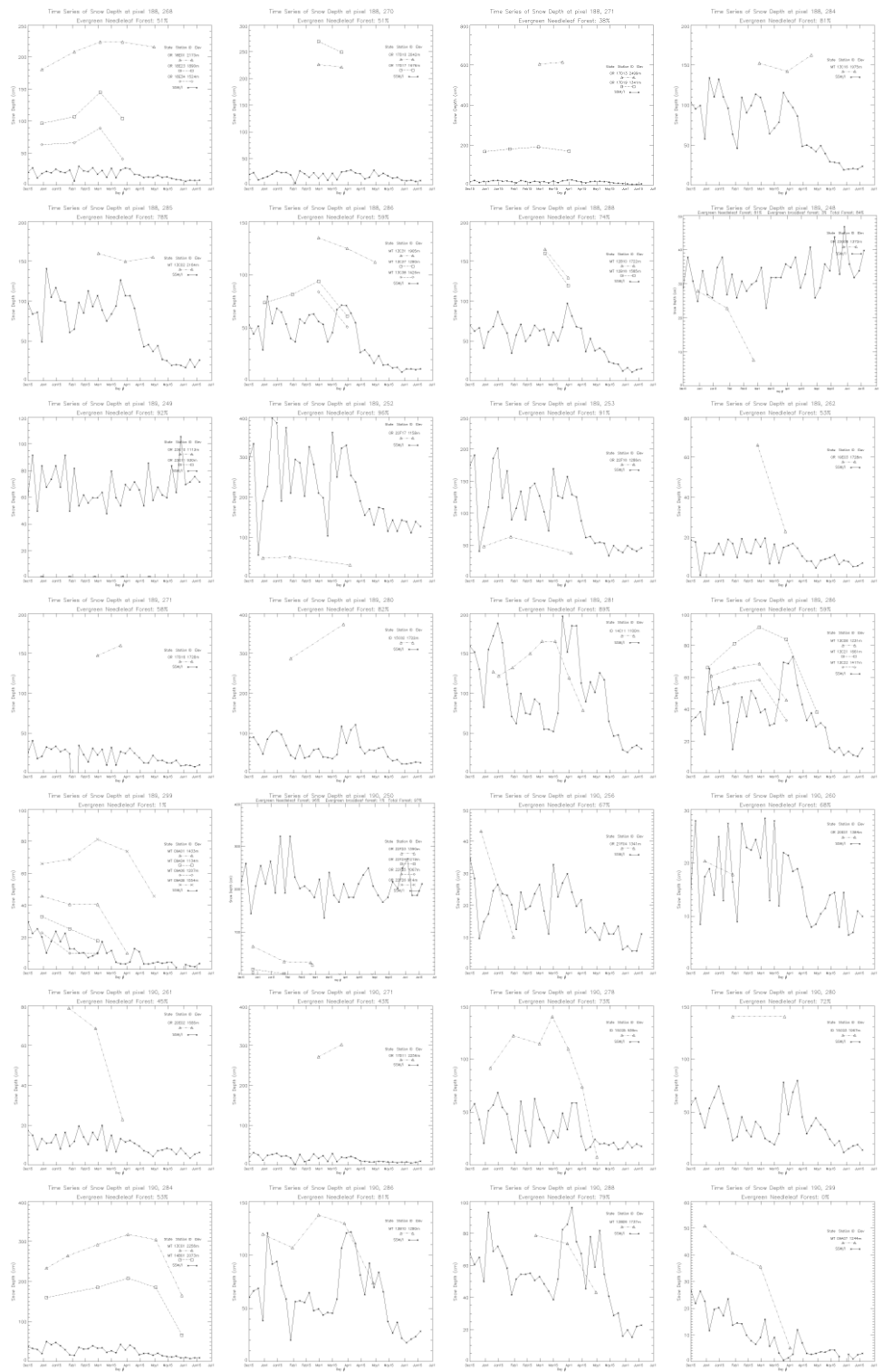


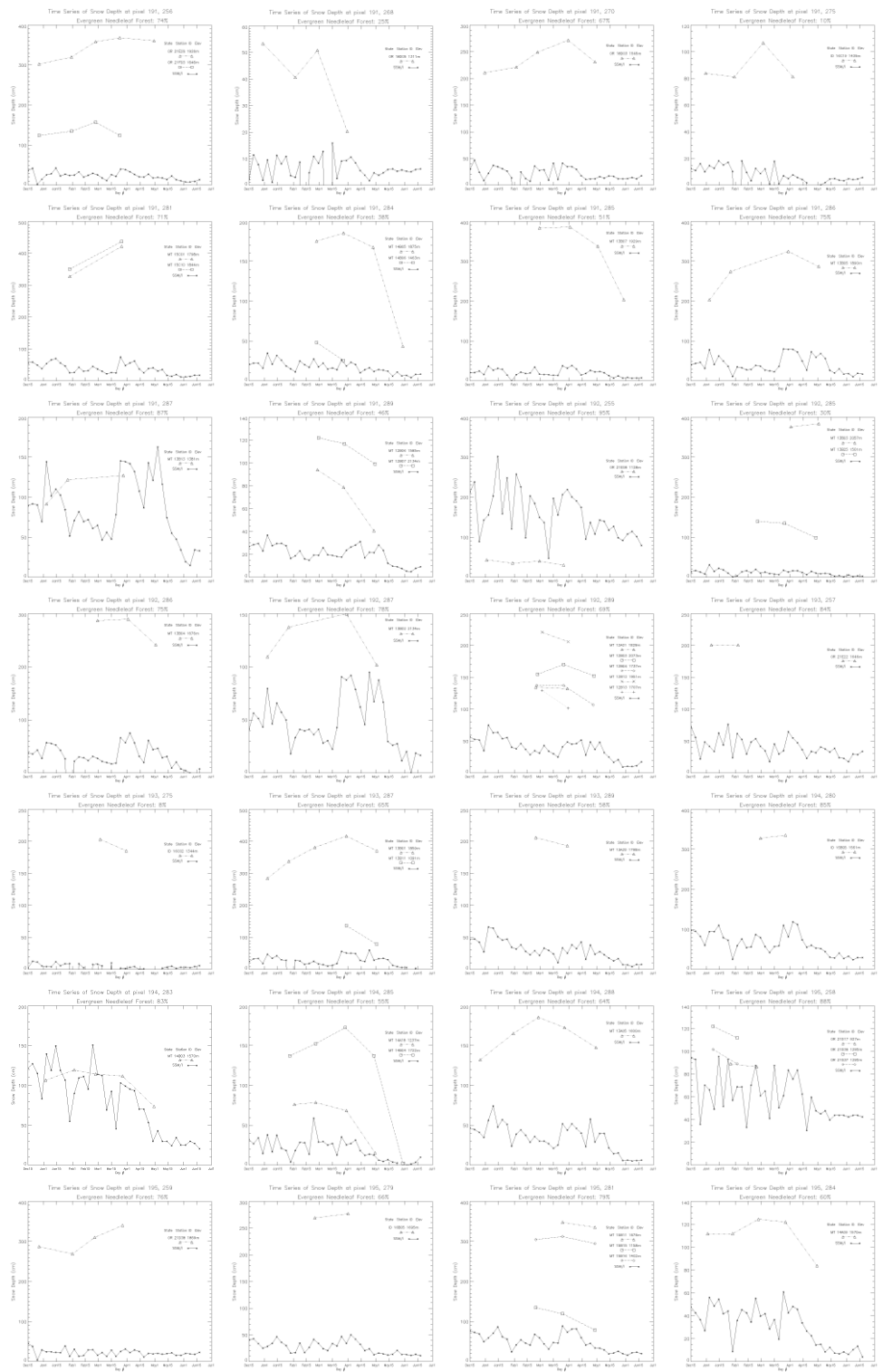


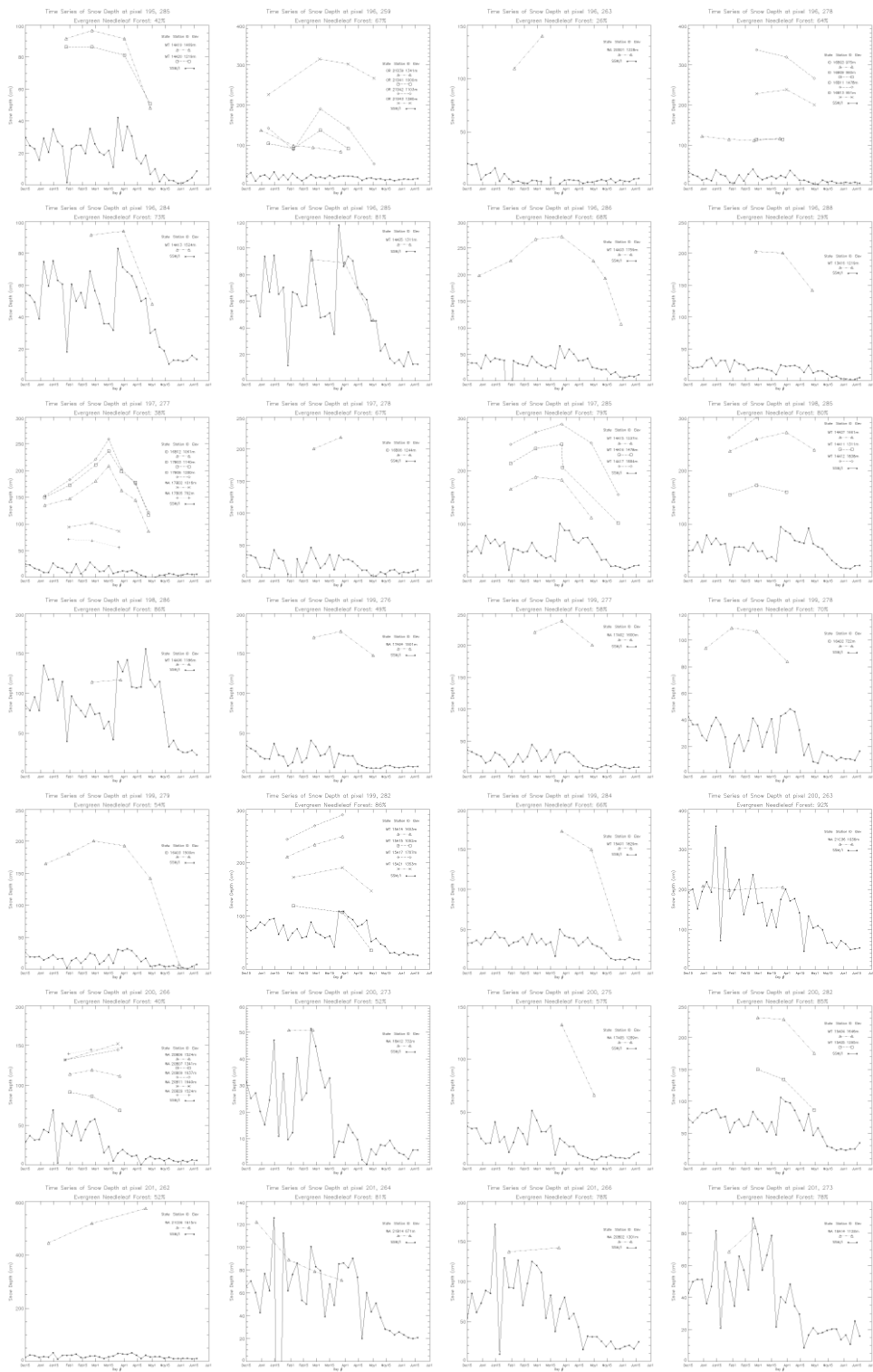


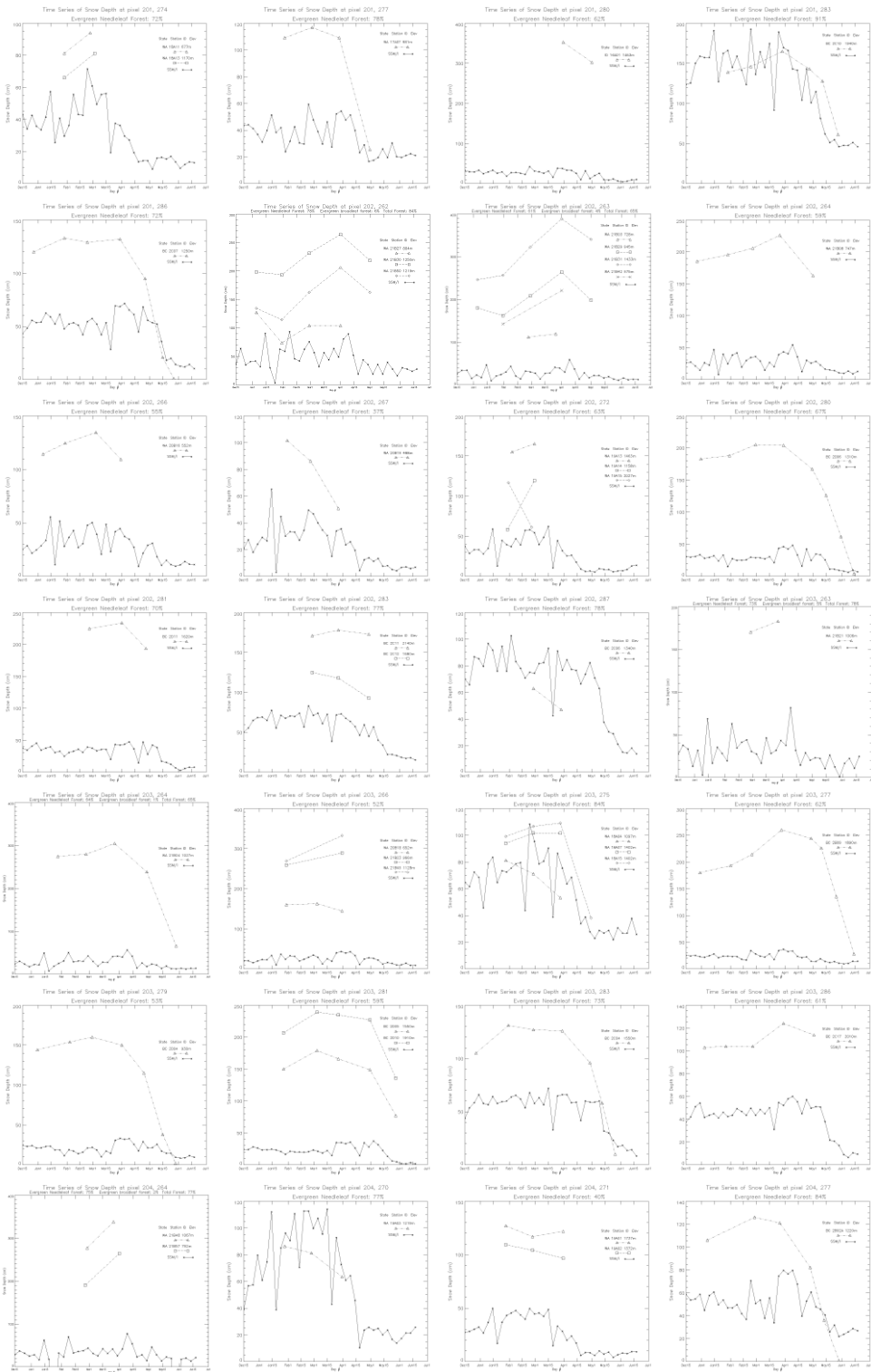


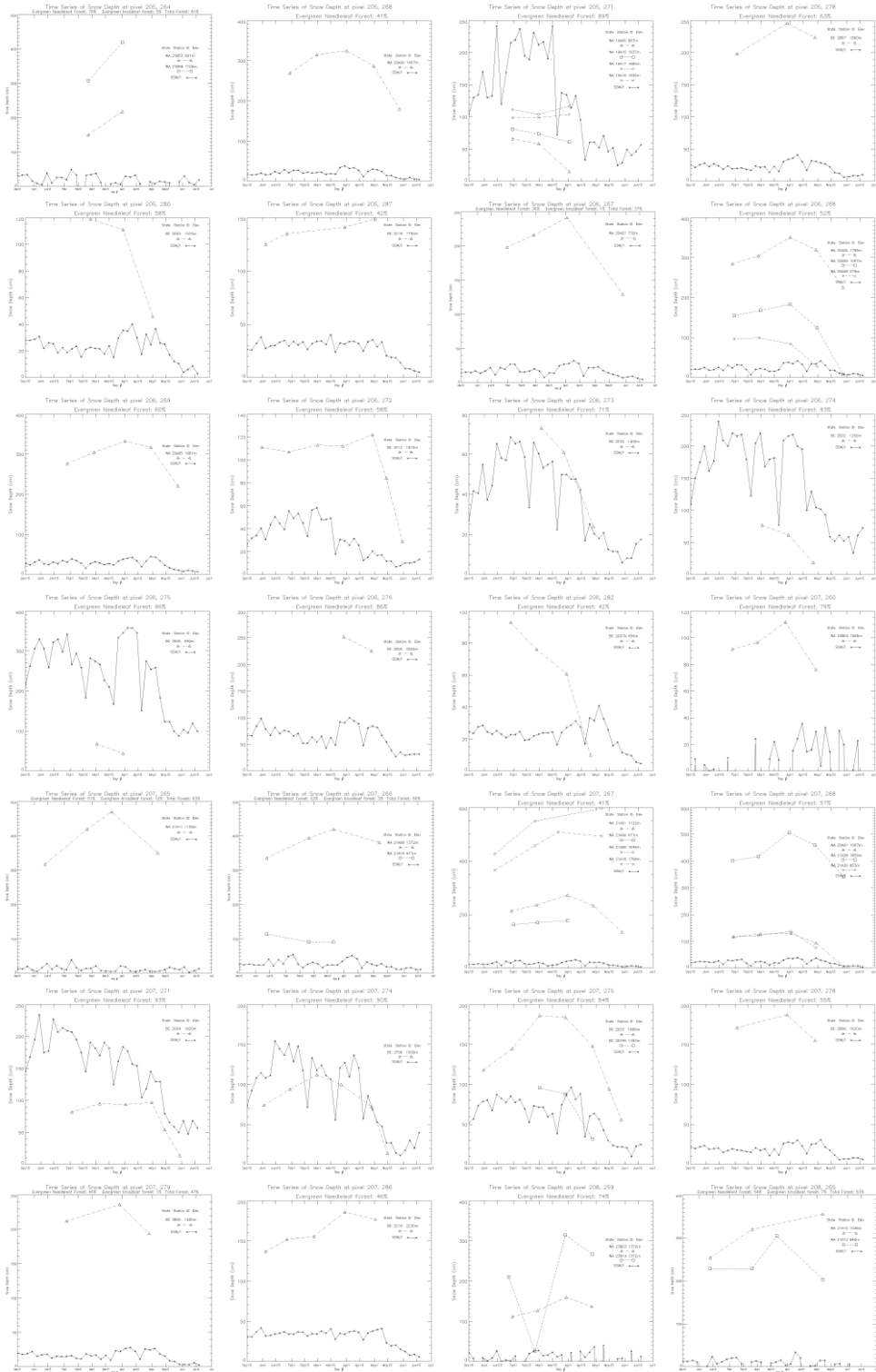


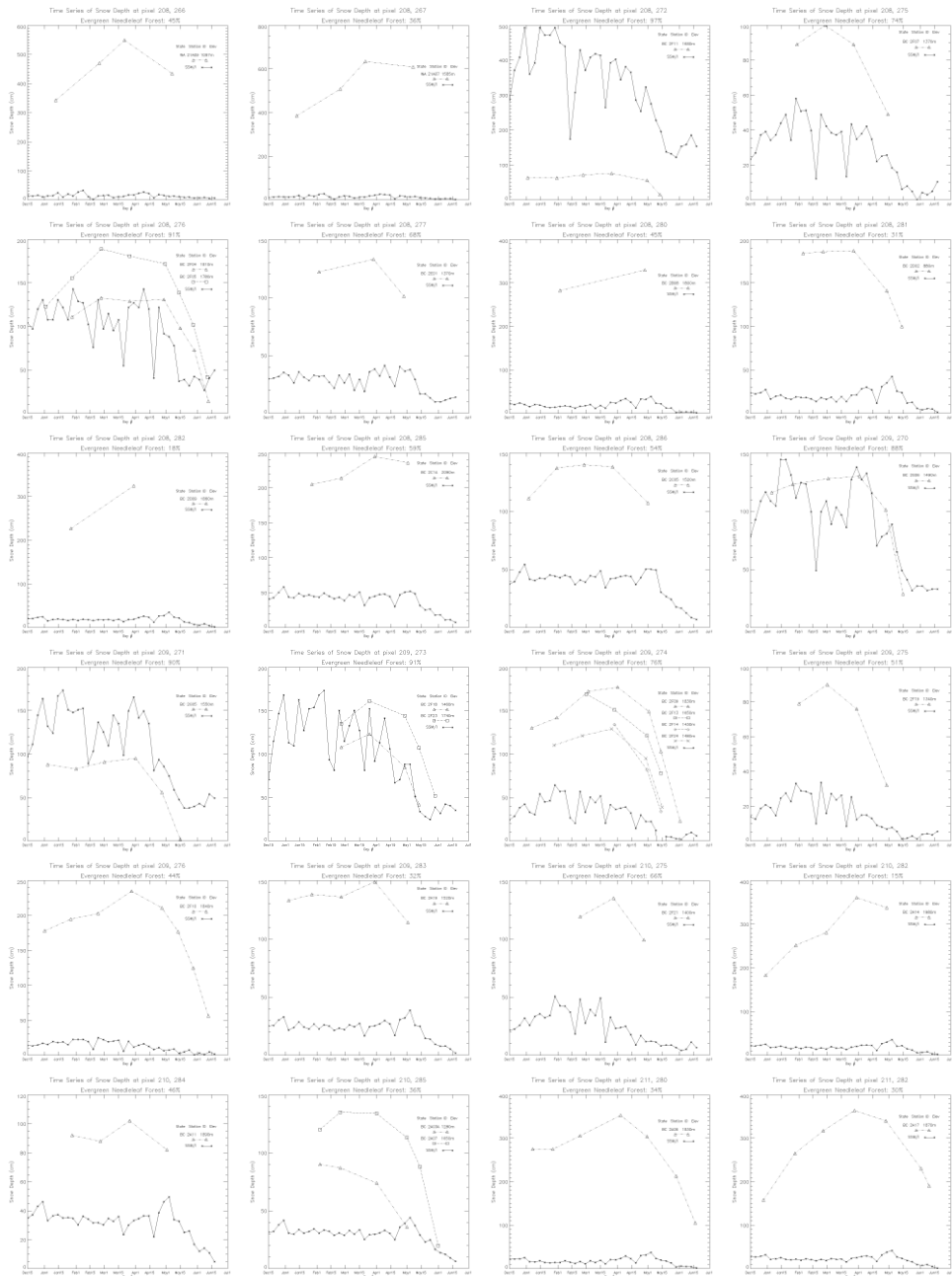


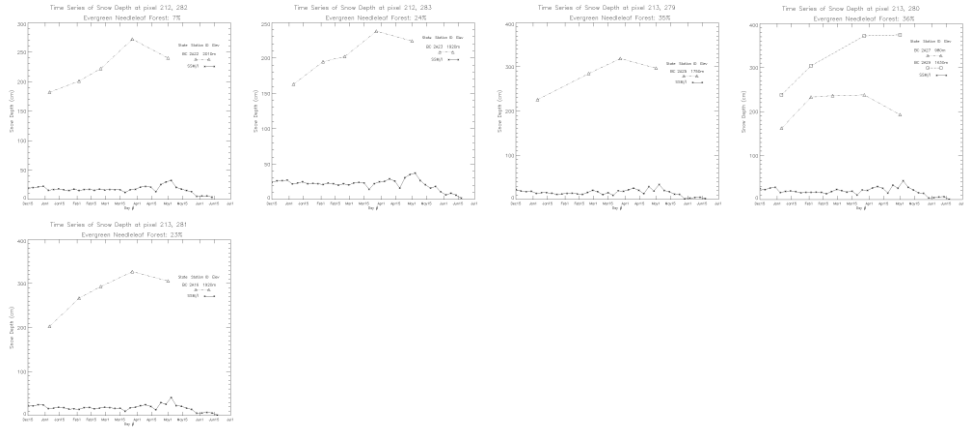








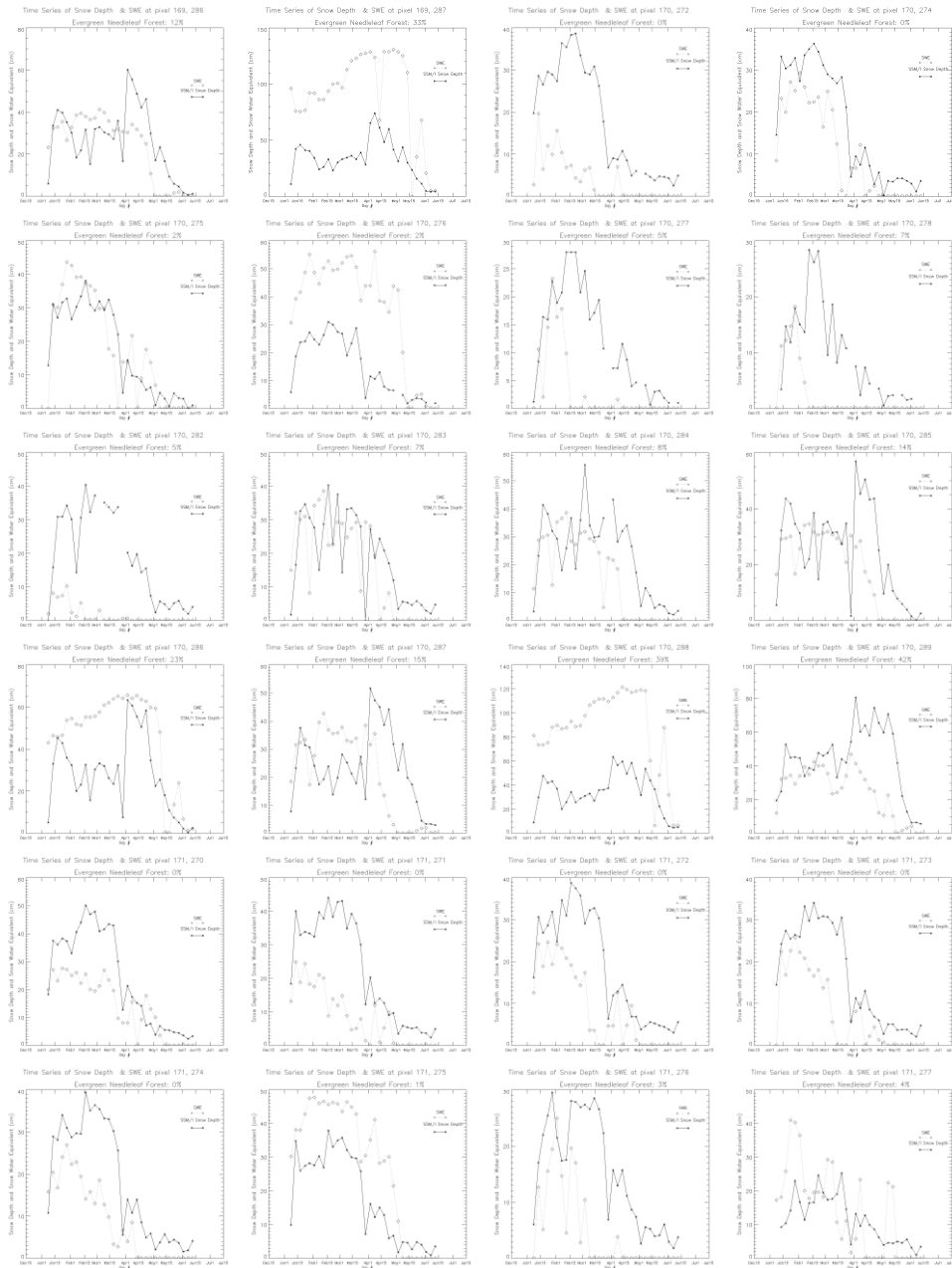


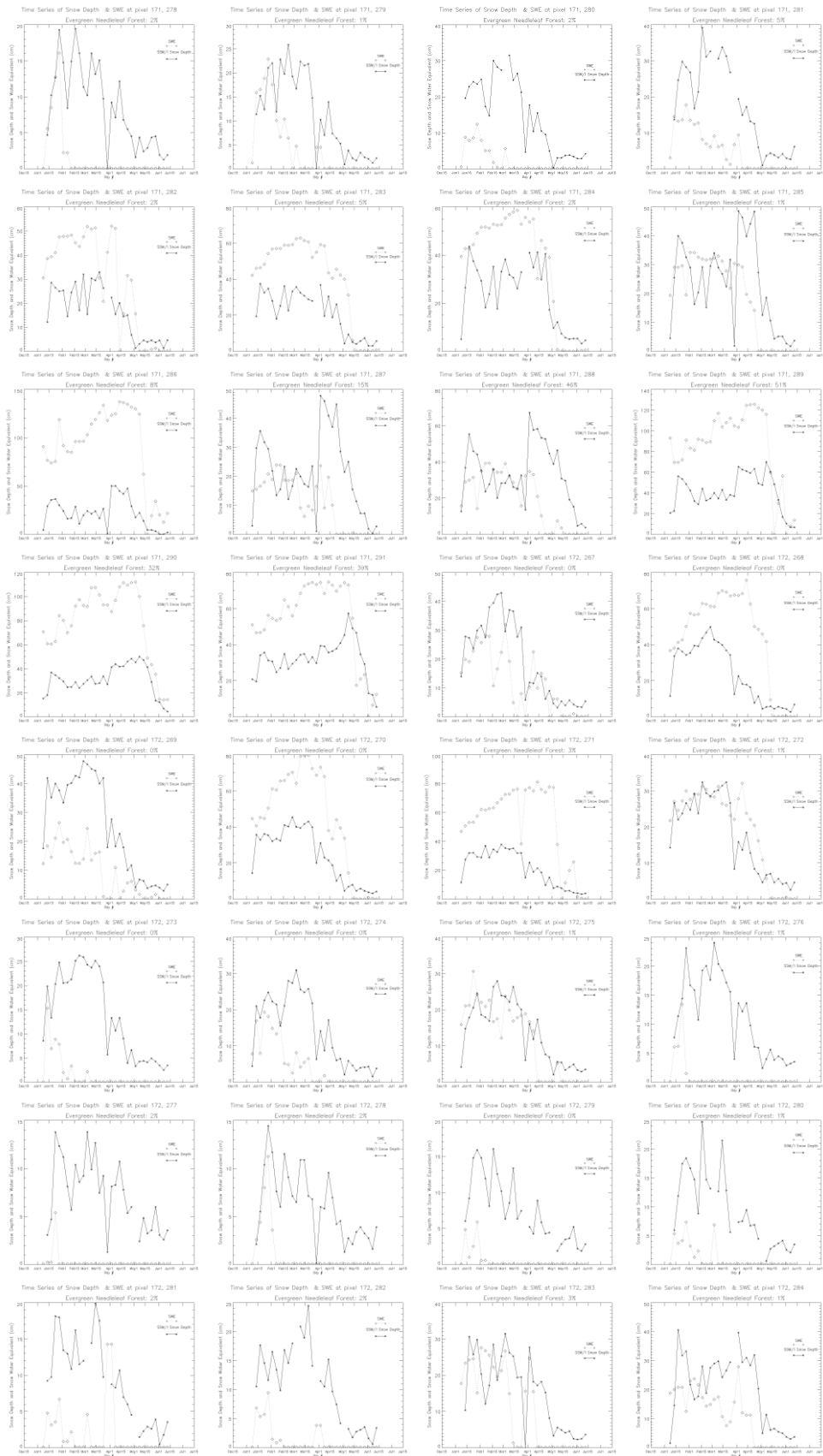


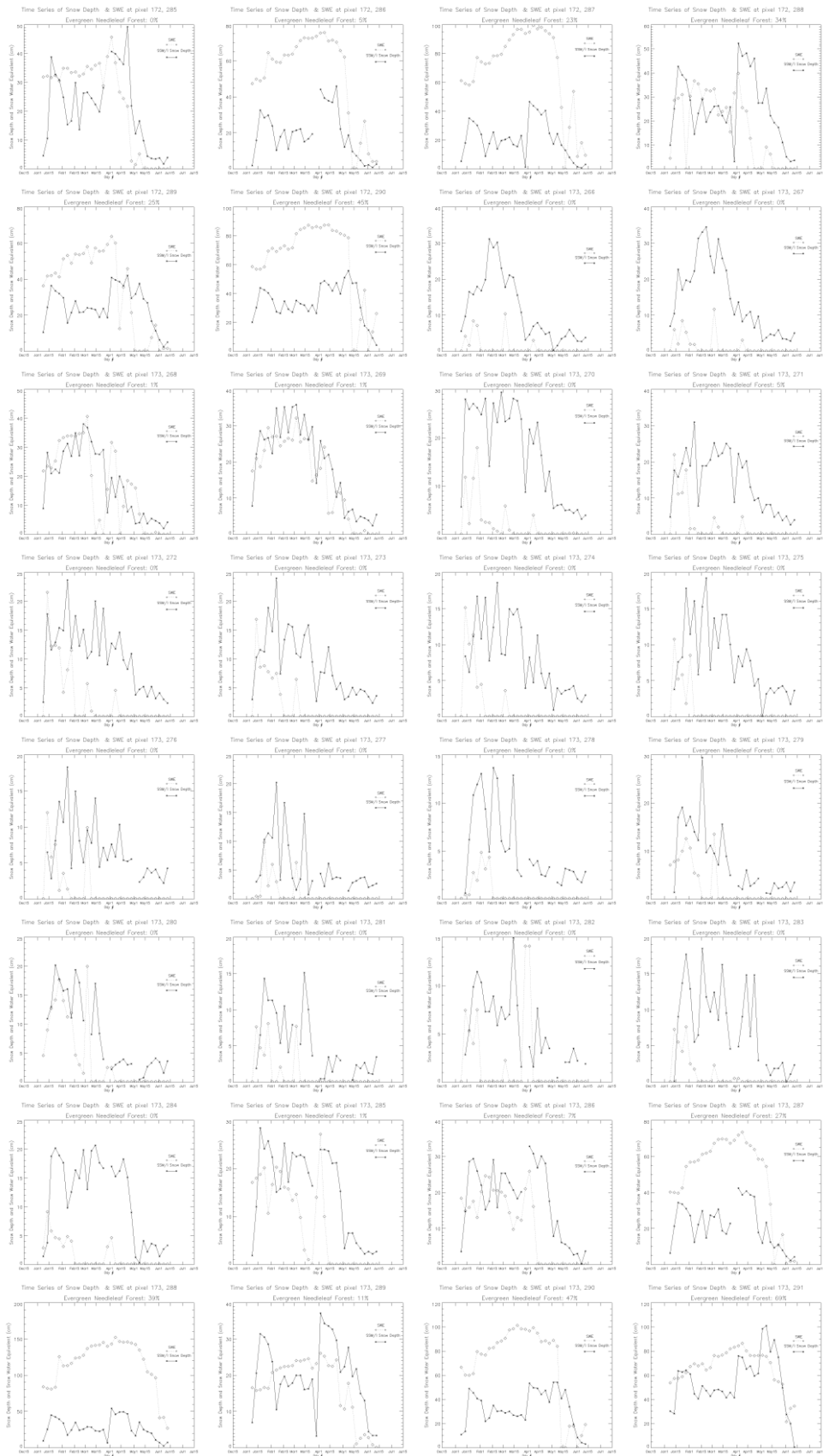
Appendix D

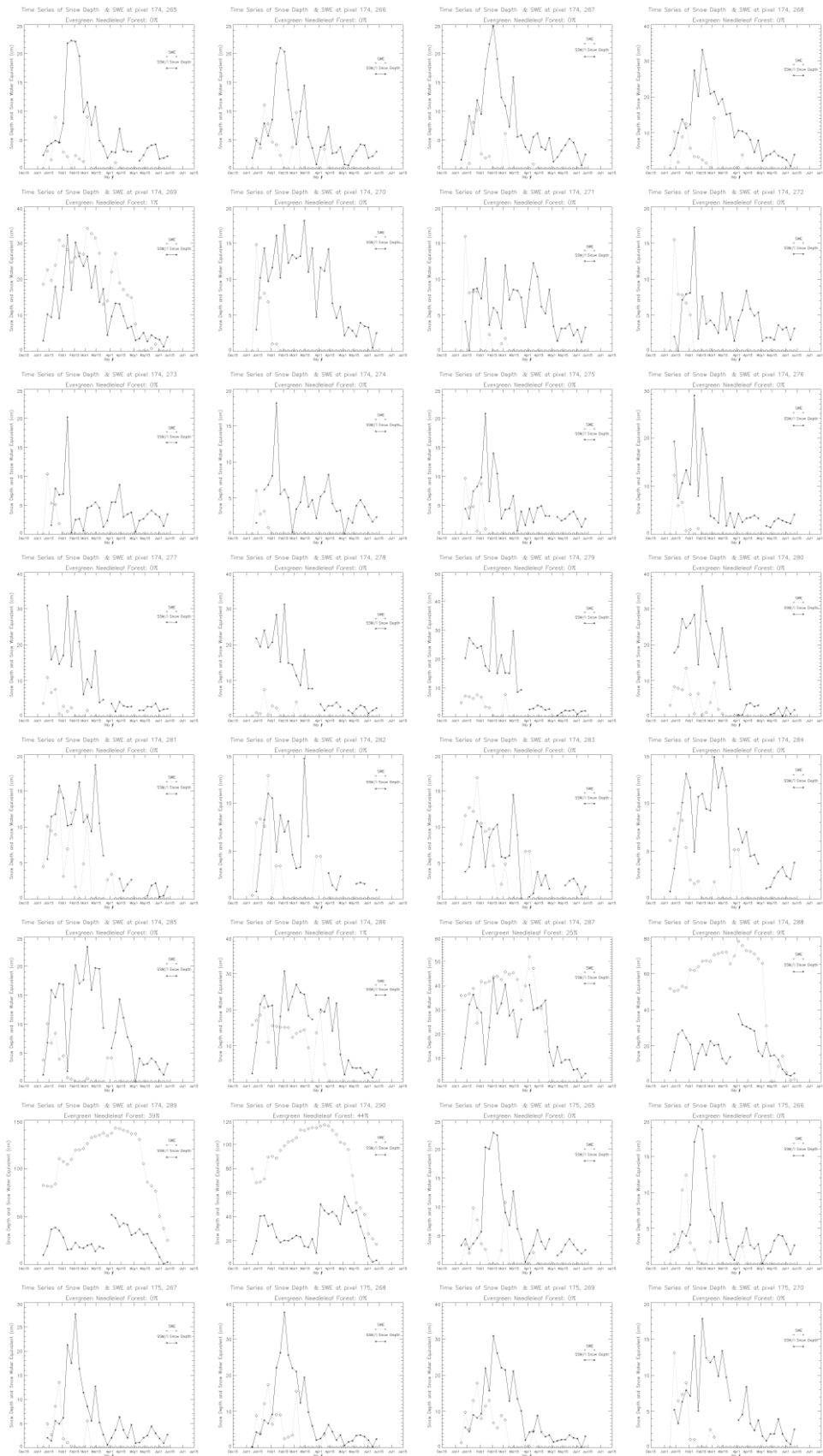
Time Series Graphs of SSM/I Snow Depth and NOHRSC SWE for Pixels in the Columbia Basin

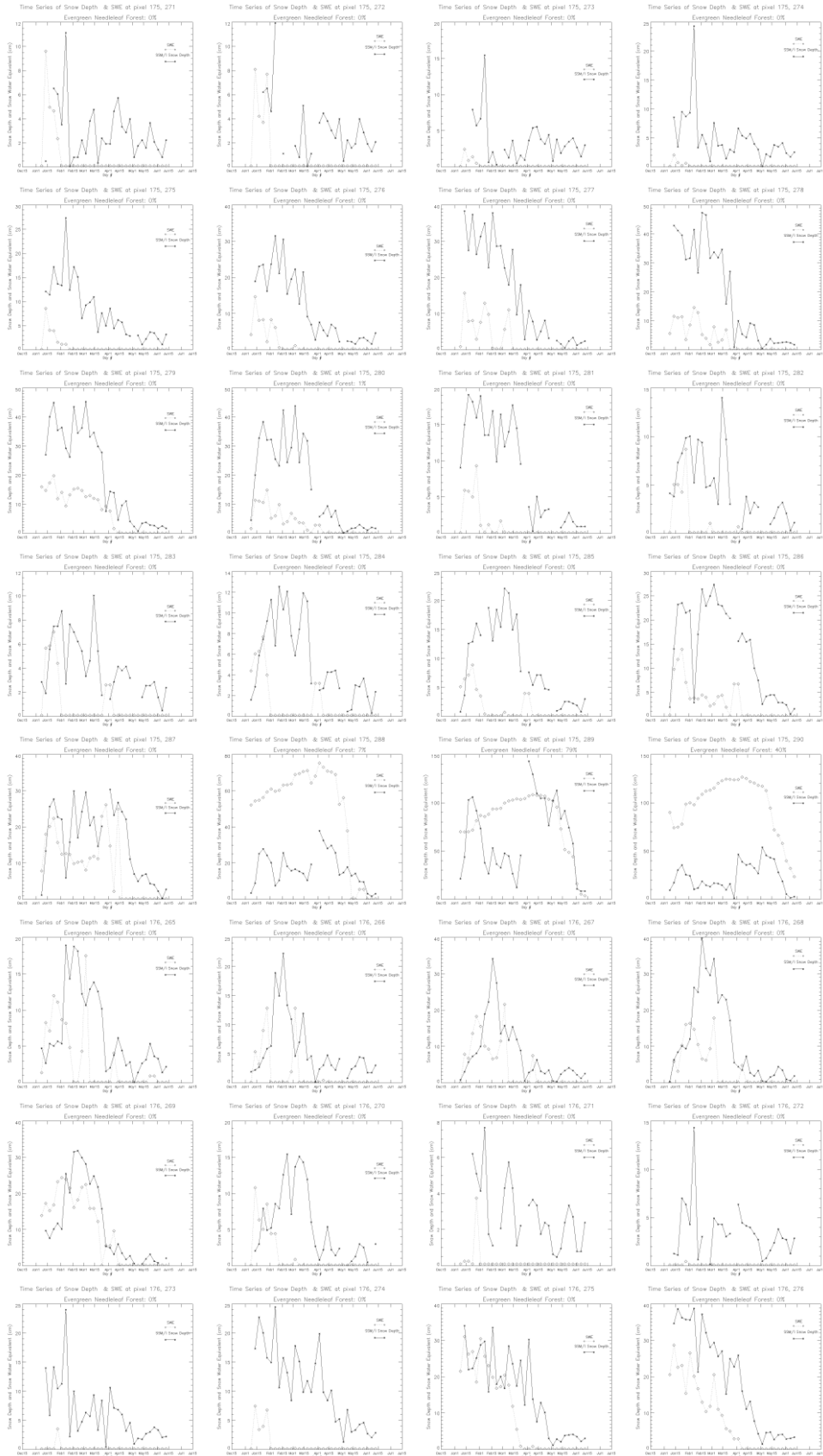
The index map #2 in Appendix A gives the (column, row) coordinates that identify the pixels in the Columbia Basin.

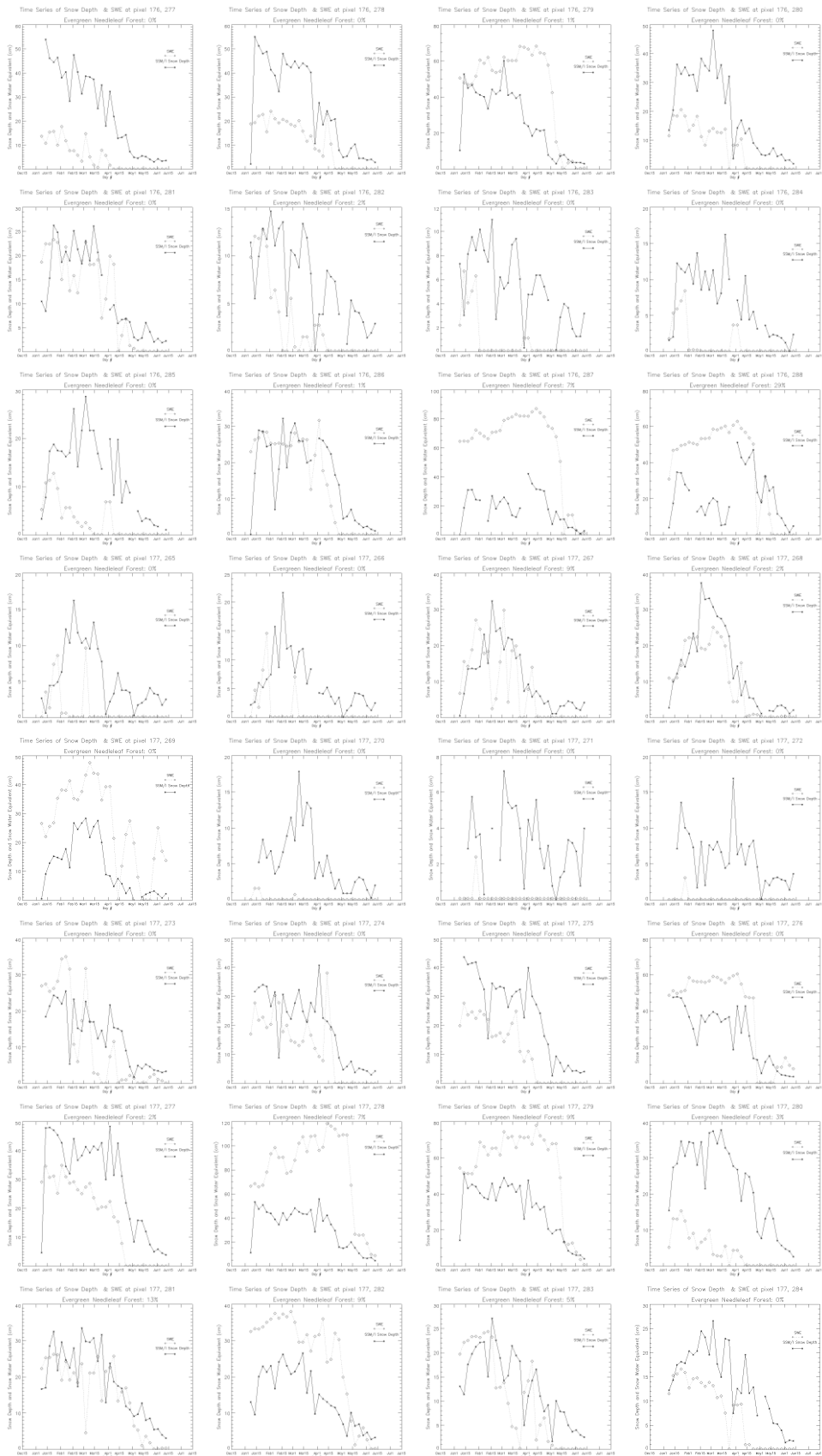


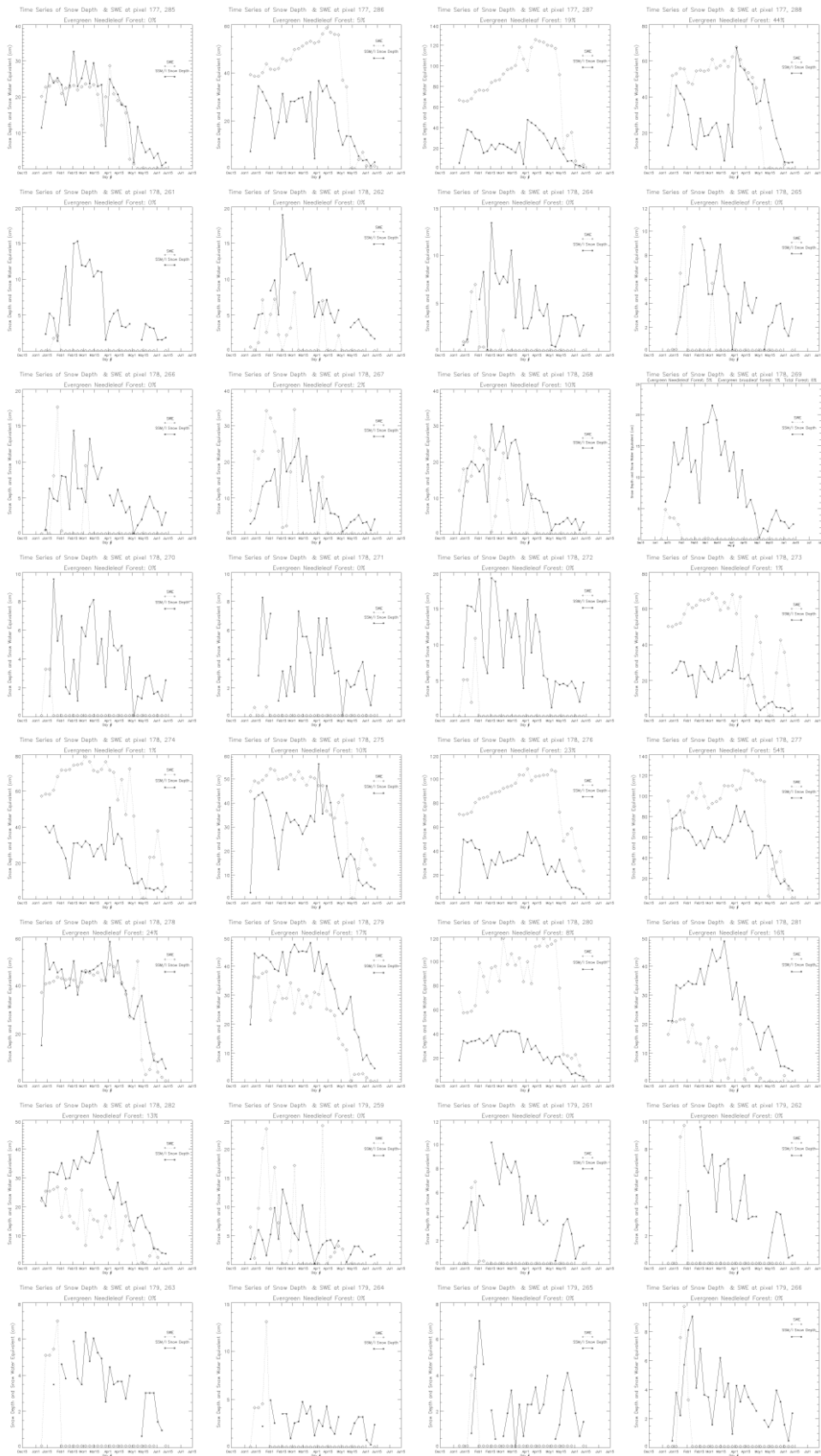


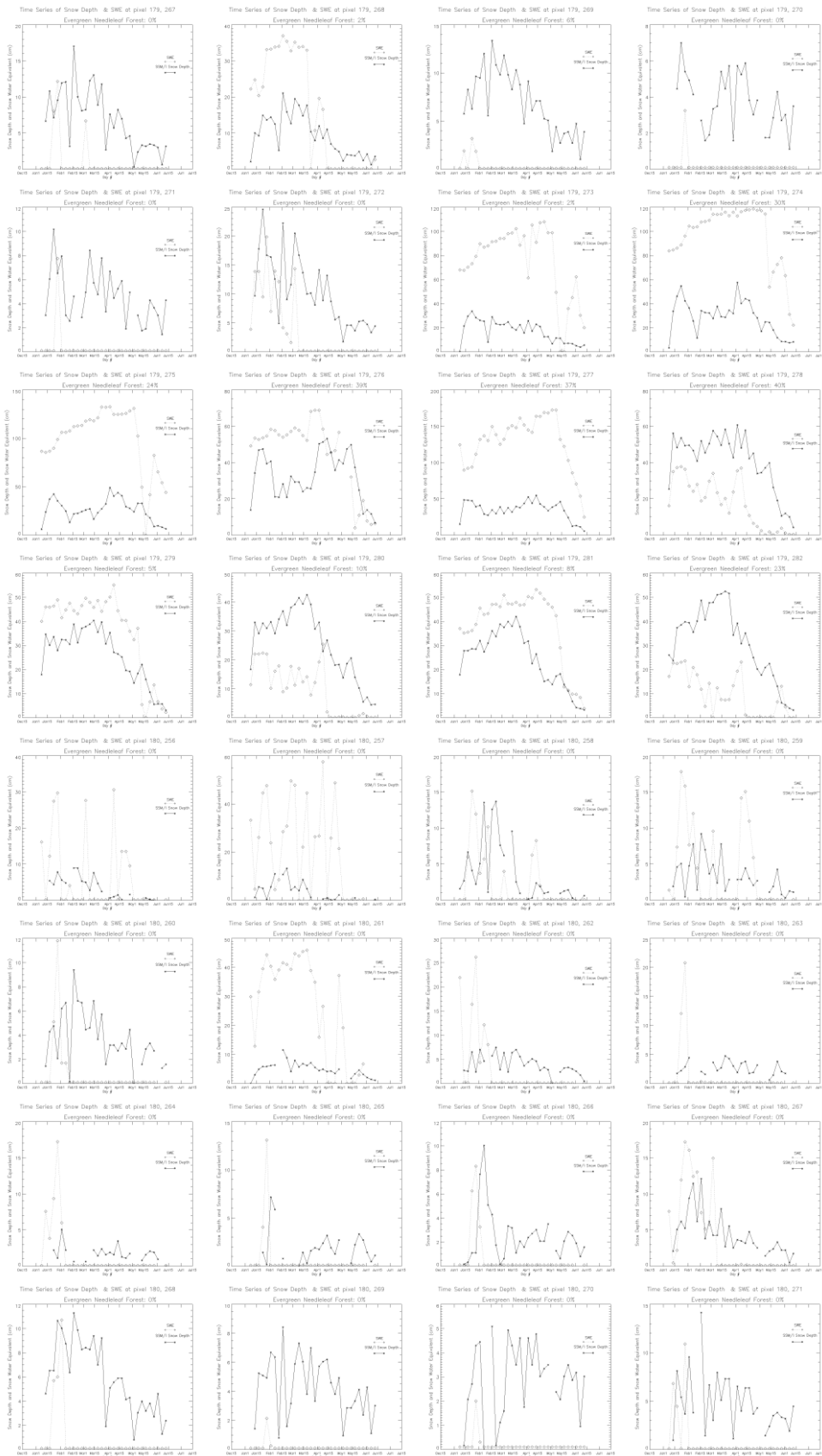


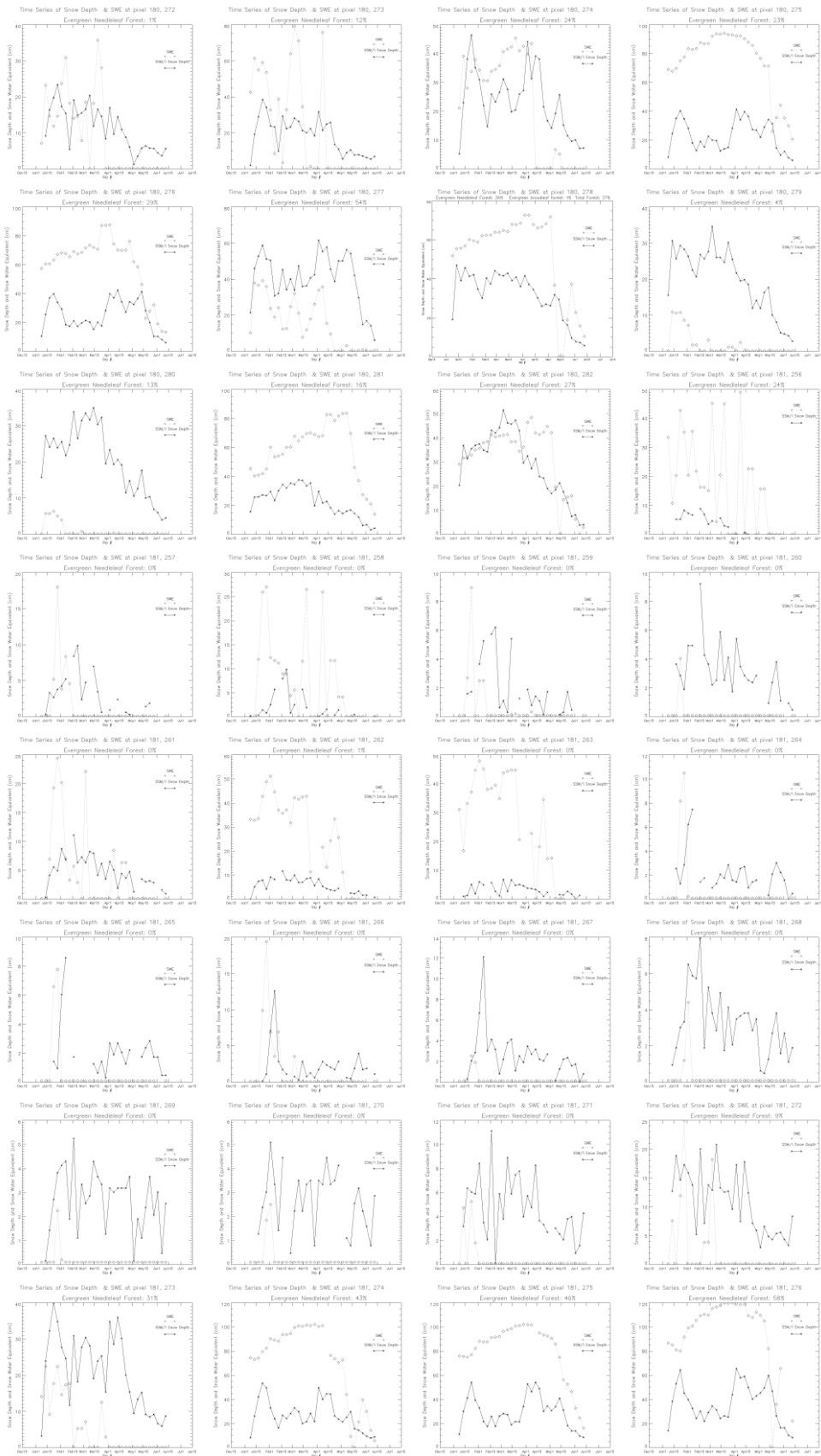


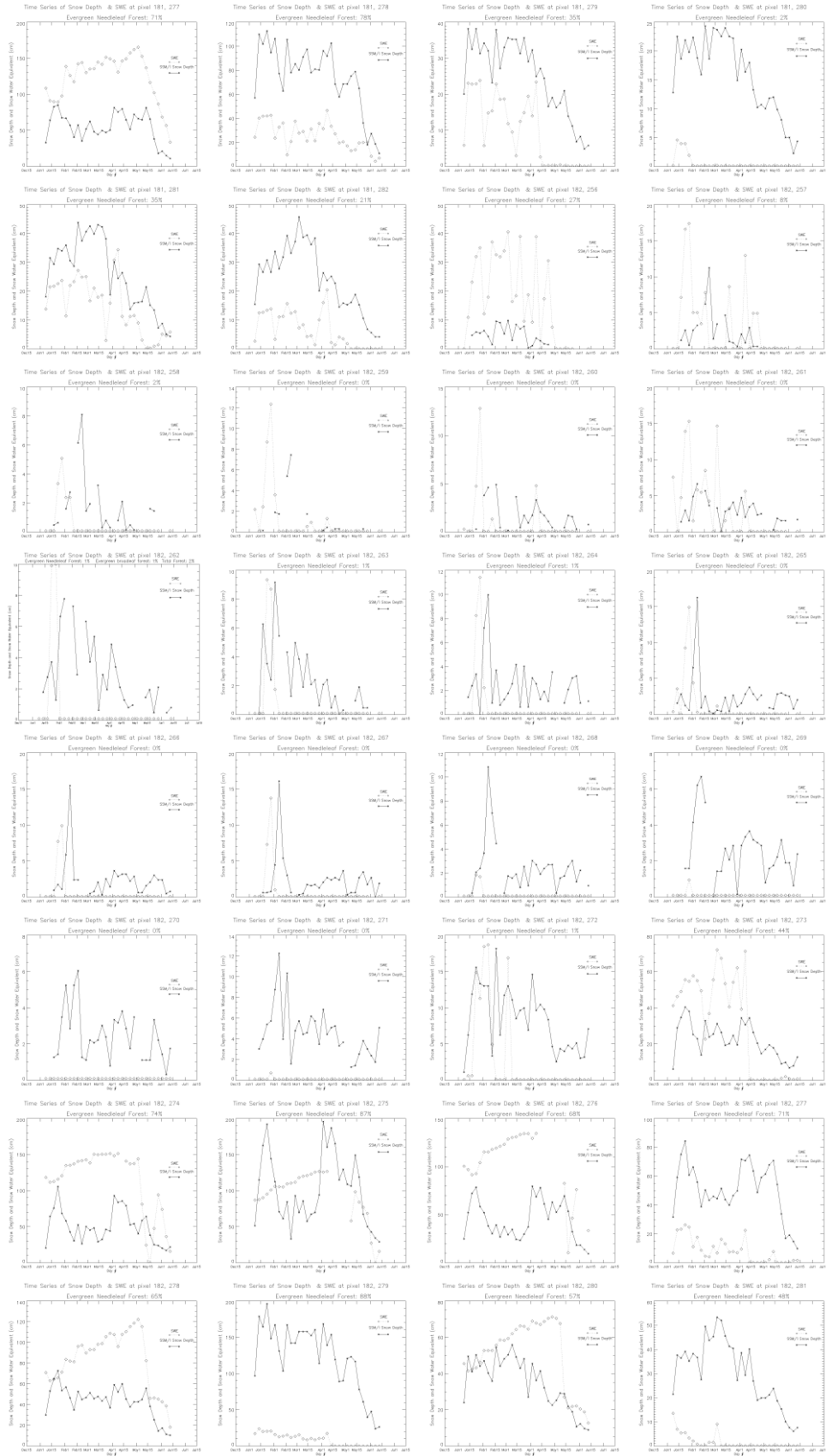


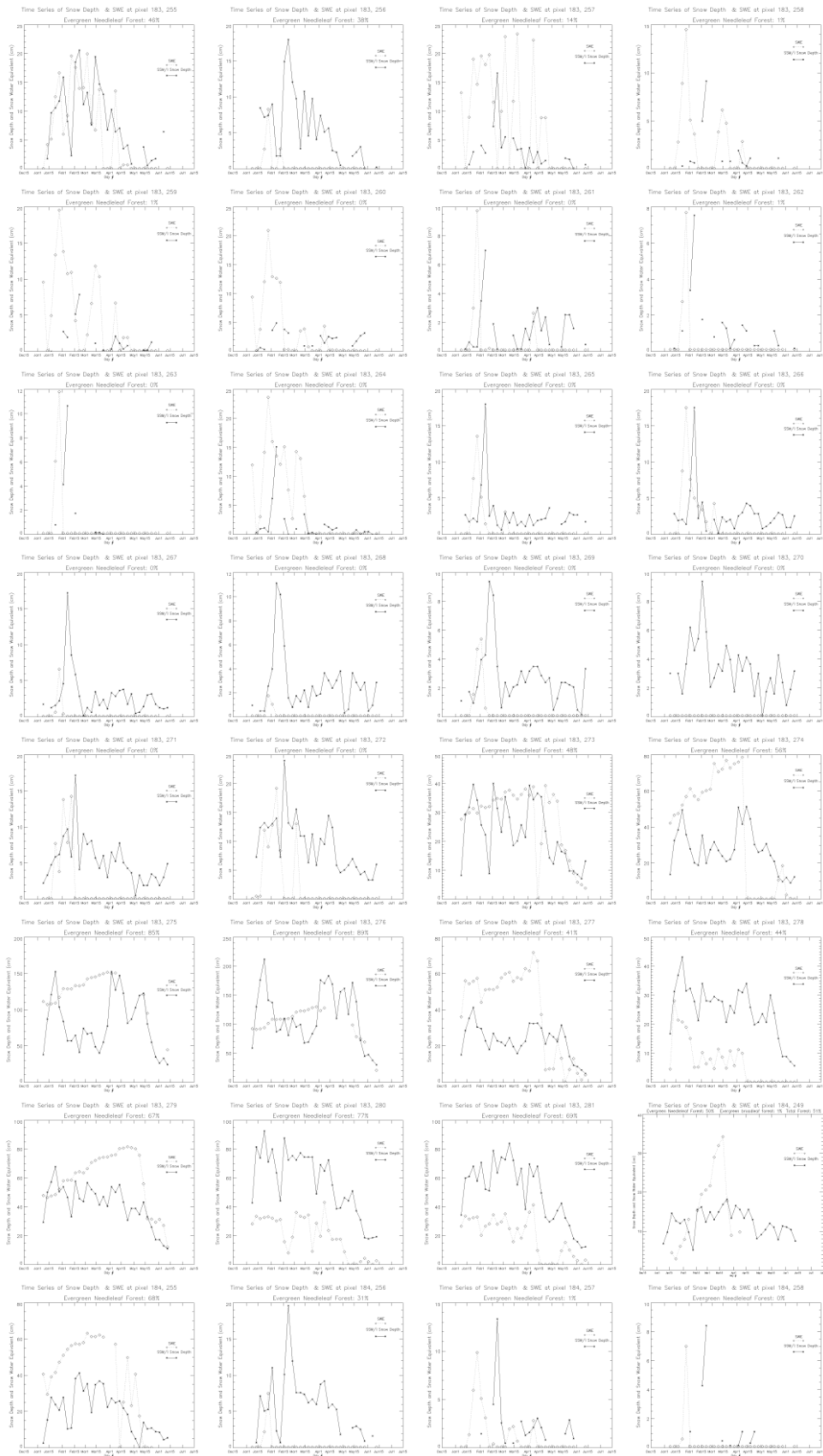


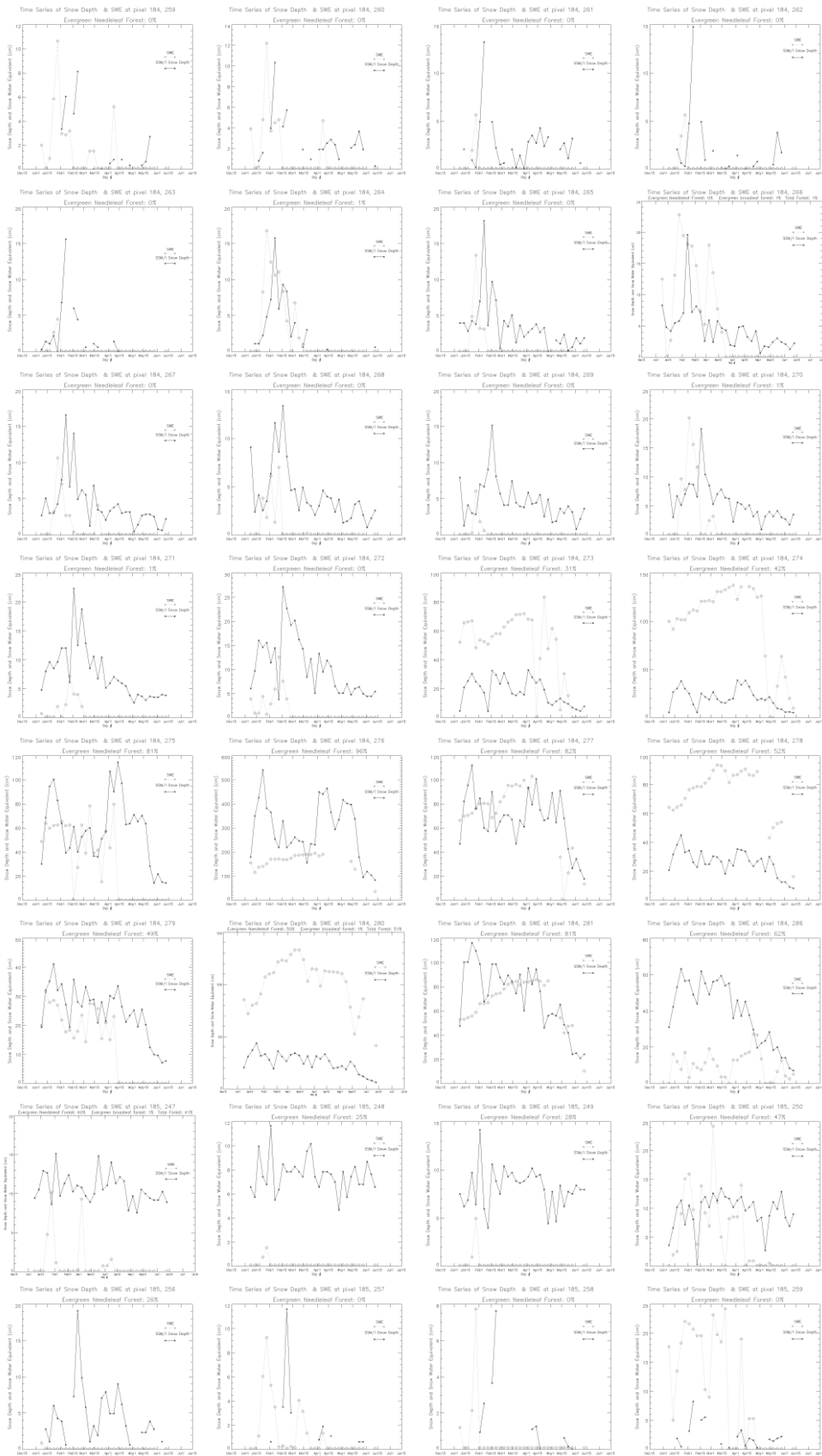


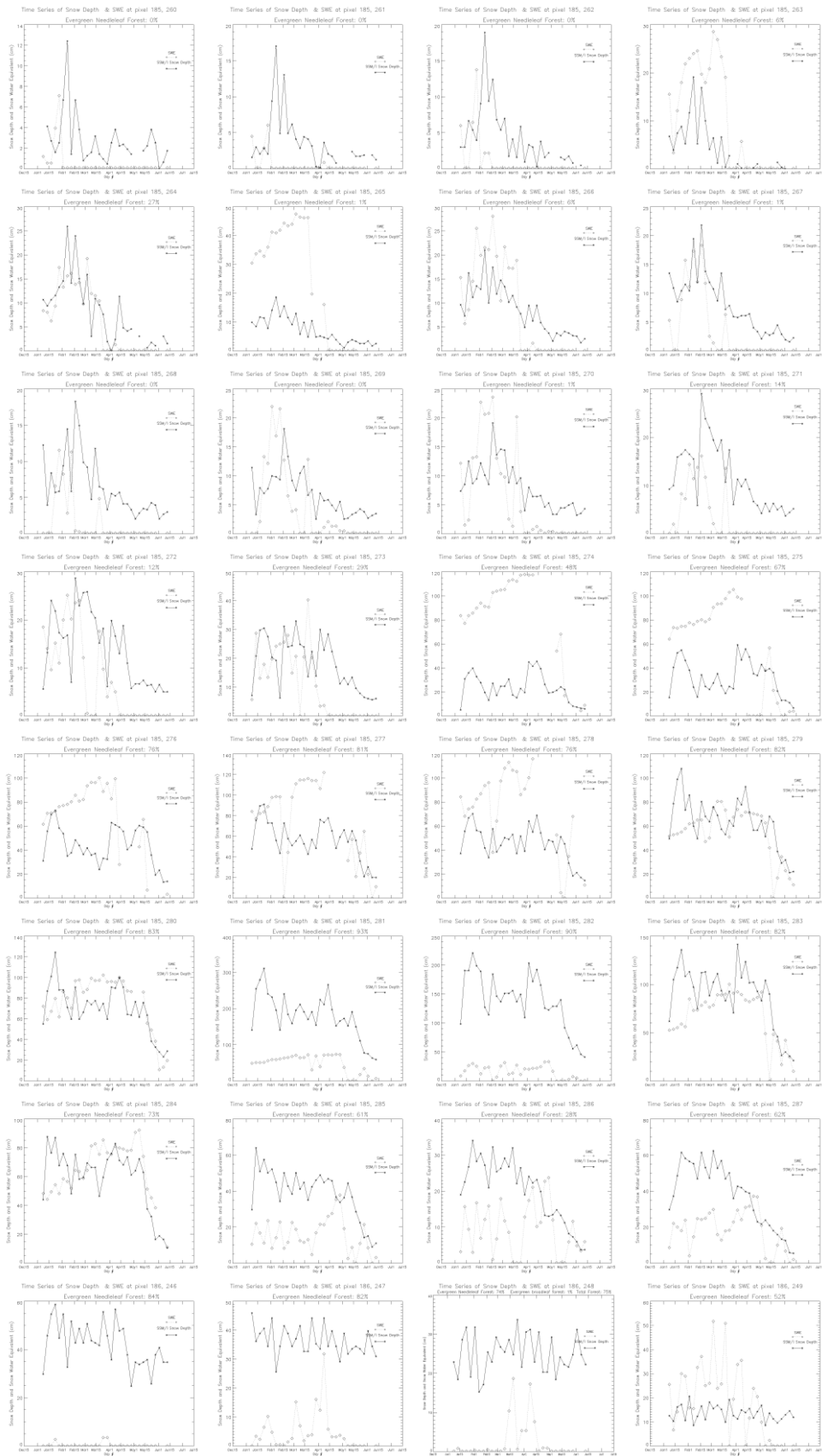


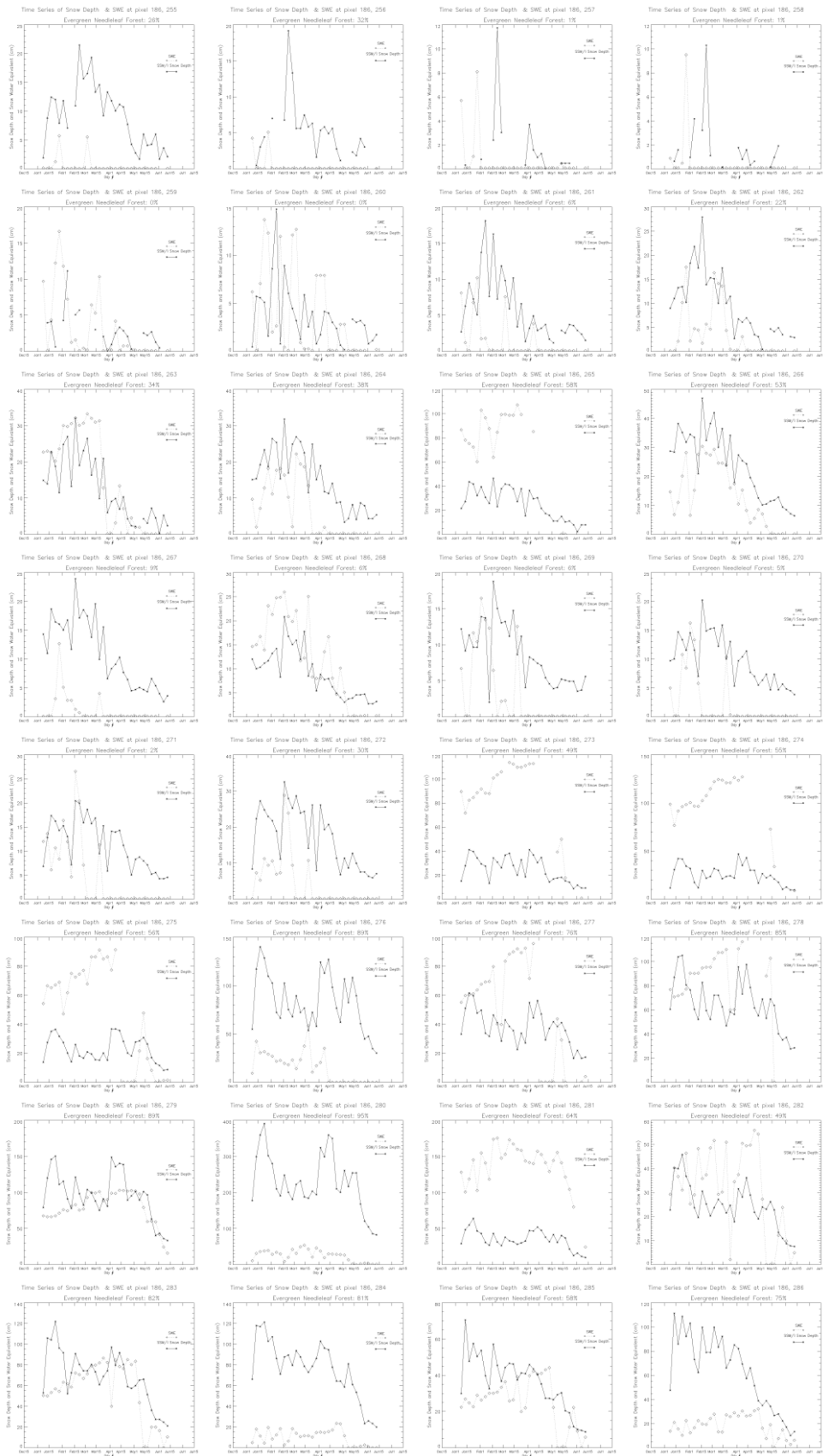


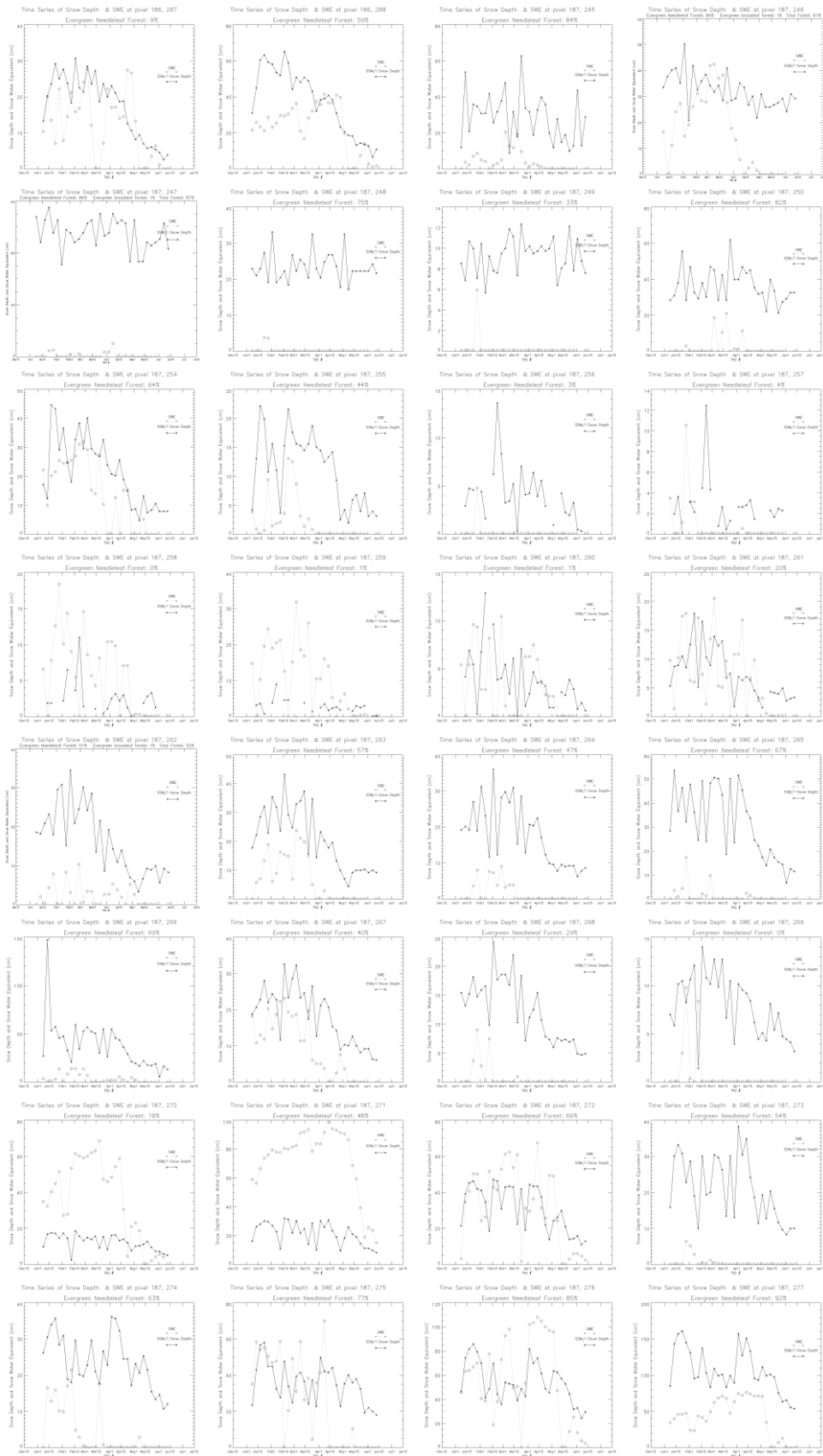


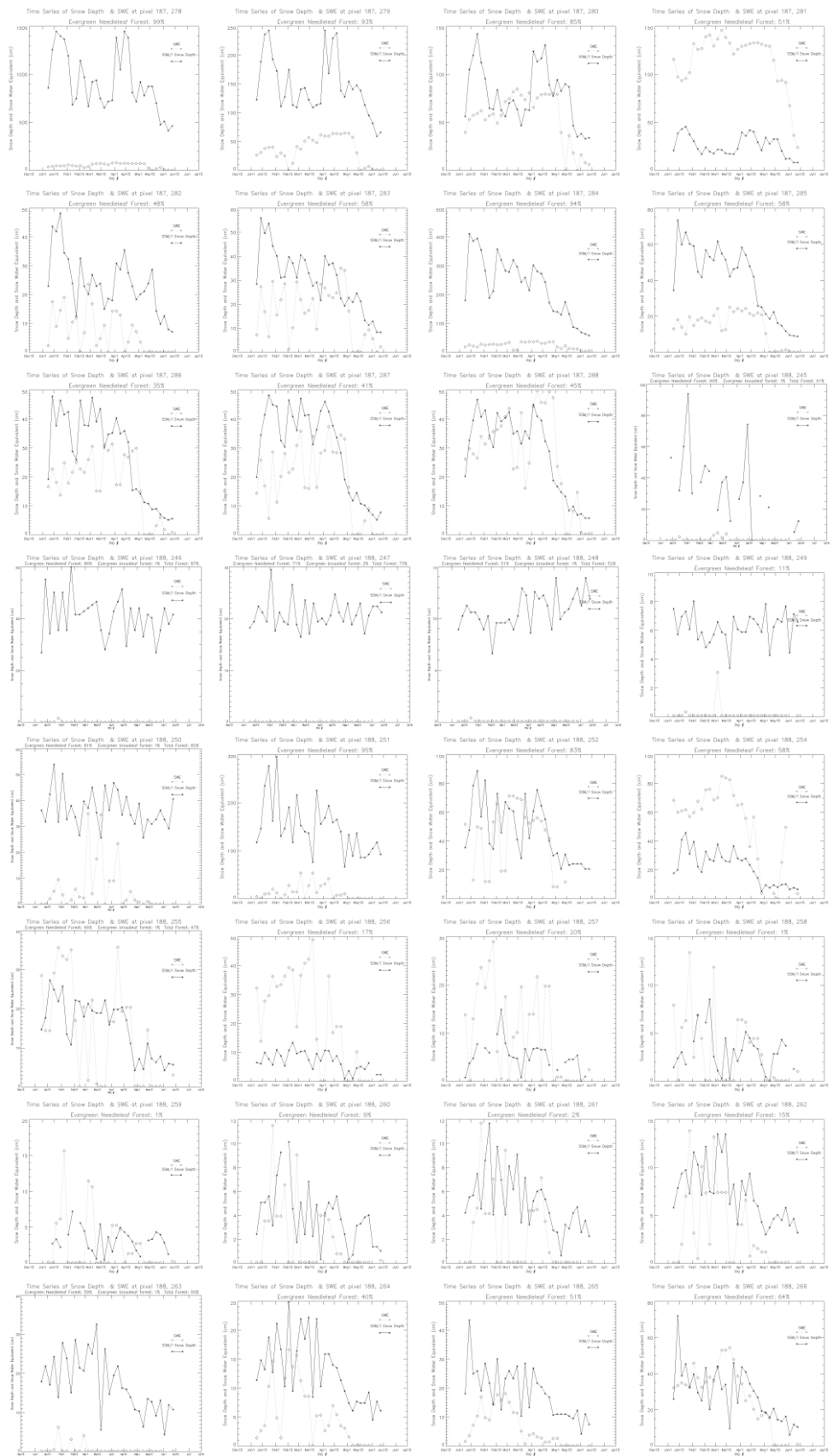


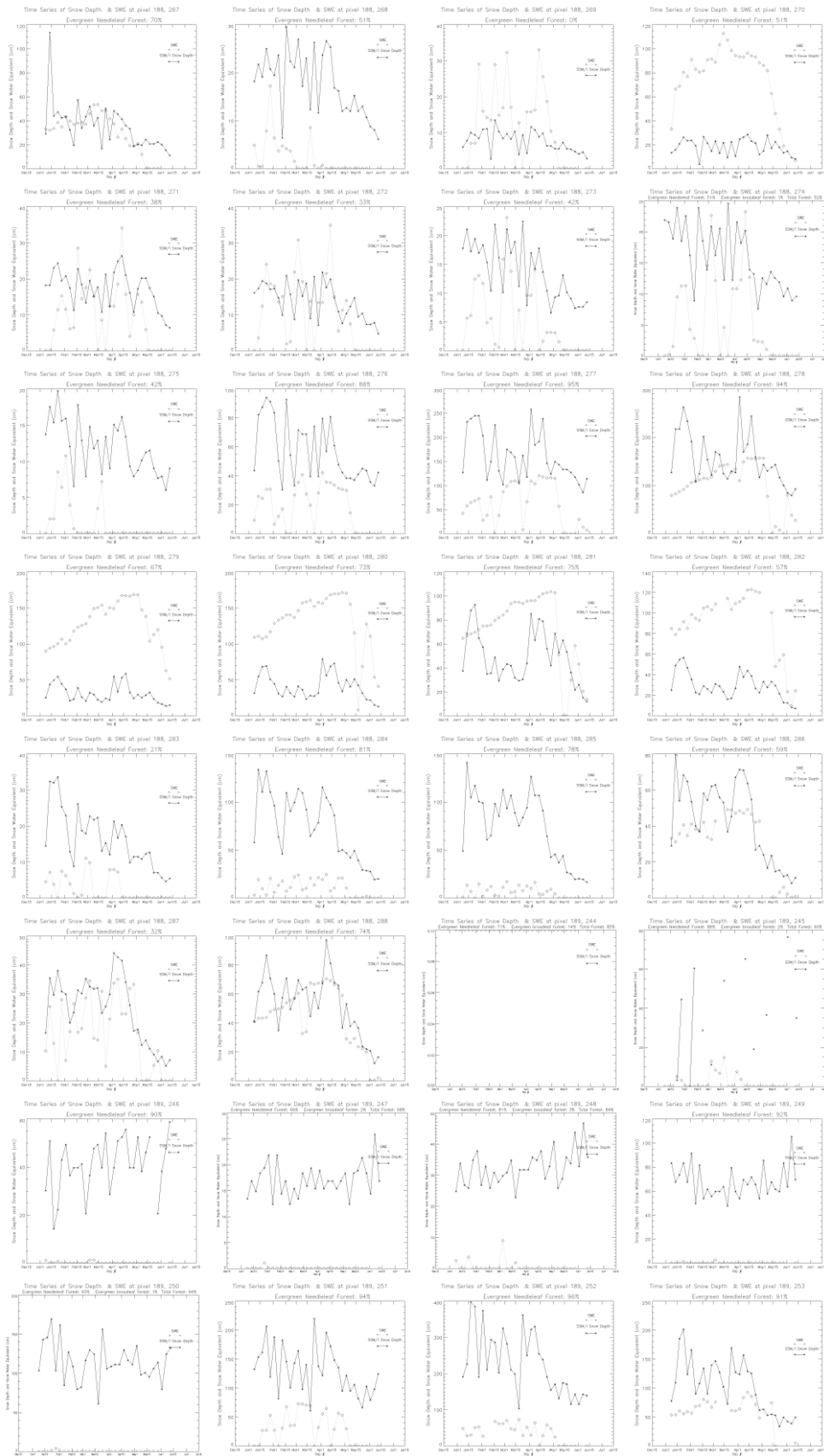


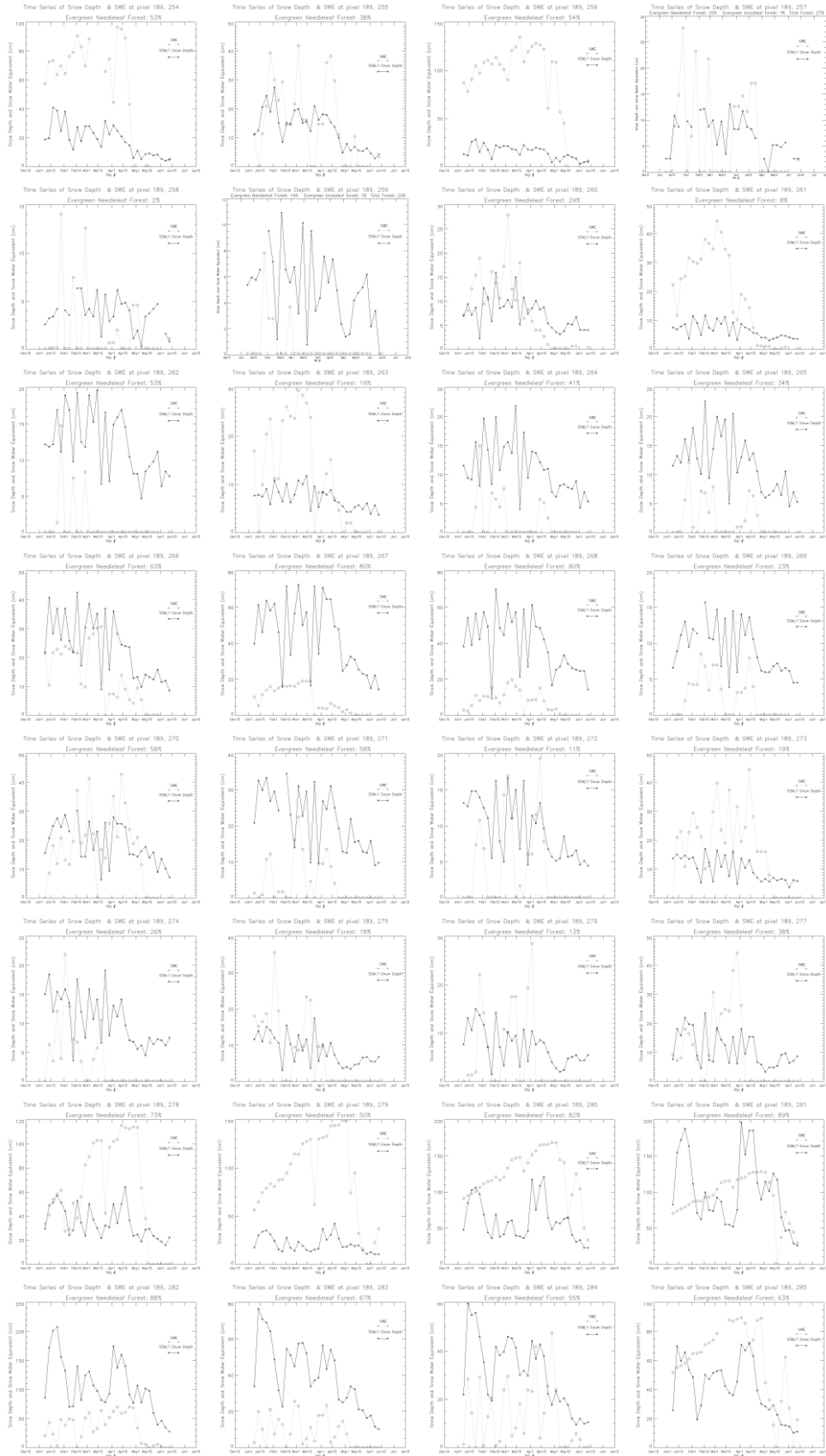


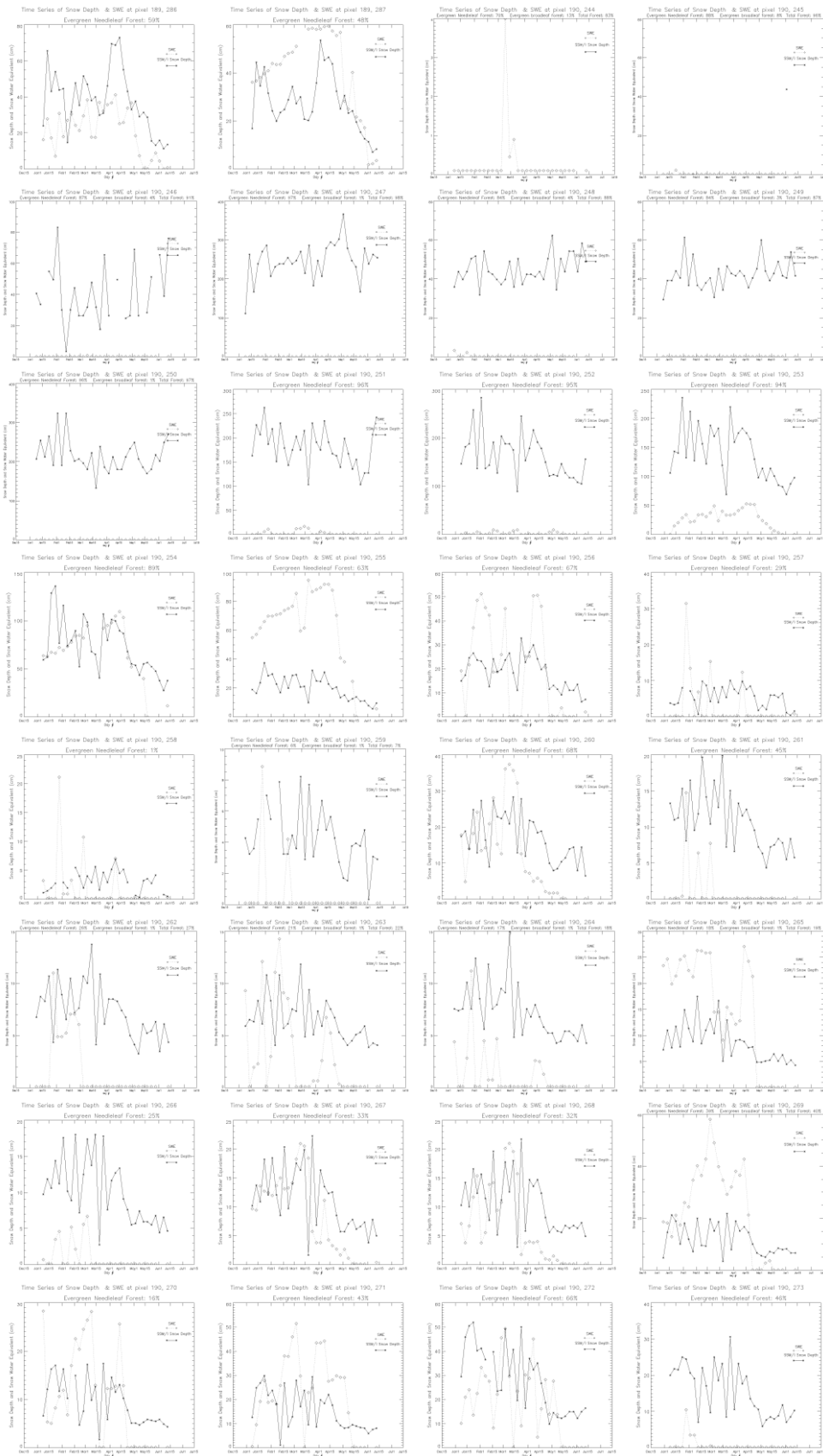


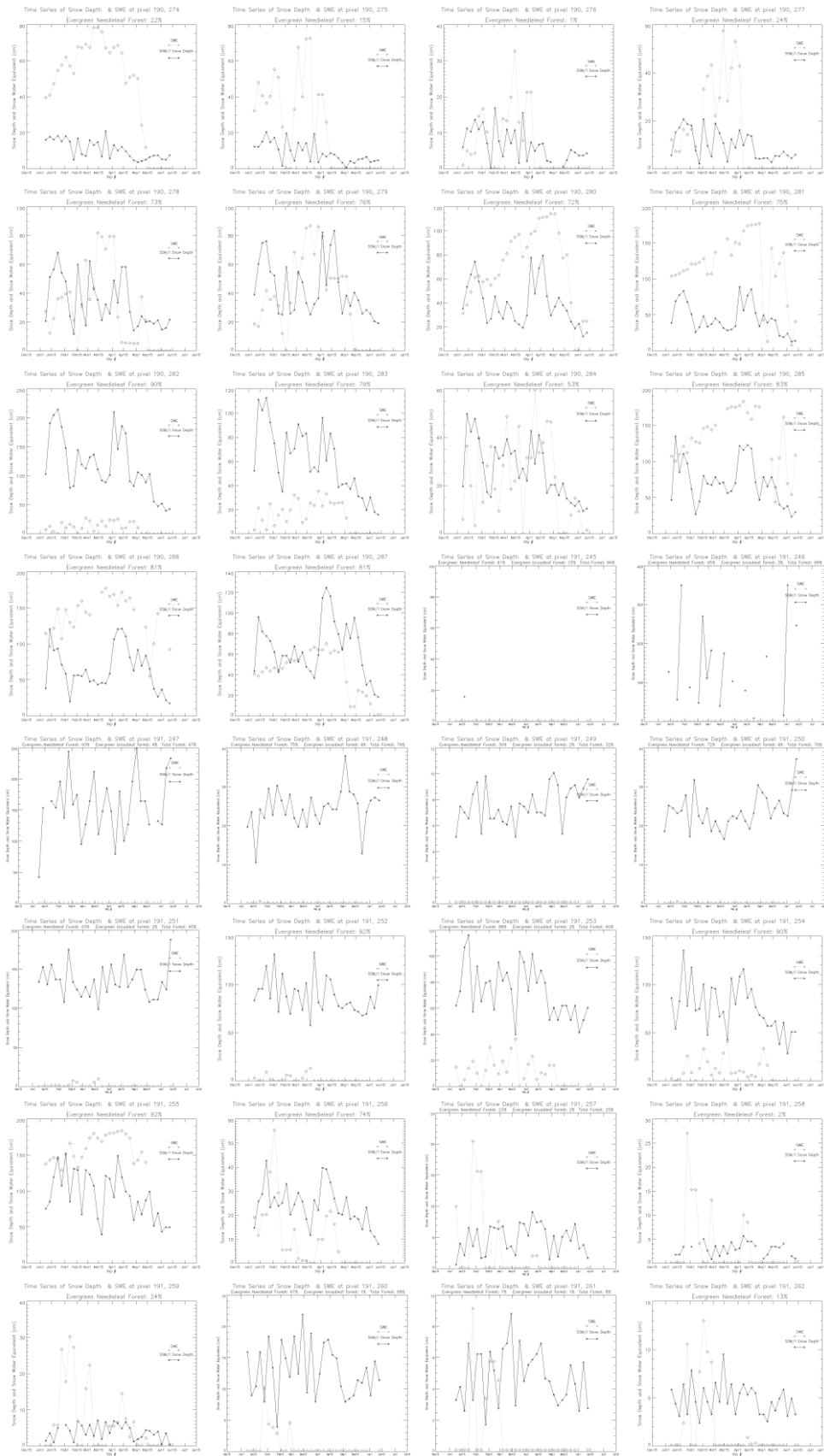


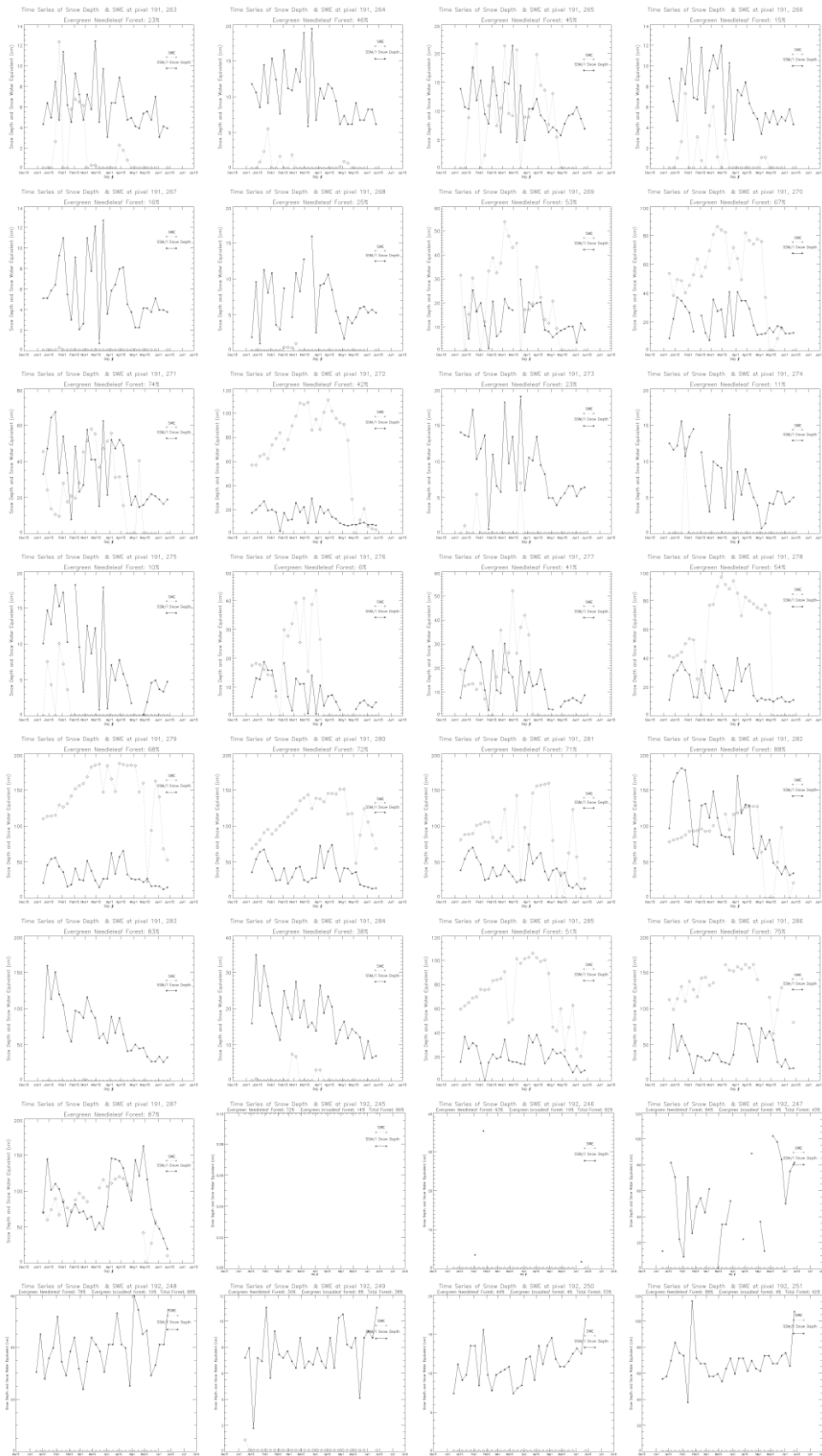


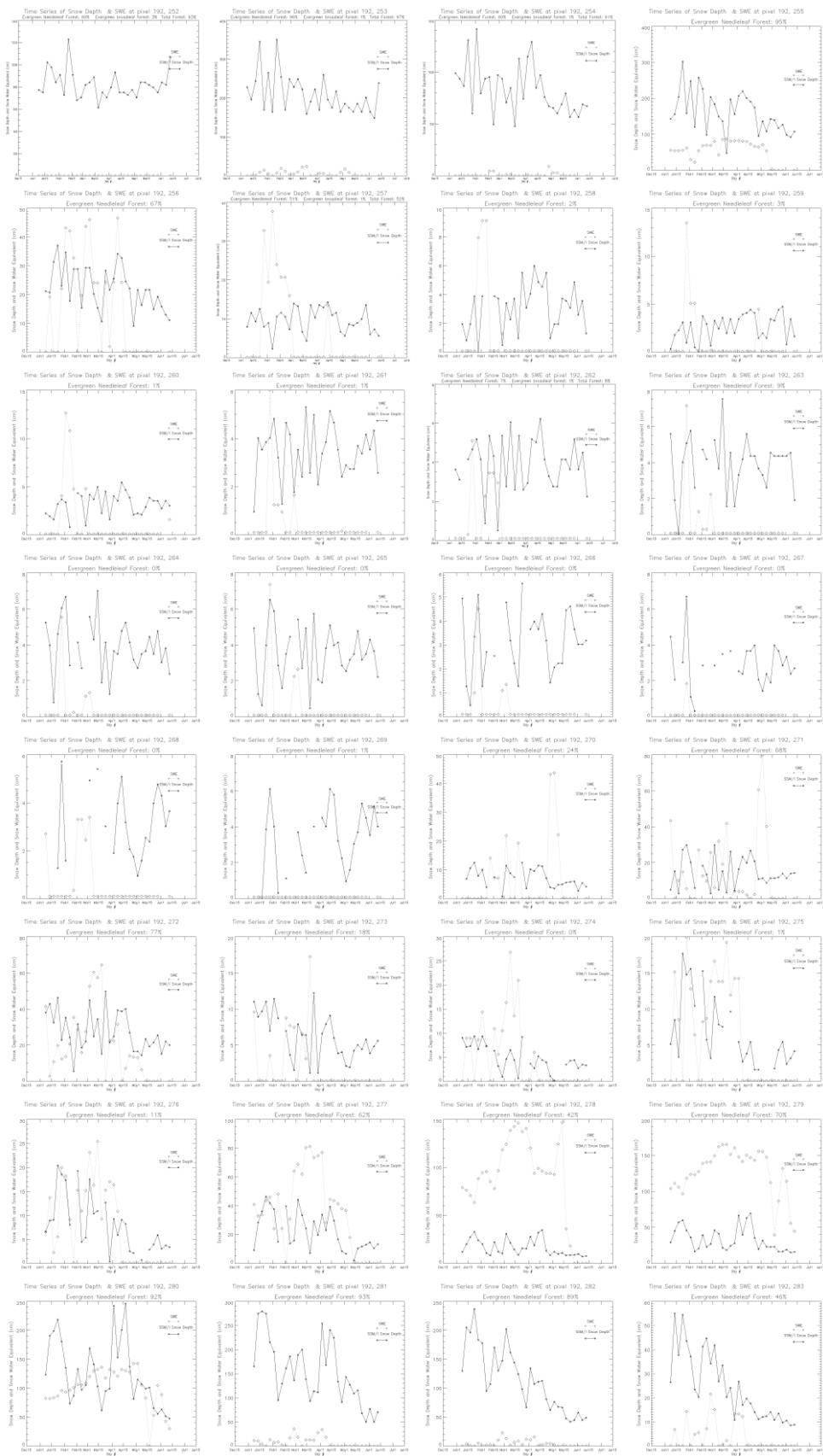




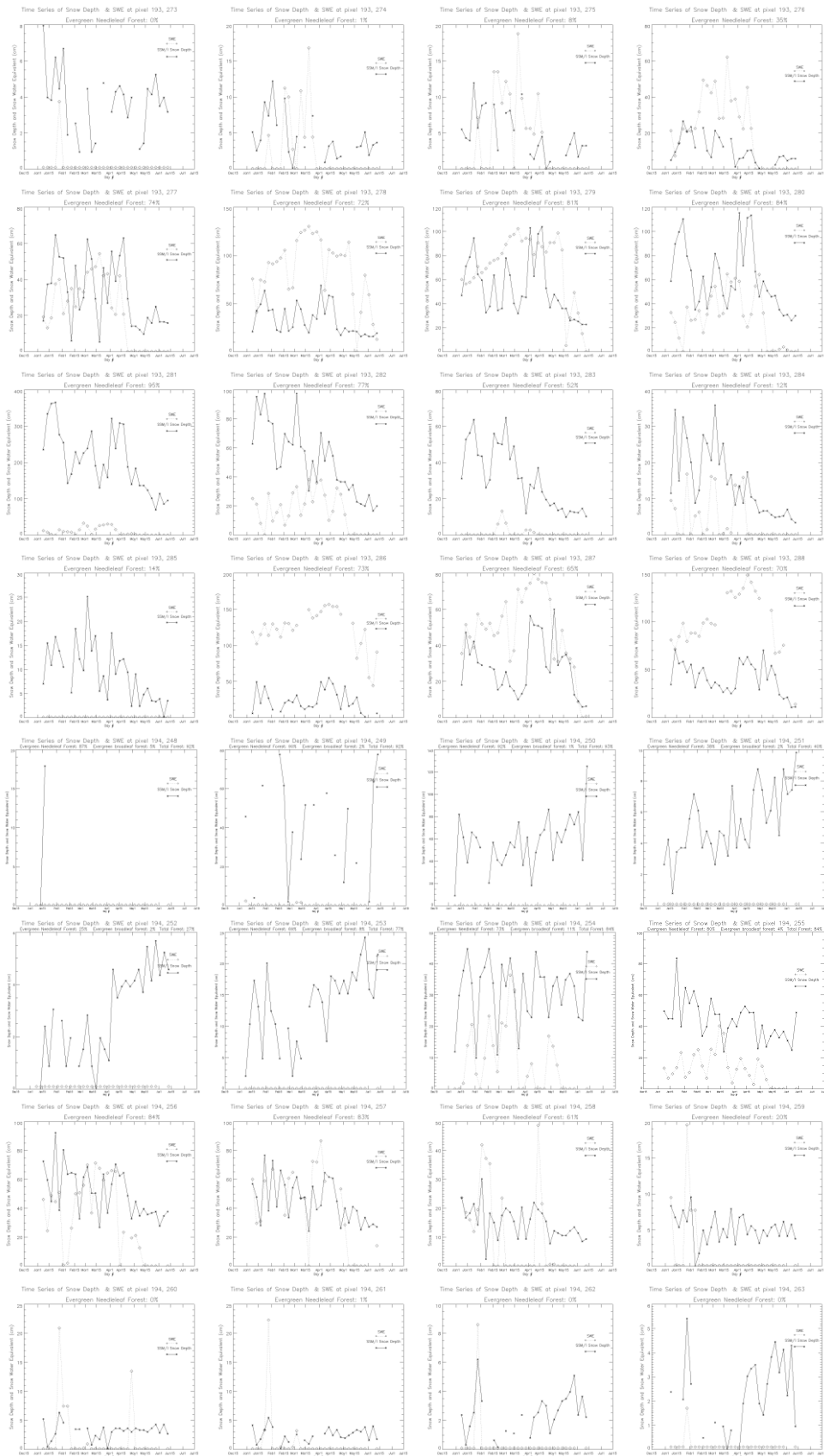


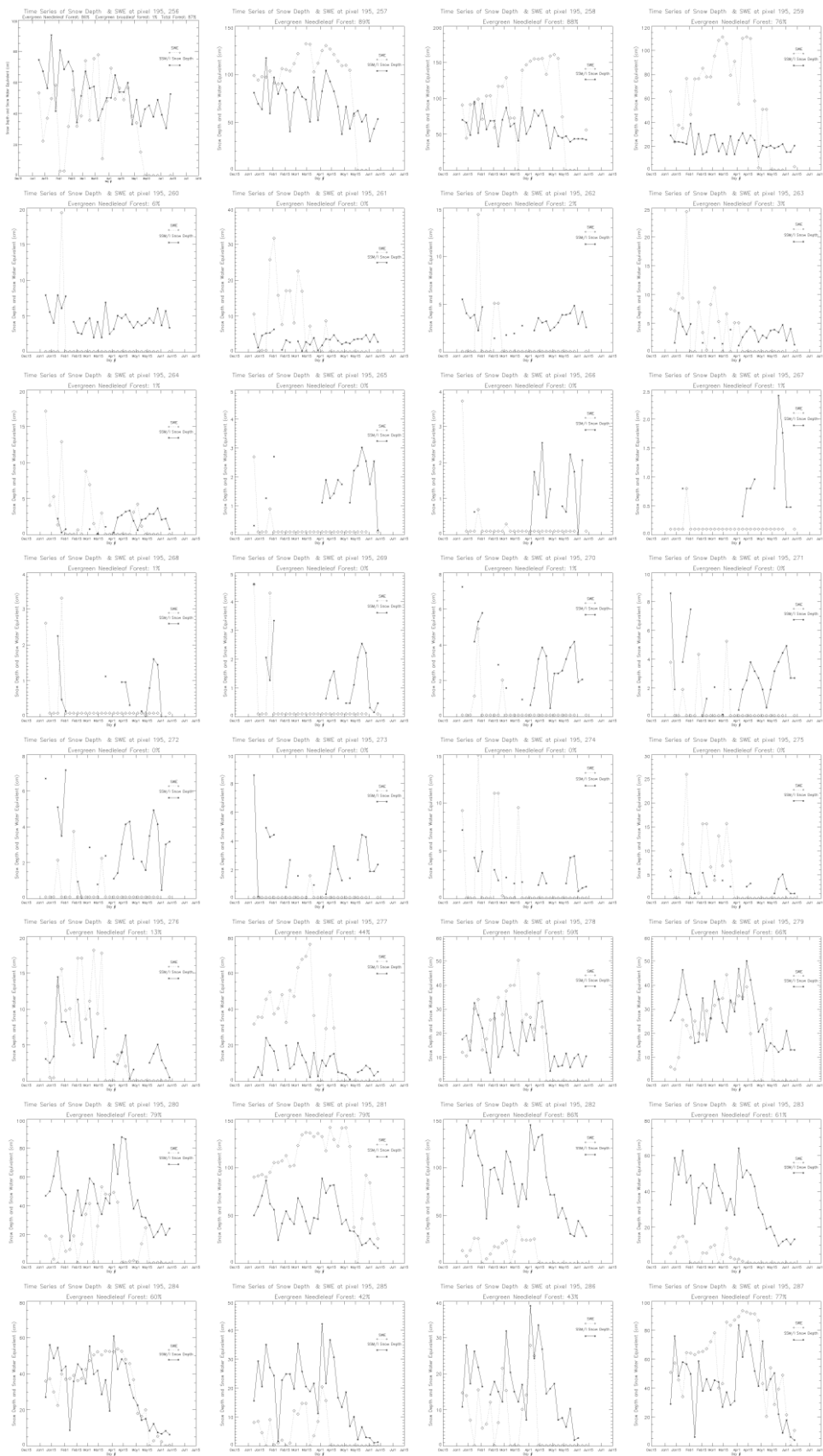


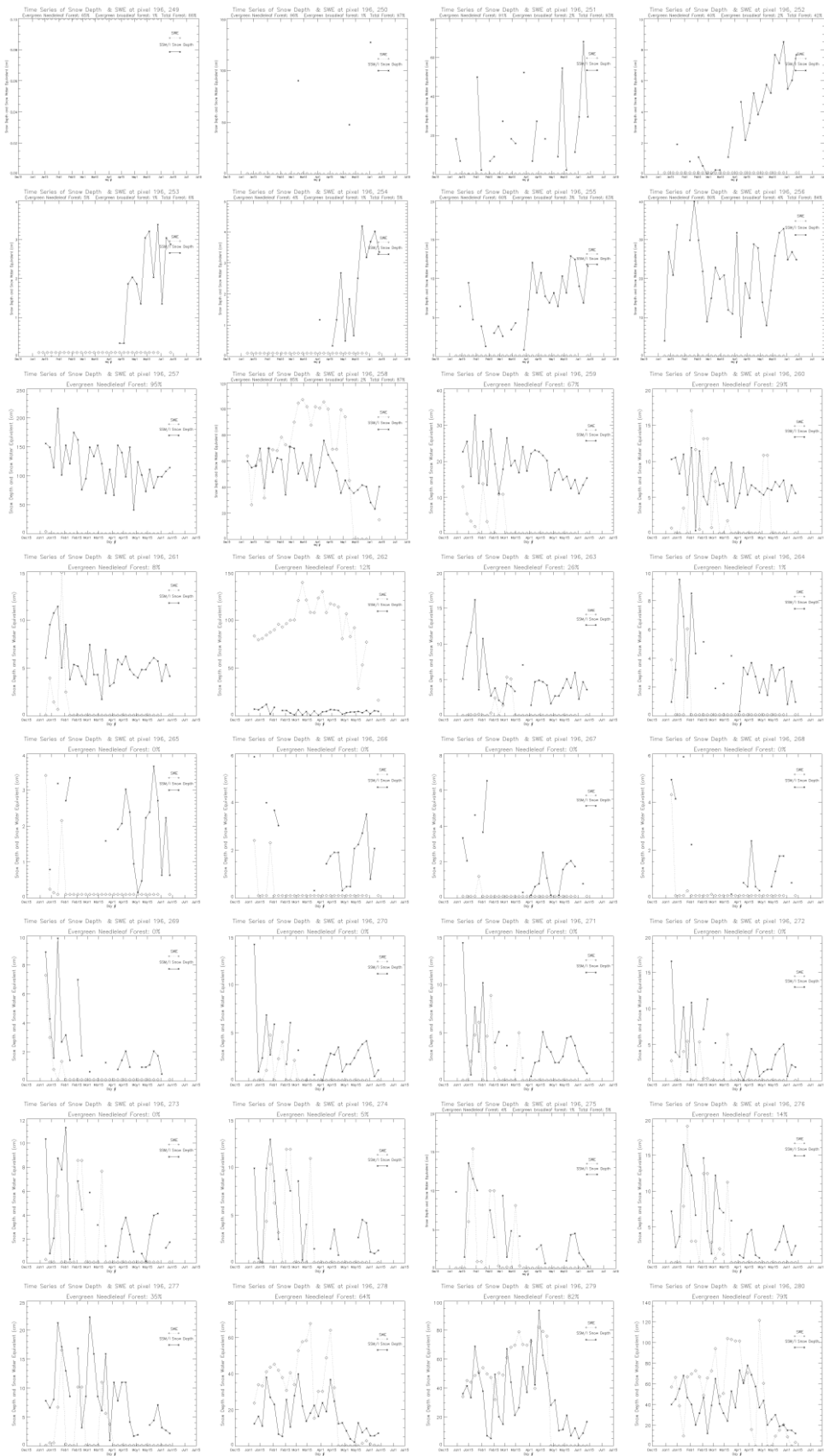


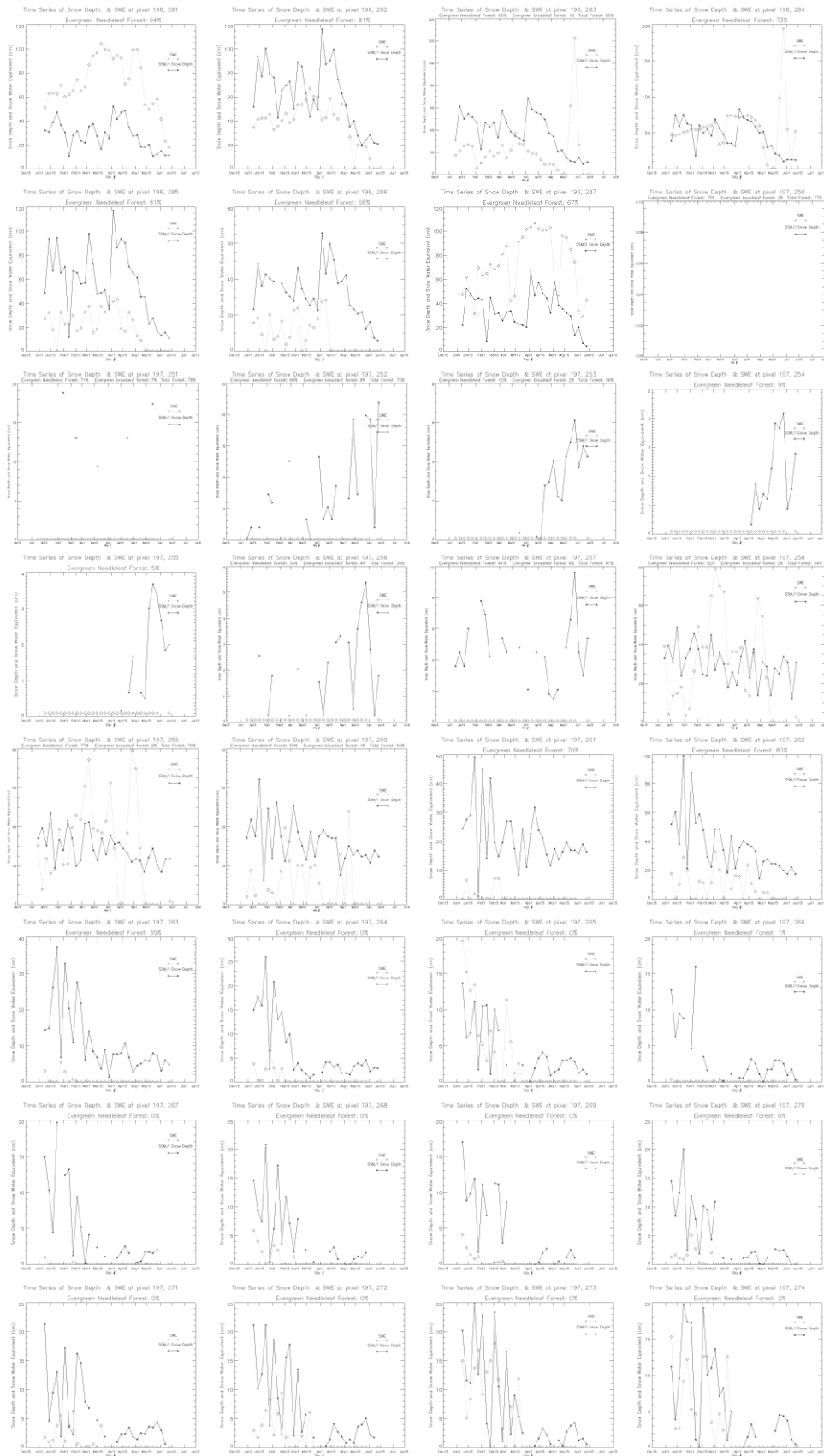


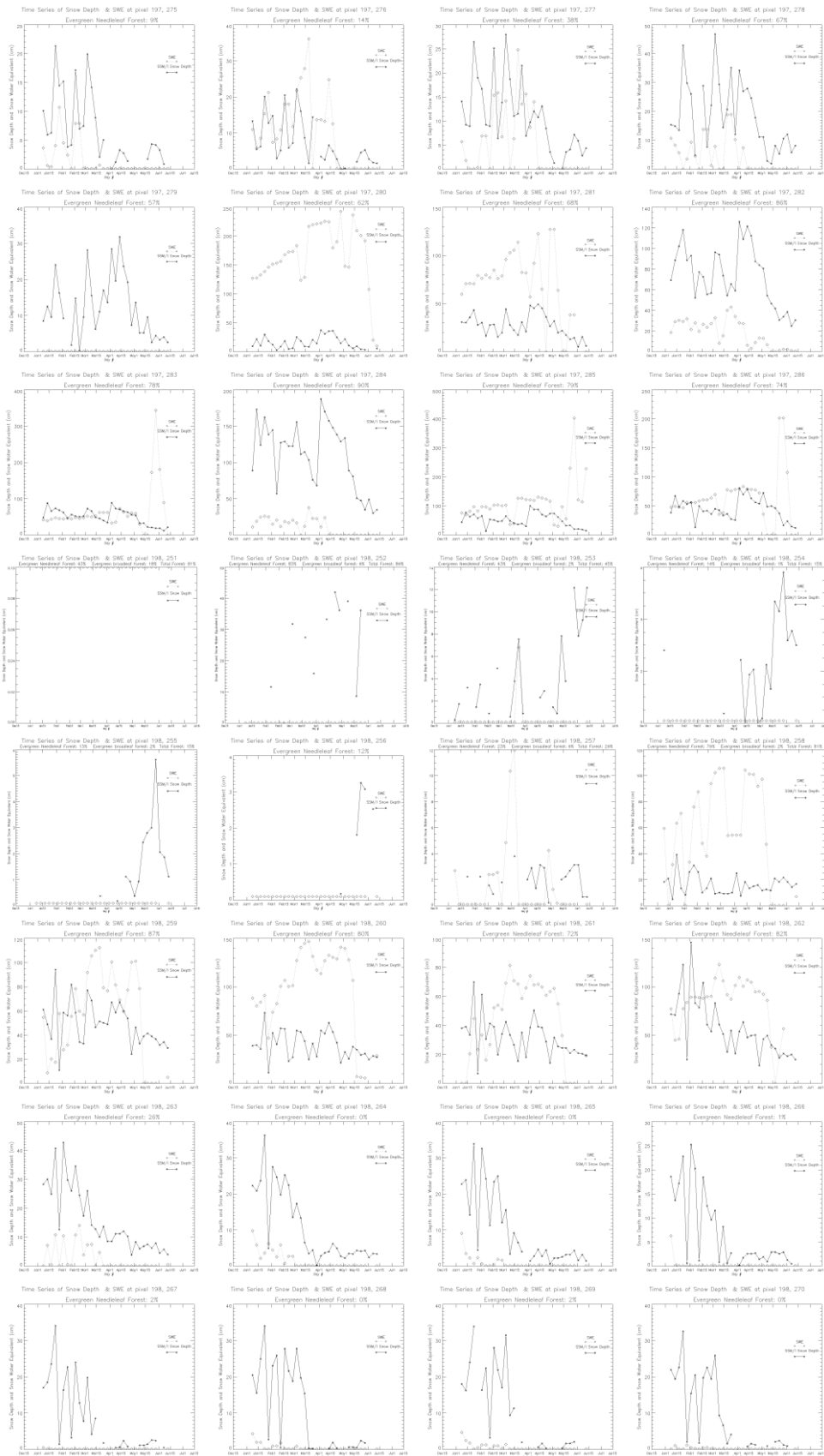


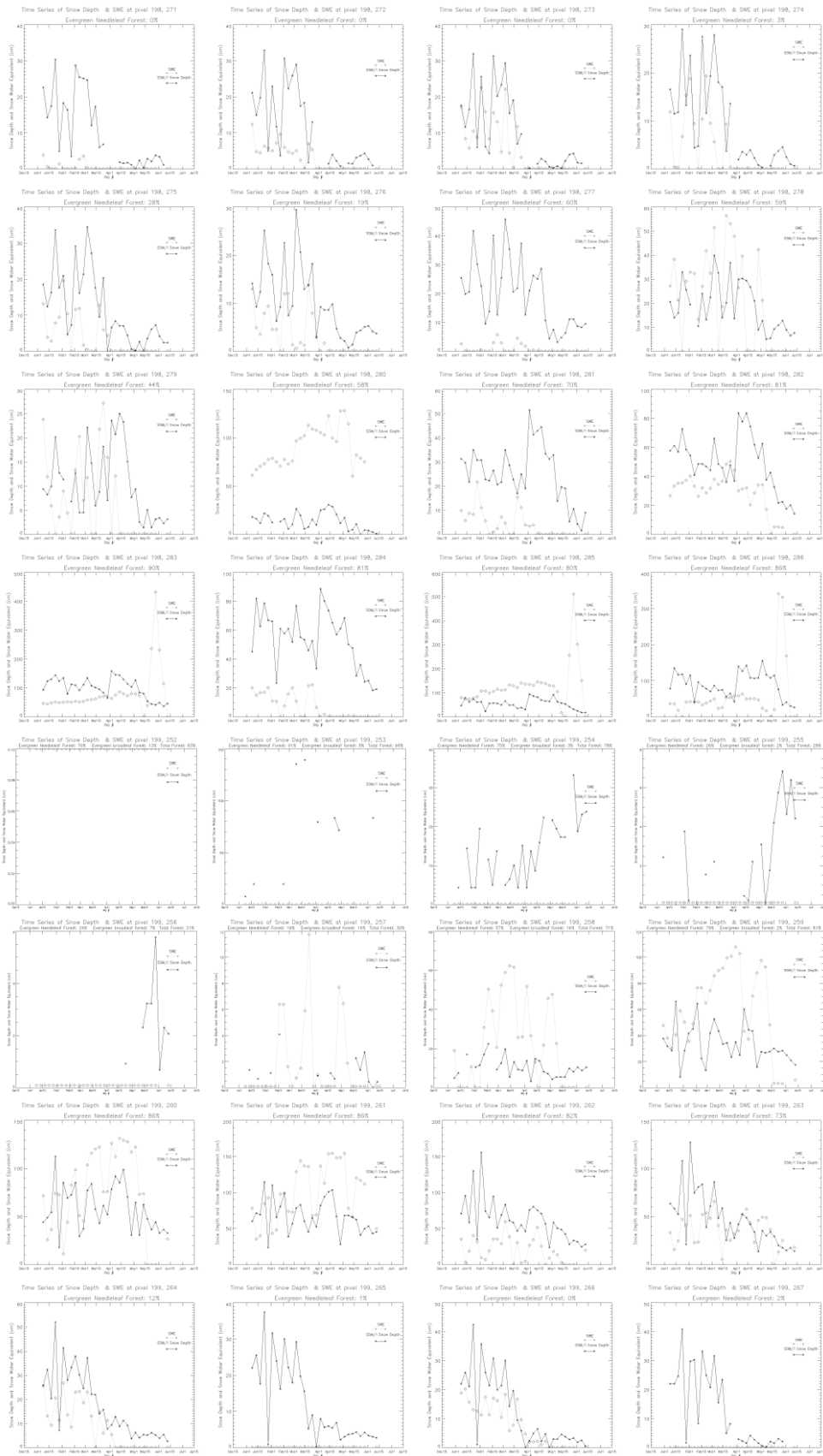


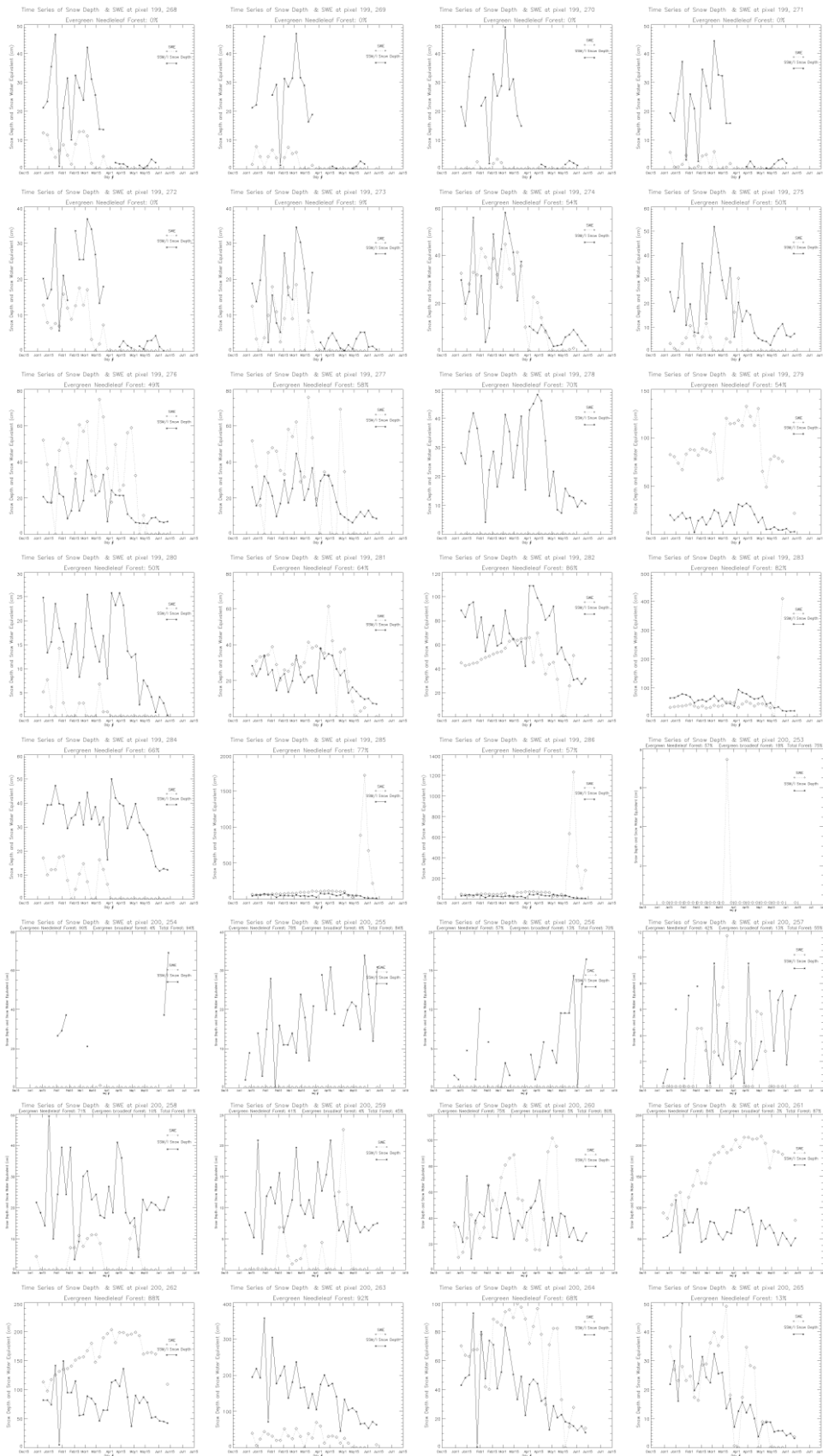


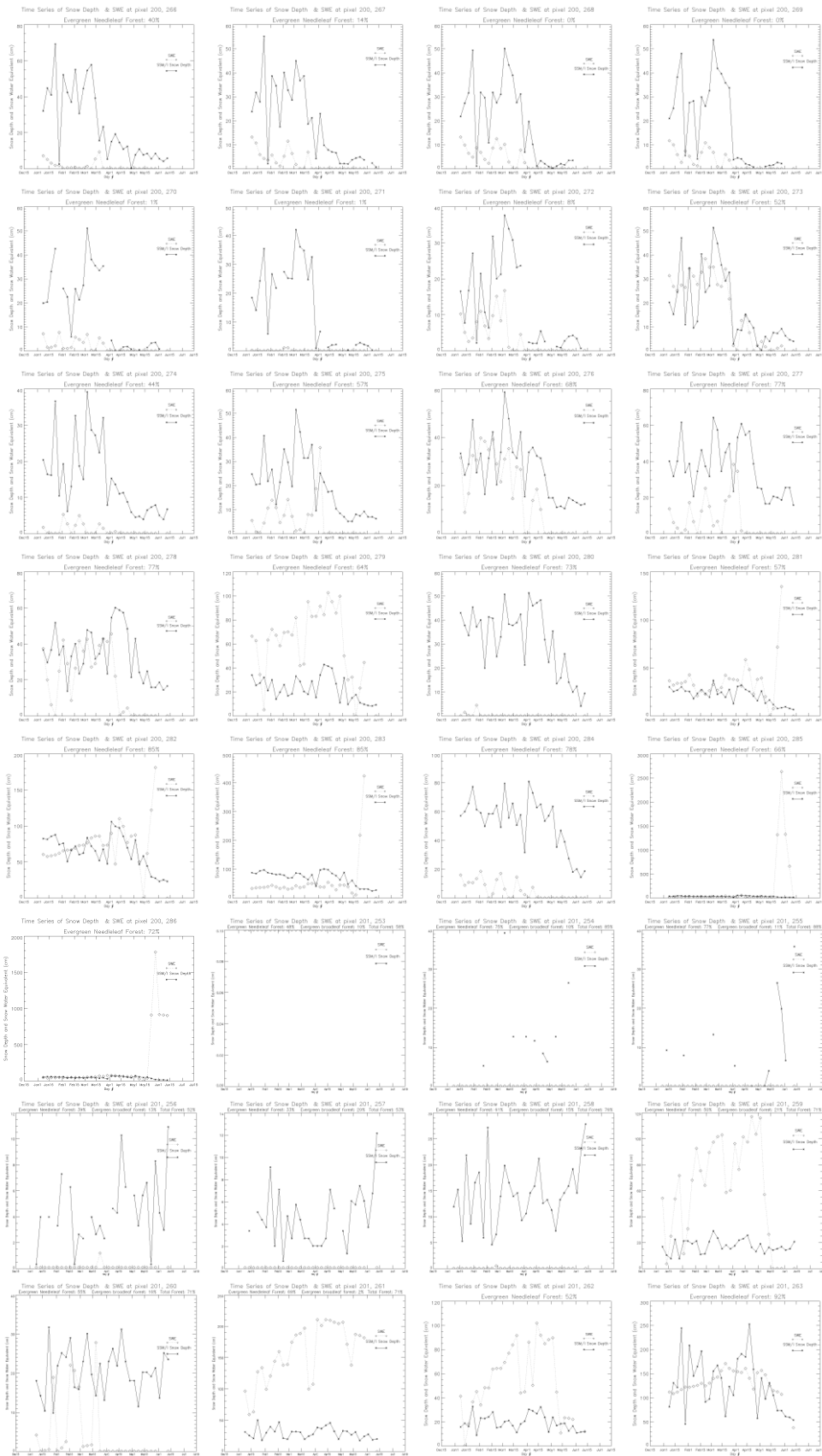


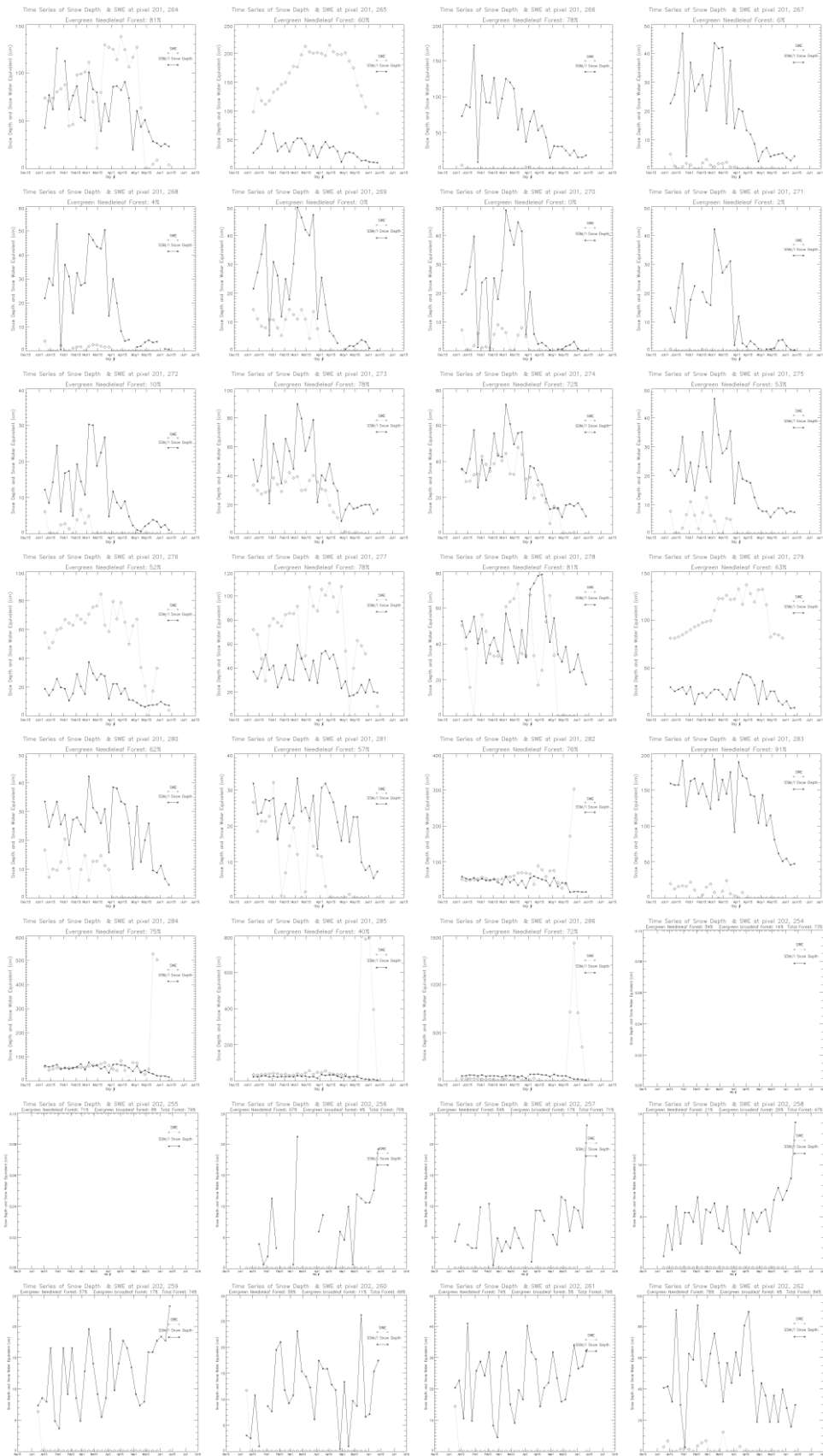


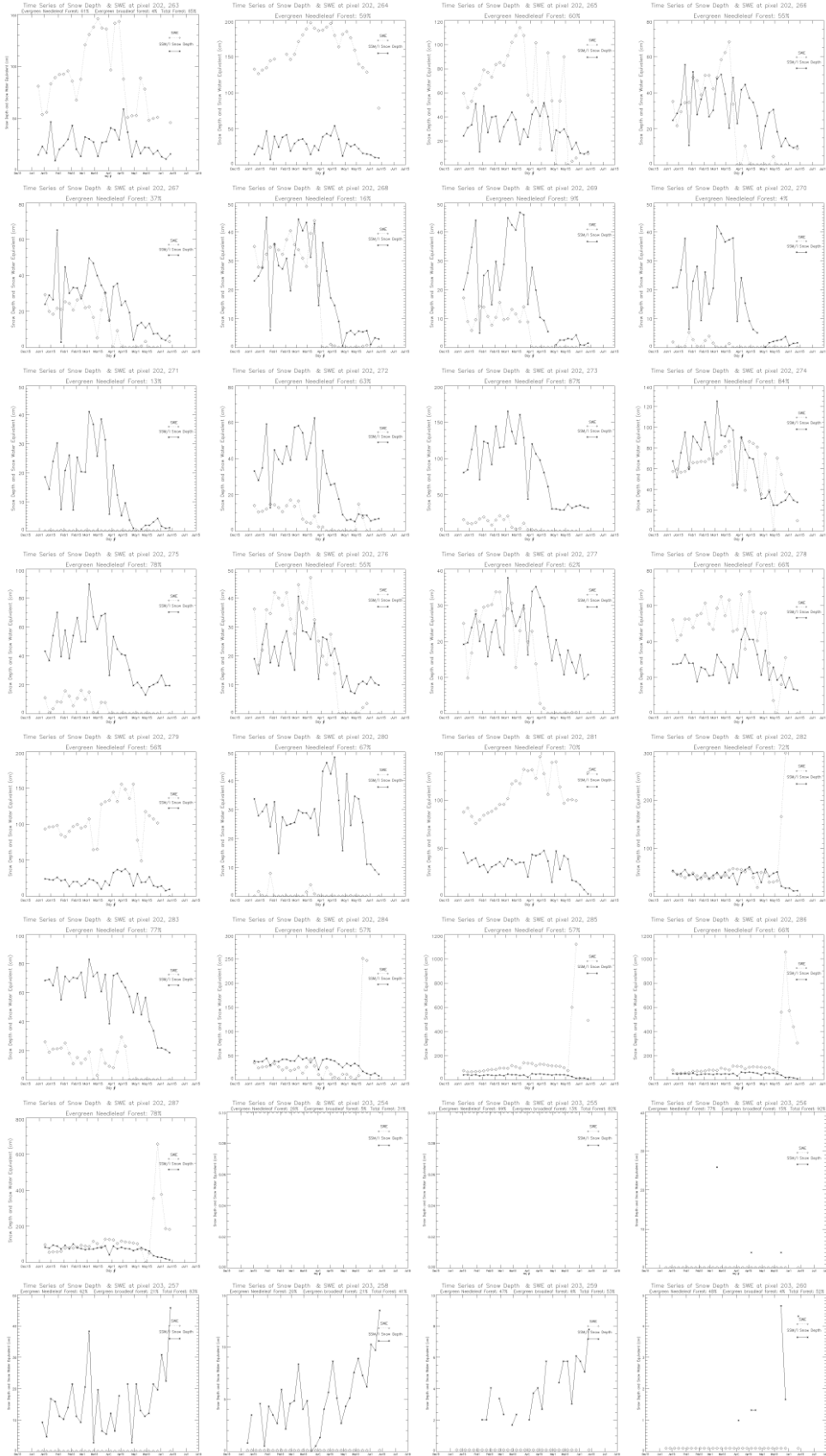


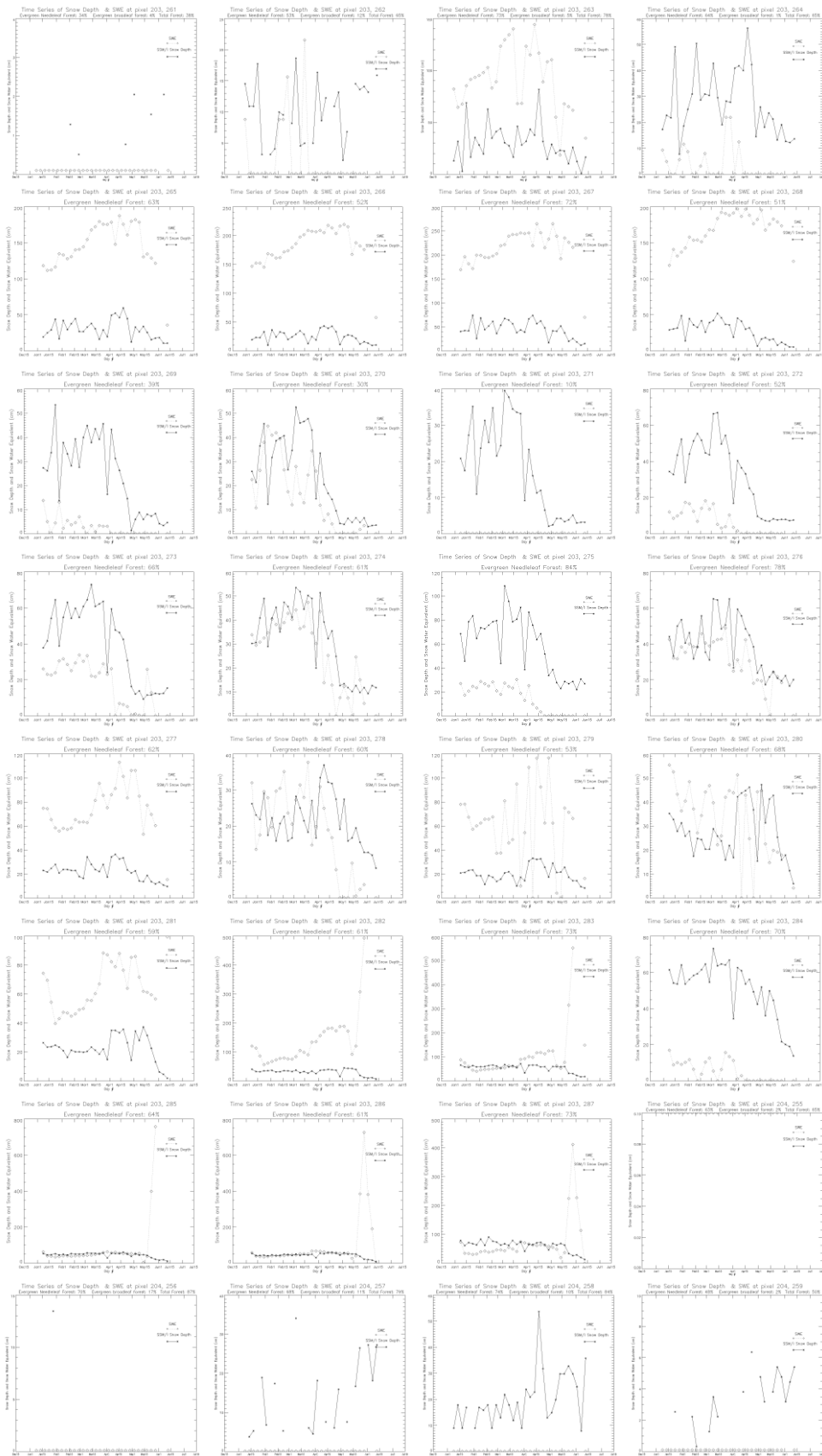


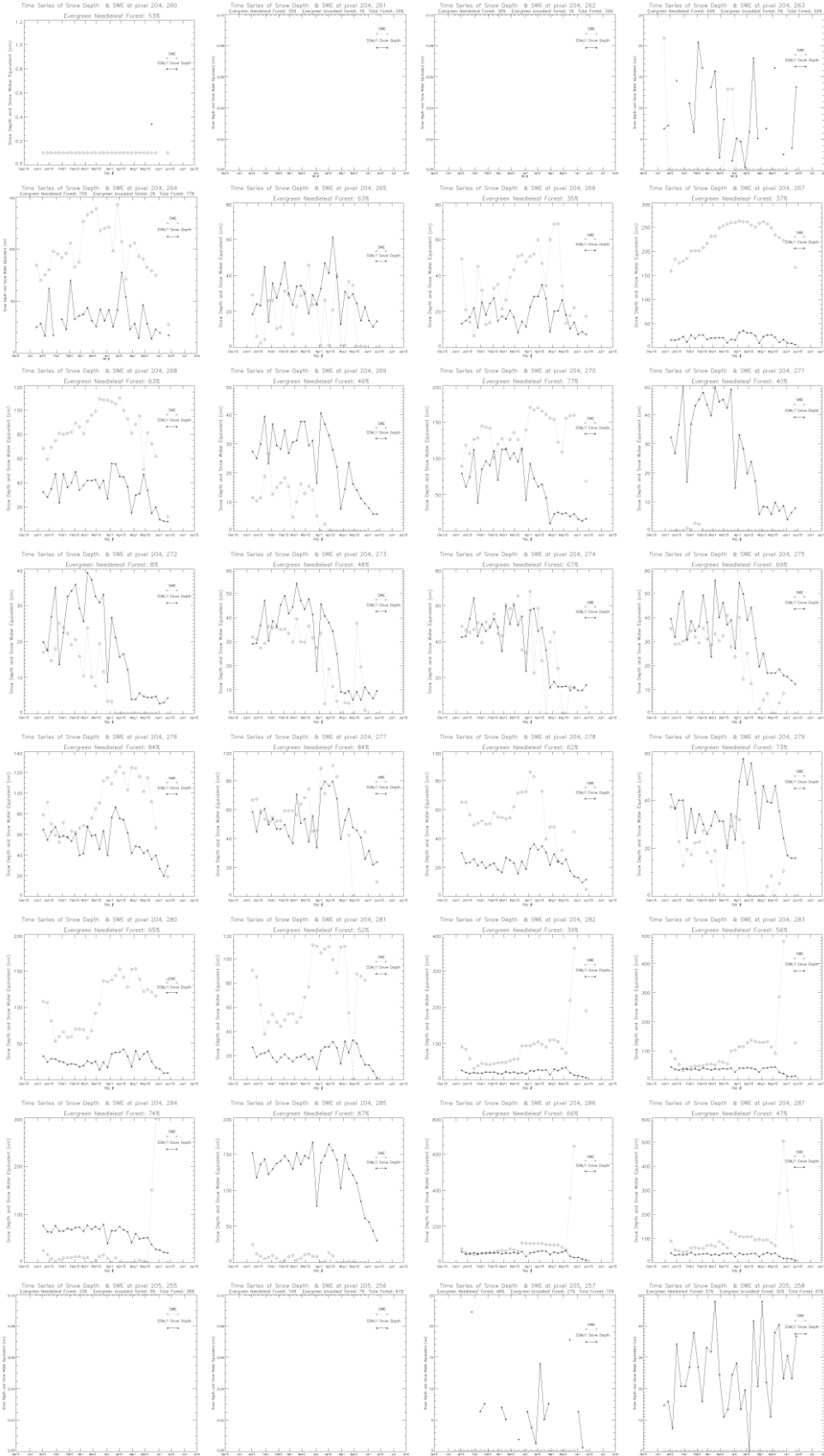


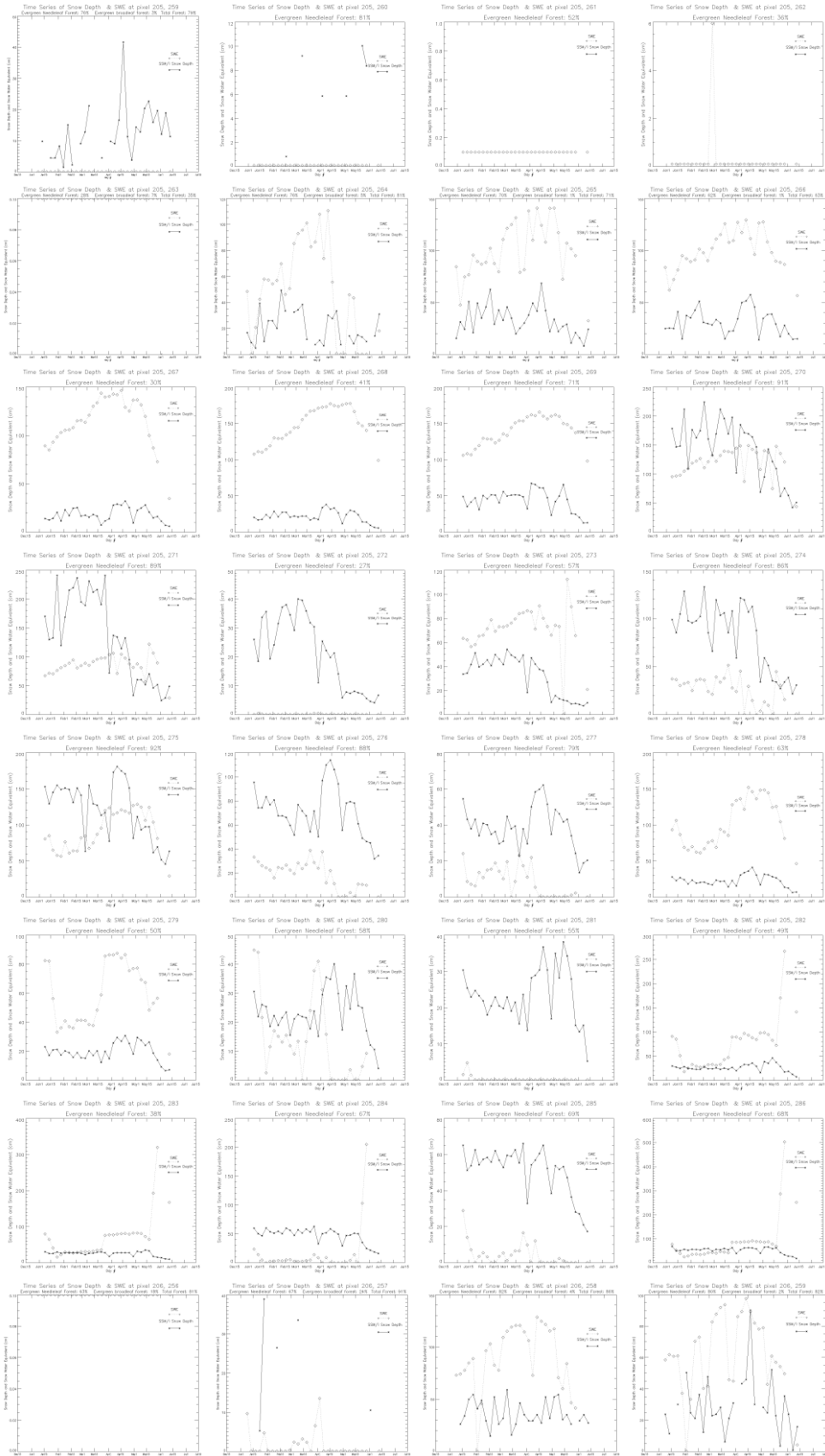


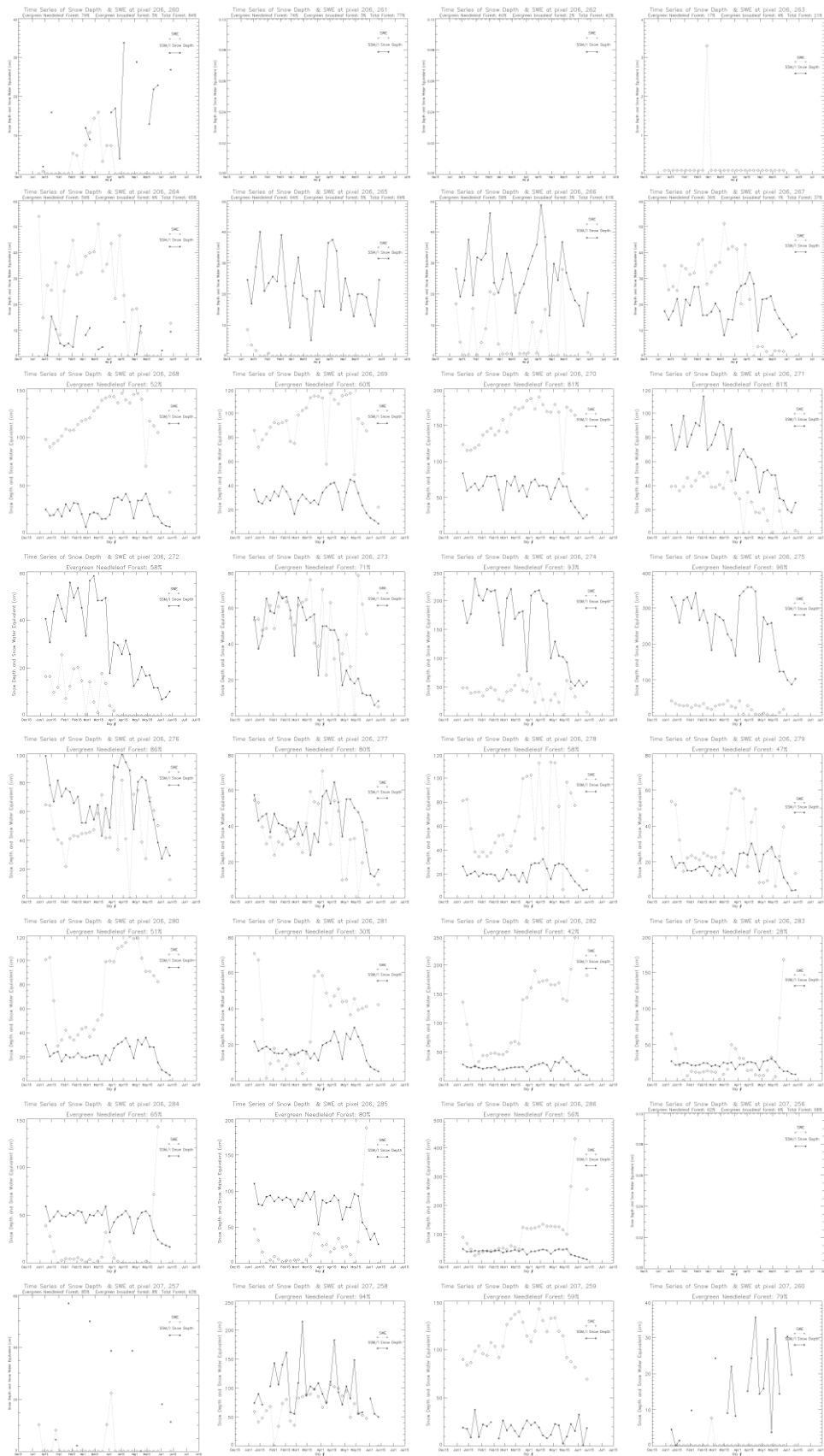


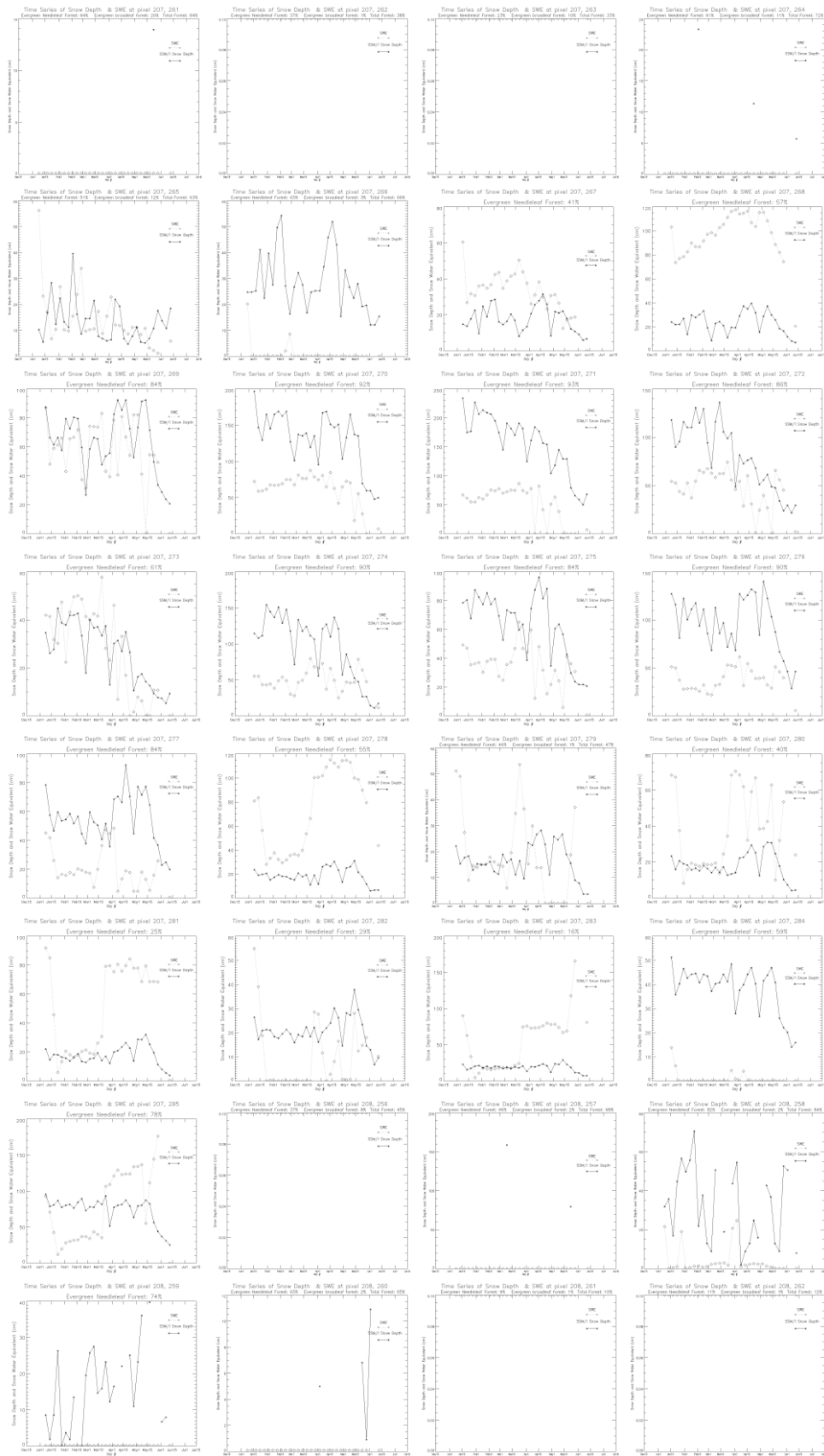


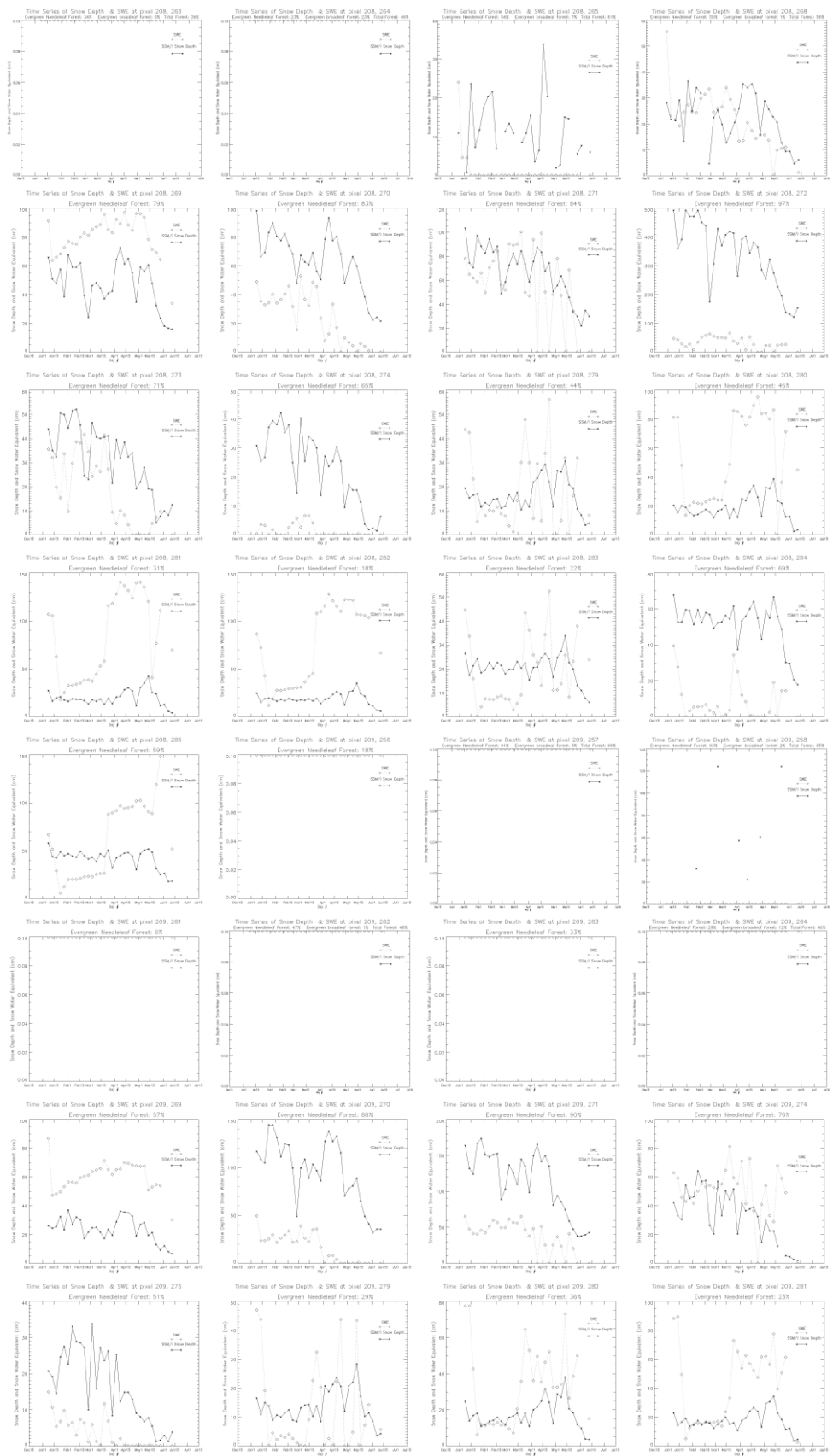


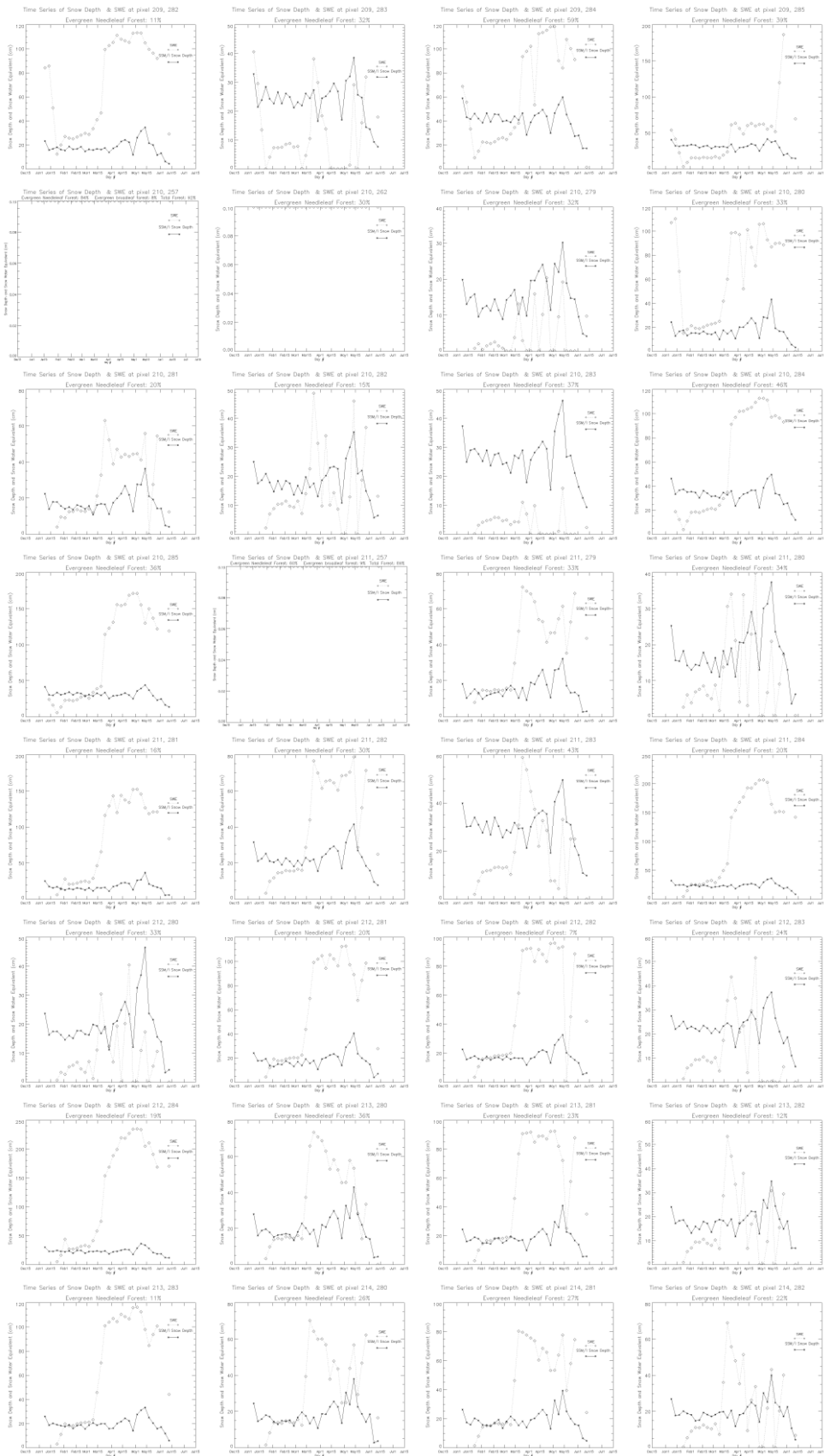


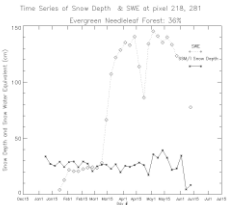
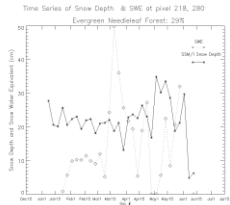
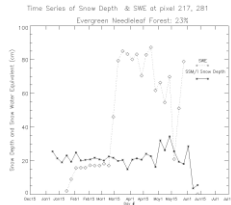
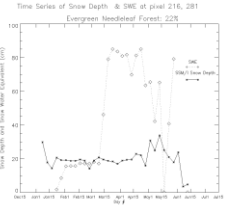
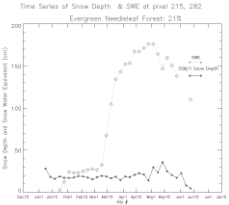
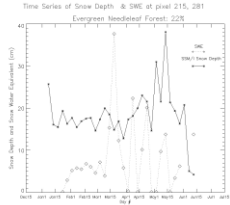
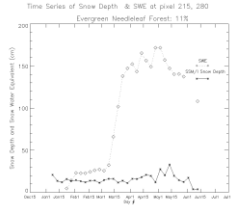












References

British Columbia River Forecast Centre, n.d., 3 Dec. 2009. “Manual Snow Survey Data”, <http://bcRFC.env.gov.bc.ca/data/survey/>

British Columbia River Forecast Centre, n.d., 3 May. 2011, “What is a Snow Survey?”, <http://bcRFC.env.gov.bc.ca/about/snow-survey.htm>

Biancamaria, S., Mognard, N., Boone, A., Grippa, M., & Josberger, E. (2008). A satellite snow depth multi-year average derived from SSM/I for the high latitude regions. *Remote Sensing of Environment*, 112, 2557–2568.

Brodzik, M. J. 1997. 10 May 2011. *EASE-Grid: A Versatile Set of Equal-Area Projections and Grids*. Boulder, Colorado USA: National Snow and Ice Data Center http://nsidc.org/data/ease/ease_grid.html

Butt, MJ (2009) A comparative study of Chang and HUT models for UK snow depth retrieval. *International Journal of Remote Sensing*, 30: 24, 6361 — 6379

Chang, A. T. C., Foster, J. L., & Hall, D. K. (1990). Satellite sensor estimates of Northern Hemisphere snow volume. *International Journal of Remote Sensing*, 11, 167–171.

Chang, A., Foster, J., Hall, D., Goodison, B., Walker, A., Metcalfe, J., & Harby, A. (1997). Snow parameters derived from microwave measurements during the BOREAS winter field campaign. *Journal of Geophysical Research*, 102(D24), 29663–29671.

Derksen, C., Walker, A., & Goodison, B. (2003). A comparison of 18 winter seasons of in situ and passive microwave derived snow water equivalent estimates in Western Canada. *Remote Sensing of Environment*, 88(3), 271–282.

Derksen, C., Walker, A., & Goodison, B. (2005). Evaluation of passive microwave snow water equivalent retrievals across the boreal forest/tundra transition of western Canada. *Remote Sensing of Environment*, 96, 315–327.

Dingman, SL (1994) *Physical Hydrology*, Prentice Hall, New Jersey.

Geer, I.W., Ed. (1996). *Glossary of Weather and Climate, with Related Oceanic and Hydrologic Terms*. American Meteorological Society, Boston, MA, 272 pp.

Hartman, R.K., Rost, A., & Anderson, n.d. May 2011 a.D.M. Operational Processing of Multi-Source Snow Data, National Operational Hydrological Remote Sensing Center (NOHRSC), <http://www.nws.noaa.gov/oh/hr/dmip/2/OPPS.html>

Hartman, R.K., Rost, A., & Anderson, D.M. n.d. May 2011b. Spatial Distribution of Snow Water Equivalent Observations in Mountainous Terrain, National Operational Hydrological Remote Sensing Center (NOHRSC), http://www.ncgia.ucsb.edu/conf/SANTA_FE_CD-ROM/sf_papers/hartman_rob/spatial.html

Hills R., McManamon, A., & Hartman, R.K. n.d. May 2011. Snow Estimations and Updating System (SEUS), National Operational Hydrological Remote Sensing Center (NOHRSC), http://www.ncgia.ucsb.edu/conf/SANTA_FE_CD-ROM/sf_papers/hills_randy/seus.html

Lowell, K & Jaton A (1999) Spatial Accuracy Assessment: Land Information Uncertainty in Natural Resources, Ann Arbor Press, Michigan.

Mizukami, N., Perica, S., & Hatch, D. (2011) Regional approach for mapping climatological snow water equivalent over the mountainous regions of the western United States. *Journal of hydrology*, 400, 72 -82.

National Snow and Ice Data Center (2011) <http://nsidc.org/>

National Snow and Ice Data Center, n.d., May 2011a, EASE-Grid Map Parameters: Northern Azimuthal Equal-Area Map. http://nsidc.org/data/ease/ease_grid.html

National Snow and Ice Data Center, n.d., 12 May 2011b, Ancillary Data. Land cover – IGBP Land Cover Classes, http://nsidc.org/data/ease/ancillary.html#igbp_classes

Natural Resources Conservation Service, n.d. December 2009a. Snow Course Data, Background Information, <http://www.wcc.nrcs.usda.gov/snowcourse/sc-hist.html>

Natural Resources Conservation Service, n.d. December 2009b. Snow Course and Monthly SNOTEL Historical Data, <http://www.wcc.nrcs.usda.gov/snow/snowhist.html>

Rango A (1997) Spaceborn remote sensing for snow hydrology applications, *Hydrological Sciences* (4) August 1996, 477-494.

Singh, P. R., & Gan, T. Y. (2000). Retrieval of snow water equivalent using passive microwave brightness temperature data. *Remote Sensing of Environment*, 74, 275– 286.

Singh P & Singh VP (2001) Snow and Glacier Hydrology, Kluwer Academic Publishers, the Netherlands.

United State Geological Survey (USGS), n.d. 1 May 2011. Seamless Data – Landcover – NLCD 2001 Forest Canopy: <http://seamless.usgs.gov/website/seamless/view.htm>